Sensor Development for Physiological and Environmental Monitoring

by

Kevin William Nichols

A Thesis Presented in Partial Fulfillment
of the Requirements for the Degree
Master of Science

Approved April 2018 by the
Graduate Supervisory Committee:

Sangram Redkar, Chair
Brad Rogers
Thomas Sugar

ARIZONA STATE UNIVERSITY

May 2018

ABSTRACT

The sensor industry is a growing industry that has been predicted by Allied Market Research to be a multi-billion industry by 2022. One of the many key drives behind this rapid growth in the sensor industry is the increase incorporation of sensors into portable electrical devices. The value for sensor technologies are increased when the sensors are developed into innovative measuring system for application uses in the Aerospace, Defense, and Healthcare industries. While sensors are not new, their increased performance, size reduction, and decrease in cost has opened the door for innovative sensor combination for portable devices that could be worn or easily moved around. With this opportunity for further development of sensor use through concept engineering development, three concept projects for possible innovative portable devices was undertaken in this research. One project was the development of a pulse oximeter devise with fingerprint recognition. The second project was prototyping a portable Bluetooth strain gage monitoring system. The third project involved sensors being incorporated onto flexible printed circuit board (PCB) for improved comfort of wearable devices. All these systems were successfully tested in lab.

TABLE OF CONTENTS

CHAPTER Page

CHAPTER Page

LIST OF TABLES

LIST OF FIGURES

Figure Page

Figure Page

Figure Page

Figure Page

Figure Page

CHAPTER 1

INTRODUCTION

Humans use their five senses to interpret what is happening around them, on the other hand, electric systems have no way to perceiving what is occurring outside the microcontroller without the aid of sensors. All electronic sensor provide some form of signal to the processor to evaluate and/or process about the physical quantity the sensor is being used to detect. Wilhelm Von Siemens developed in 1860 one of the earliest sensors which was a temperature sensor (Staff 1995). Today, the global sensor market has grown into a multibillion dollar industry. In a recent market forecast report by Allied Market Research, it was reported that the global sensor market is expected to a $241 billion market by 2022 which translates to a compound annual growth rate of 11.3%. There are many driving factors behind this expected growth rate. Some of the driving factors that were mentioned in the Allied Market Research Sensor Market Overview report are advancement in sensors themselves, advancement in consumer electronic products, increasing usage of sensors in smartphones, robust demand in automation industry, surge in the automotive sector and growing demand of wearable devices (Bajpai, Shukla and Singh 2016). Additional, as the objects in our world become more interconnected, like with smart home devices, the demand for sensors will continue to grow. As Figure 1 illustrates, there is more than just the sensor's development itself that is increasing the demand and value for sensors. Two early links in this value chain that provides areas for research are "Concept and Engineering Test" and "Measurement System." An important factor in deciding what type of sensor to use in developing a

concept and testing to become a marketable system involves looking at what sectors of the industrial markets are highly involved in the expected growth for that particular sensor. Besides the Electronic industry, there are the Aerospace, Defense, and Healthcare industries who are all looking at new and efficient ways to incorporate sensors into products.

Figure 1. Illustrate Value Chain Analysis for Sensor Market (Bajpai, Shukla and Singh 2016).

Sensor are classified by the form of energy that the sensor will be interacting with. Mechanical, thermal, electrical, magnetic, radiant, and chemical are the six common energy forms which a sensor element receive (Staff 1995). Within each of these energy forms, there can be many different physical quantity or property which can be measured. For example, some of the elements that could be measured within the electrical energy form are voltage, current, resistance, capacitance, or frequency. Table 1 show a more complete list of measurable properties in relationship to the different energy form classifications (Staff 1995).

Table 1. Measurable Properties Grouped by the Different Energy Forms for Sensors (Staff 1995)

Energy Form	Example Property Measured
Mechanical	Length, volume, velocity, acceleration, force, torque, pressure, acoustic wavelength
Thermal	Temperature, heat flow, entropy, specific heat
Electrical	Voltage, current, resistance, capacitance, electric field, frequency, inductance
Magnetic	Field intensity, flux density, magnetic moment
Radiant	Intensity, phase, wavelength, transmittance
Chemical	Composition, concentration, pH, reaction rate

Sensors, in their most generalistic form, are comprised of three basic components which are a sensor element, sensor packaging, and sensor signal processing hardware. The sensor element is the mechanism that converts the measured energy form into another energy form which can be processed into a meaningful energy signal. Sensor elements can be divided further by whether they are self-generating/passive or modulating/active sensors. Active sensors have an external, modulated, energy that is add to the sensor element which is a needed part of transforming the input energy into the desired output energy form. The packaging for a sensor provides the physical means to protect, move, and connect to the sensor. Within the sensor package there is often more than just a sensor element as shown in Figure 2. There could be LEDs, multiple sensor elements, secondary sensor element, and calibration controls. If the sensor includes an on-chip signal processing system, the sensor is referred to as a smart sensor. By having the signal processor hardware embedded into the sensor package, this minimizes the

external hardware that would otherwise be needed to complete the sensor system that would have been incorporated and integrating with the sensor's energy output to transform it into a signal form that a microcontroller can process (Staff 1995).

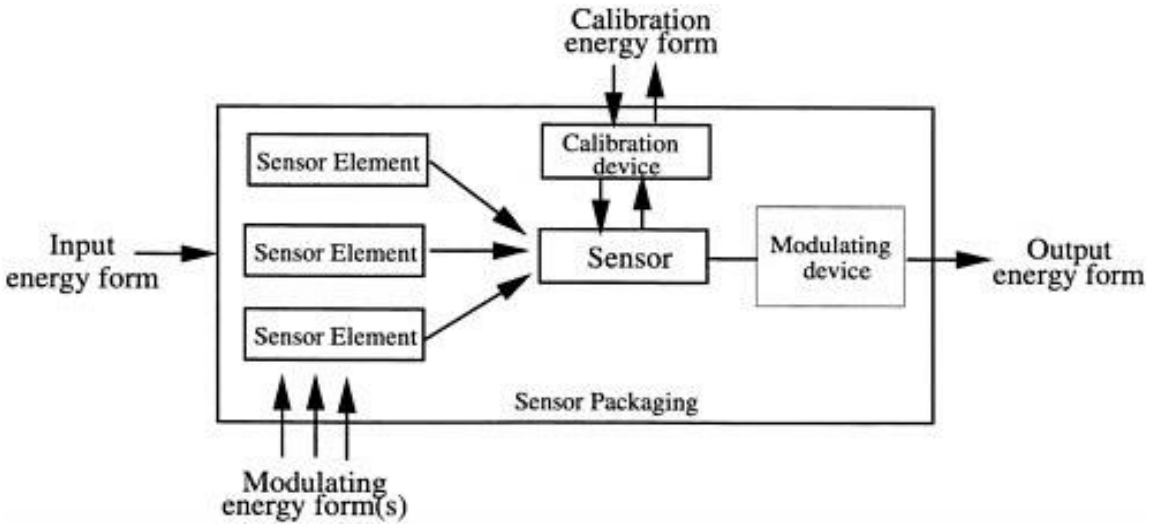

Figure 2. Illustration of Anatomy of a Sensor System (Staff 1995)

While wearable devices are a portable device that have become a popular term since pre-millennial, the first portable devise was a heart rate monitor that Dr. Norman Holter introduced in 1957 (Lemay, et al. 2014). Wearable and portable devices development has a lot of focus application development for health care application. Advancing wearable healthcare technology has been identified by the United States National Academy of Engineering as one the fourteen great challenges for the twenty-first century (Poon, et al. 2014). Wearable healthcare device for use outside of a clinical facilities are used in many ways for improving the care, monitoring, and detection of medical problems. For example, there are many cardiovascular disease, like Hypertension, that are not identified until it is too late. But with a wearable blood pressure devise, long-term monitoring, in an economical way, is now means in which

doctors can detect the variation in one's blood pressure to which can aid in the diagnosing heart disease and asses the risks factors the patient could be facing (Poon, et al. 2014).

Beside disease recognition, wearable healthcare devices can be used as part of the recovery treatment plan. Wearable devices that monitors the human gait actives to observe the balance and walking patterns to provide information which can be used in refining the care and physical treatment the patient receives. Wearable body temperature devices can be used to monitor the process and treatment sleeping disorders. Epilepsy patients benefit from wearable device by monitoring their seizure activities by the aid of accelerometers and gyroscope sensors (Poon, et al. 2014).

This thesis is organized by presenting in the following chapters the developmental work and research of some novel sensors. Chapter two presents the design of a wireless pulse oximeter with fingerprint recognition. This is followed by chapter three discussing the development of a wireless multipurpose data acquisition device. The last design that is presented in chapter four includes information about some flexible physiological sensors developed. This is then wrapped up in the conclusion which is presented in chapter five.

CHAPTER 2

WIRELESS PULSE OXIMETER WITH A FINGERPRINT SENSOR

Motivation

As part of this research in wearable devices, a pulse oximetry wireless device for possible clinical medical application was developed. With this project, the initial challenges were making this device unique since there are many commercial off-the-shelf options available. To make this pulse oximeter unique, a fingerprint reading and wireless communication functionality was to be integrated to the pulse oximeter that was powered by a rechargeable battery. This would allow medical personnel to identify and/or confirm the identity of the wearer of the device while transmitting the vital signs of pulse and SpO2 (peripheral capillary oxygen saturation) level. By being able to transmit a variety of information wirelessly would allow the devices to work in a variety of settings from combat field aid situation to emergency efforts at a disaster site. This would allow medical personnel the ability to monitor the measurement of the SpO2 level which is typically a key parameter in assessing how stable or critical the condition is of someone who needs medical attention without the need of setting up a network system at the site.

Operation Methodology for a Pulse Oximeter Component

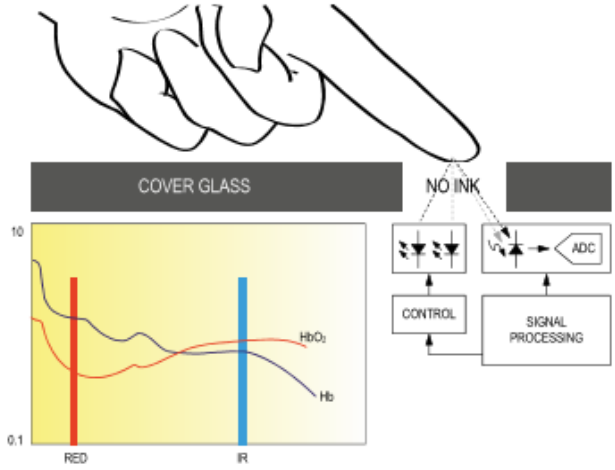

Figure 3. System Block Diagram of the MAX30100 (Integrated 2014)

A pulse oximeter is a noncontact device, which can measure pulse and oxygen saturation in the blood. Typically, the sensor consists of two LEDs emitting light: one in Red spectrum (RED-650nm) and the other in Infrared (IR-950nm) (Integrated 2014). This type of sensor can be placed on a finger or an earlobe, where the skin is not too thick so that both light signals can easily penetrate the tissue. An overview of the operating principle for a pulse oximeter sensor is shown above in Figure 3. Once both light rays penetrate through finger, the absorption is measured with a photodiode. One such pulse oximeter device is the Pulse Oximeter and Heart-rate sensor MAX30100 whose product package is shown in Figure 4. The MAX30100 is reflectance type pulse Ox sensor made

by Maxim Integrated. This sensor also has the capable of heartbeat detection and temperature reading (Integrated 2014).

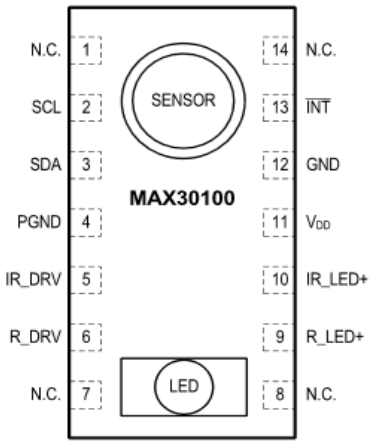

Figure 4. MAX30100 Pin Configuration (Integrated 2014)

The SpO2 levels are an estimated percentage of the amount of oxygenated hemoglobin compared to the total amount of hemoglobin in the blood (Nokia 2017). The SpO2 value is the oxygenated Hemoglobin level over the total Hemoglobin level.

$$SpO2 = \frac{HbO2}{Total\ Hb} \text{ (Strogonovs 2017)}$$

Depending on the amount of oxygen in the blood, the ratio (R) between the absorbed Red light and IR light will be different. This ratio R is calculated as

$$R = \frac{AC_{RMS\ RED}/DC_{RED}}{AC_{RMS\ IR}/DC_{IR}} \text{ (Strogonovs 2017)}$$

where $AC_{RMS\ RED}$ correspond to RMS value of the AC signal of the RED light measured and DC_{RED} correspond to the DC component of the RED light measured. Similarly, $AC_{RMS\ IR}$ corresponds to RMS value of the AC signal of the IR light measured and DC_{IR} corresponds to the DC component of the IR light measured. It is assumed that DC

component is the result of absorption by the body tissue and veins and the AC component is the result of the absorption by arteries.

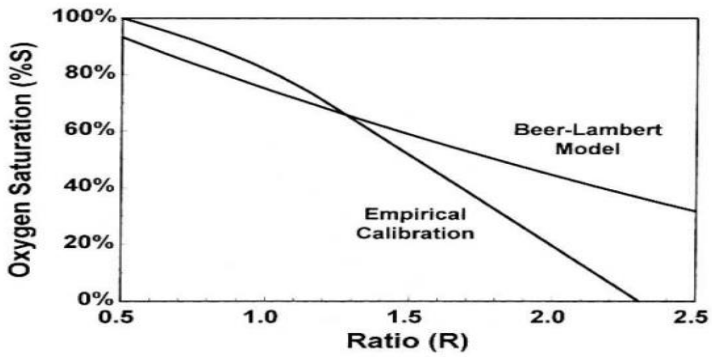

Figure 5. Empirical and Theoretical R to SaO2 (Strogonovs 2017)

From this ratio, it is possible to calculate oxygen level in blood hemoglobin. To get SpO2 from R, an empirical or a theoretical linear relationship with a slight offset can be safely used since the Oxygen Saturation level seldom drops below 80% (Chan and Underwood 2005). This relationship between the Empirical and Theoretical of SpO2 and R can be observed in graph shown in Figure 5 above.

Operation Methodology for a Fingerprint Recognition Reader

Fingerprint scanner use the sensing element(s) within the sensor to extract and/or compare various features of a fingerprint patterns such as fingerprint ridges (arch, loop, and whorl) and minutia features of fingerprint ridges (ridge ending, bifurcation, and short ridge). Two minutia fingerprint features are shown below in Figure 6.

Figure 6. Two of the Minutia Fingerprint Features in a Fingerprint (John 2011)

The way a fingerprint sensors captures a digital image of the fingerprint is divided into three main categories which are optical, solid-state, and ultrasonic sensing. Within each of these categories, there are advantages and disadvantages.

The Frustrated Total Internal Reflection (FTIR), is one of the oldest and most used technique for live-scan fingerprint scanning, is which is also part of the optical sensing group (Maltoni, et al. 2003). With FTRI, a figure is placed on top of a glass prism which ends up leaving the valleys of the fingerprint's feature a distance away from the glass. The scanner will illuminate light into one of the other sides of the prism with a LED. This will causes the light to be reflected from the valleys and absorbed at the ridges of the fingerprint. This reflection and absorb of reflected light will result in distinguishable light and dark areas. The light ray pattern will then exit out the other side

of the prism and be focused onto a CCD or CMOS image sensor (Maltoni, et al. 2003). An illustration of this process is shown below in Figure 7. As a way of reducing the cost of these type of FTIR devises, plastic is often used instead of glass for the prisms and lenses, and CMOS cameras are mounted instead of more expensive CCDs. Being the largest type of fingerprint sensor means the FTIR type of sense will be easy to acquire at a low cost while have numerous documents, examples, and support.

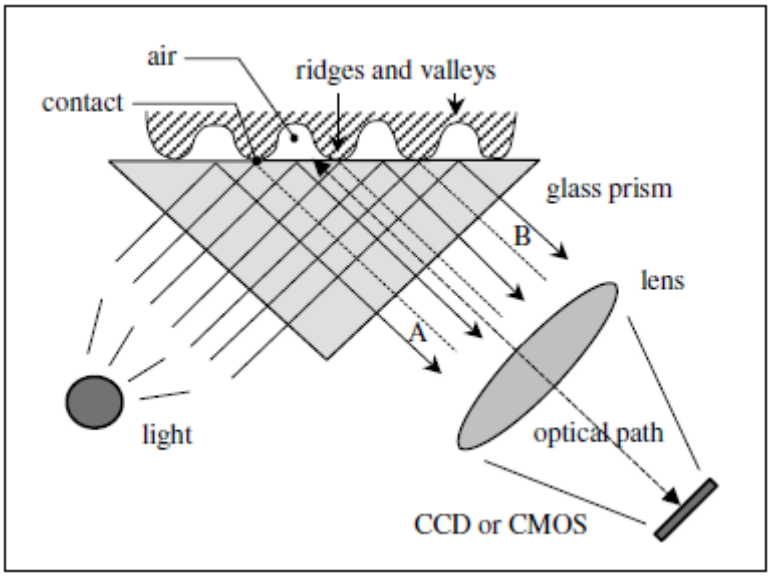

Figure 7. Illustration of the Working Principle of Optical FTIR Sensing (Maltoni, et al. 2003)

The disadvantage of this technique is fingerprint quality is affected by the cleanliness of the fingertip and camera lens, quality of contact between lens and skin, erosion of skin surface, and quality of screen, i.e. scratch free, no smudges on screen etc. Another disadvantage to FTIR technic of fingerprint sensing is that it cannot be miniaturized due to constants of the optical path length between the finger surface the prism to the image sensor (Maltoni, et al. 2003).

Solid-state sensors, also known as silicon sensors, consist of an array of pixels, each pixel being a tiny sensor itself. The user directly touches the surface of the silicon which eliminates the need for optical components or external CCD/CMOS image sensors. Capacitive, thermal, electric field, and piezoelectric are the four main effects that are used to convert the physical information into electrical signals (Maltoni, et al. 2003).

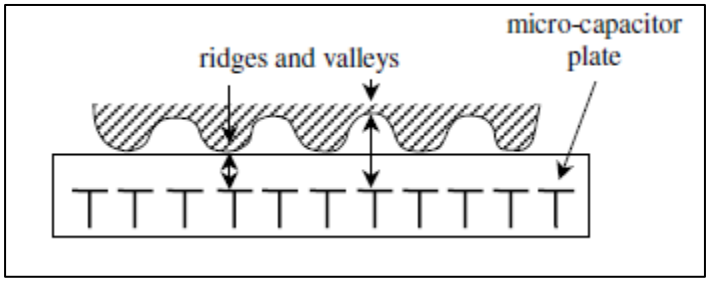

Figure 8. Illustration of the Working Principle of Capacitive Sensing (Maltoni, et al. 2003)

A capacitive fingerprint sensor measures is the most common used of the solid state methods. A capacitive sensor is a two-dimensional array of micro-capacitor plates embedded in a chip as shown in Figure 8 above. The finger's skin itself is the second plate and the fingerprint pattern is the micro-capacitor that has a unique identifying pattern. When a finger is placed on the chip, small electrical charges are created between the surface of the finger and each of the silicon plates. The magnitude of these electrical charges depends on the distance between the fingerprint surface and the capacitance plates. Thus the capacitance varies across the array of capacitors between the ridges and valleys found within a fingerprint to form a digital image of the user's fingerprint.

Some of the advantages of the capacitive sensors are the possibility of adjusting some electrical parameters to deal with non-ideal skin conditions like wet and dry fingers.

Also the sensor package size can be made compact. Disadvantages to this type of fingerprint reading is the need for frequently cleaning the surface to prevent the grease and dirt from compromising image quality. Additional two other important things are needed to keep the capacitive sensor working. One is that the sensor most have proper protection and grounding to avoid electrostatic discharge that could come from the figure tip and damage the sensor. The second important things is with the protective surface coating over the silicon chip. This protective layer protects the silicon chip from chemical substances that are present on the finger and abrasion (Maltoni, et al. 2003).

Ultrasound sensing is a kind of echography that can be used to capture a fingerprint image. The sensor uses acoustic signals are transmitted towards the fingertip and then captures the returning echo signals. Since this method ends up imaging the subsurface of the skin, gloves, dirt, oil and minor injuries do hinder its ability to acquire a good image of the fingerprint. This working principle is shown below in Figure 9. Disadvantage to ultrasound sensing is that it is primarily mechanical, expensive, and the technology behind it has not matured enough for large-scale production (Maltoni, et al. 2003).

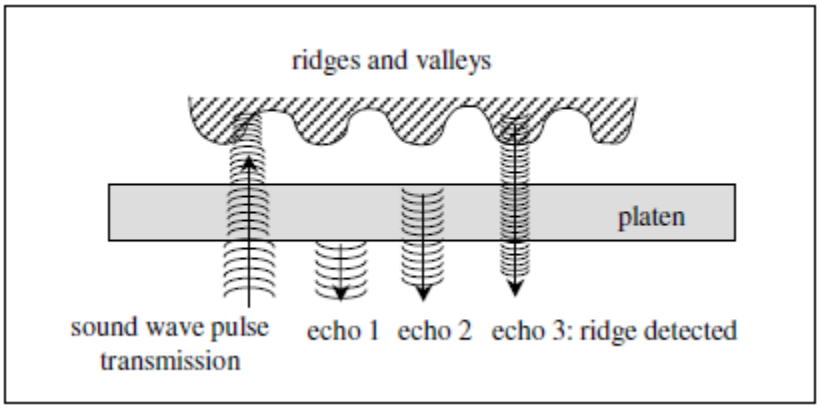

Figure 9. Illustration of the Working Principle of the Ultrasound Sensing Technique (Maltoni, et al. 2003)

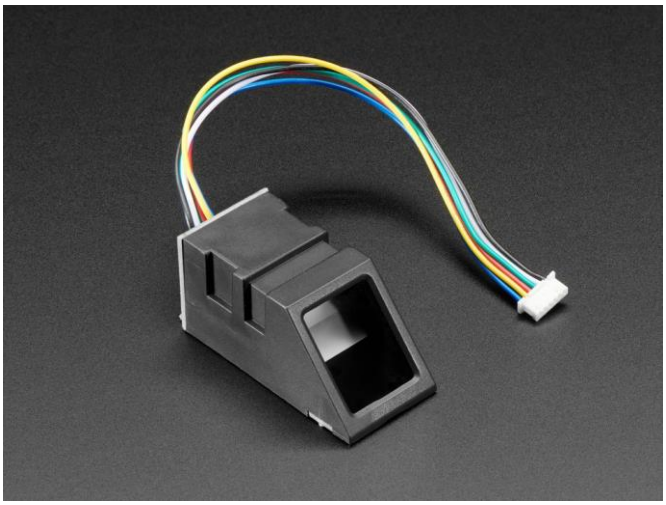

Figure 10. ZFM20 Fingerprint Sensor (Adafruit 2012)

The point-of-departure prototype used the ZFM20 optical fingerprint sensor made by Zhiantec Technologies Co, shown above in Figure 10, which performs a series of functions like fingerprint enrollment, image processing, fingerprint matching, searching and template storage (ZhianTec 2008). This sensor can store 162 fingerprint templates (images) and has a False Acceptance Rate: <0.001% (Security Level 3), and a False Reject Rate: <1.0% (Security Level 3) (S. Technology 2010). Since this sensor works on

the optical sensing principle, it requires a clean fingertip and scratch/smudge free screen. The sensor has a Digital Signal Processor chip that performs pattern recognition. When matching fingerprints, the users the fingerprint enters the system through optical sensor and is then compared with the fingerprints that have been stored in the sensors library. If the sensors is setup for 1:1 matching, system will compare the live fingerprint with specified template designated within the ZFM20 module. If the setup configuration is for 1:N matching, the system will search the whole fingerprint library looking for a matching finger. In both circumstances, system will return the matching result of either success or failure.

Prototype Design

The prototype design for the wireless pulse ox with fingerprint devise formed out from five key element housed in a ridged case. These five key elements are a pulse oximeter, fingerprint reader/decoder, microprocessor, Bluetooth communication and rechargeable power. In an effort to quickly establish fully functional, point-of-departure design, the initial design for the prototype revolved about the fit and used of readily available electrical breakout boards/modules. The fingerprint reader and MAX30100 Pulse-Oximetry module took care of biometric reading of the user's finger. The microcontroller and Bluetooth communication was handled by a Bluno Beetle module. The battery was simply handled by a rechargeable, 3.7 volt Lithium-Ion with 400 milliamp hours that would plug into a recharger that was external to the prototype.

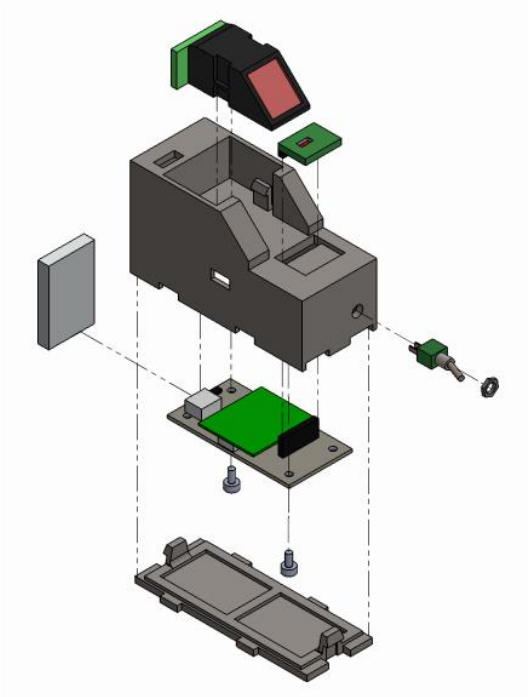

Figure 11. Exploded View of the Pulse Oximeter Design That Was Created in SolidWorks

A three-dimensional design of the Pulse Oximeter's case was created in SOLIDWORKS so that the casing could be 3D printed. The creation different elements of the system were approximated to help with the fit and form of the case in to ensure the success of creating a functional prototype. Figure 11 shows an exploded view of the mechanical design and how the different components fit within the case. The basic mechanical drawing have been added to the Appendix A for further possible reviewed.

Figure 12. Initial Assembled Prototype Design of the Pulse Oximeter Devise

Figure 12 shows the point-of-departure prototype fully assembled. The case was 3D printed and the design house the different components. From this working prototype iteration in design, the potential and insight to future design were easily able to be identified.

Prototype Validation Testing

To validate that this initial prototype is fully functional, point-of-departure design, validating testing was broken into two main parts. The first part was to validate that the fingerprint reader can distinguish the differences between different fingerprints. The second part of the testing was to validate that the pulse oximeter was providing pulse and SpO2 reading to the reading that is similar to the results from an established SpO2 commercial devices. The testing for the Bluetooth wireless communication was a simple pairing of device to Android Smartphone with BLE 4.0 and reading the transmitted information from the prototype device.

The fingerprint validation testing began by enrolling different fingerprints. Table 2 shows what identification number was enrolled to which finger.

Table 2. Enrolled Fingerprint Identification Number to Finger

Enrolled ID #	Hand	Finger
0	Right	Index
1	Right	Middle
3	Right	Little
4	Left	Index
5	Left	Middle
6	Left	Ring
7	Left	Little
8	Right	Ring

After enrolling different fingerprints, the different fingers were placed onto the fingerprint reader's window. The result from the fingerprint reader module was observed in a Serial Print window which and then compared to enrollment to check functionality. Show below in Figure 13 and Figure 14 are a couple of those validation readings.

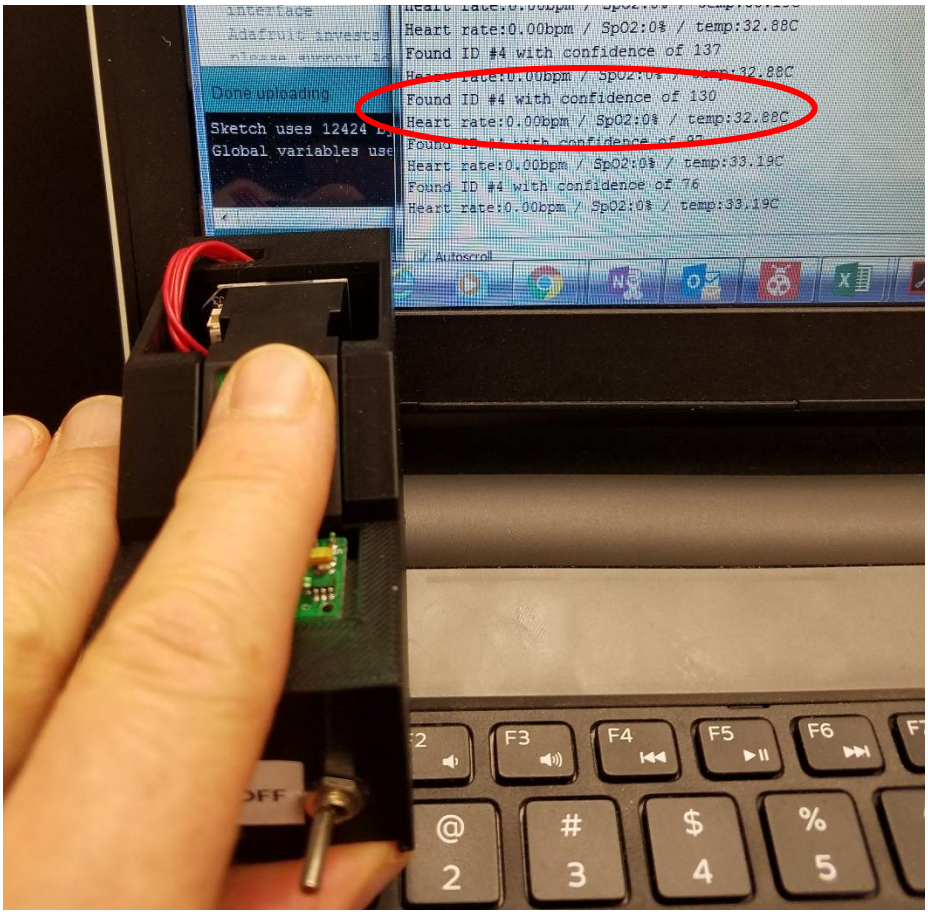

Figure 13. The Left Index Finger Shown Being Identified by the Fingerprint Reader

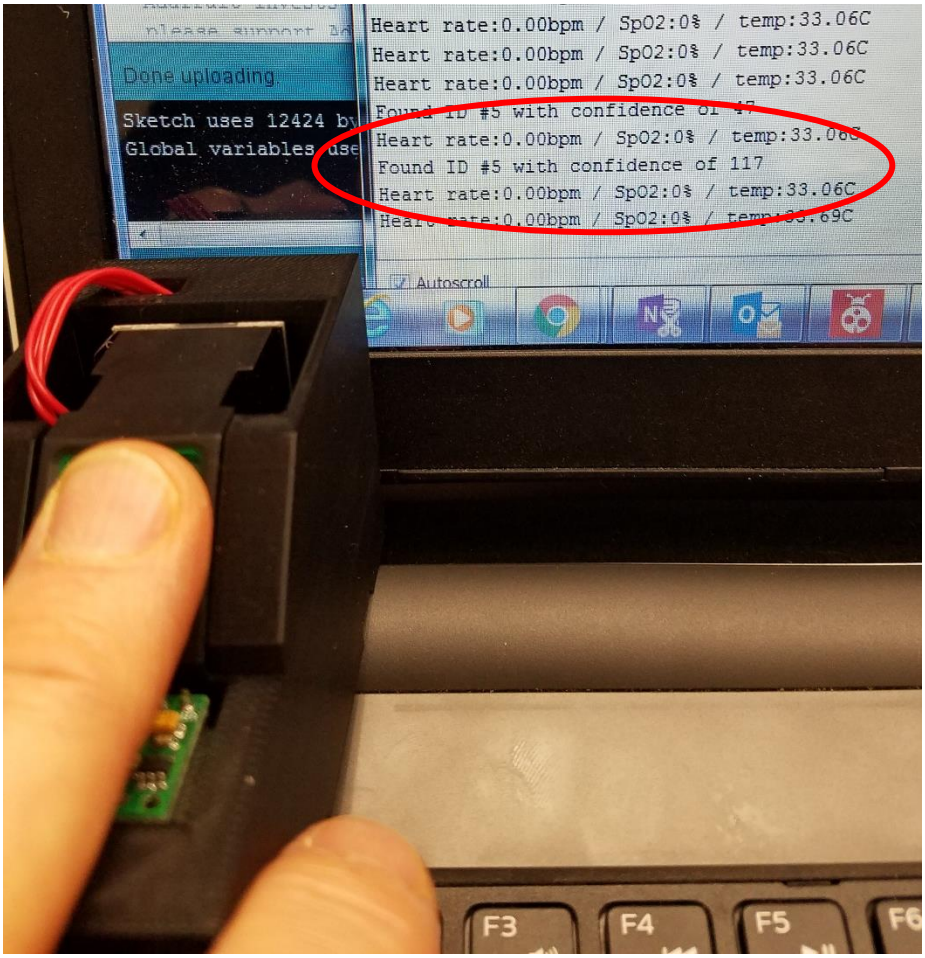

Figure 14. The Left Middle Finger Shown Being Identified by the Fingerprint Reader

The ‘confidence’ is a score number which ranges from 0 to 255 that indicates how good of a match the fingerprint is, higher is better. Note that if it matches at all, that means the sensor is pretty confident so you do not have to pay attention to the confidence number unless it is being used for high security applications.

The validate process for the functionality for the pulse oximeter was simple done by comparing results the prototype results to a commercial devices. The commercial pulse oximeter used for comparing the results is by Contec Medical Systems Company and the model number of the device was CMS50DL. To help minimize the difference in

reading of the two pulse oximeters, the reading were taken from two side-by-side figure on the same hand. The prototypes results were similar to the commercial devices. Some of those results has been captured and is shown below in Figure 15.

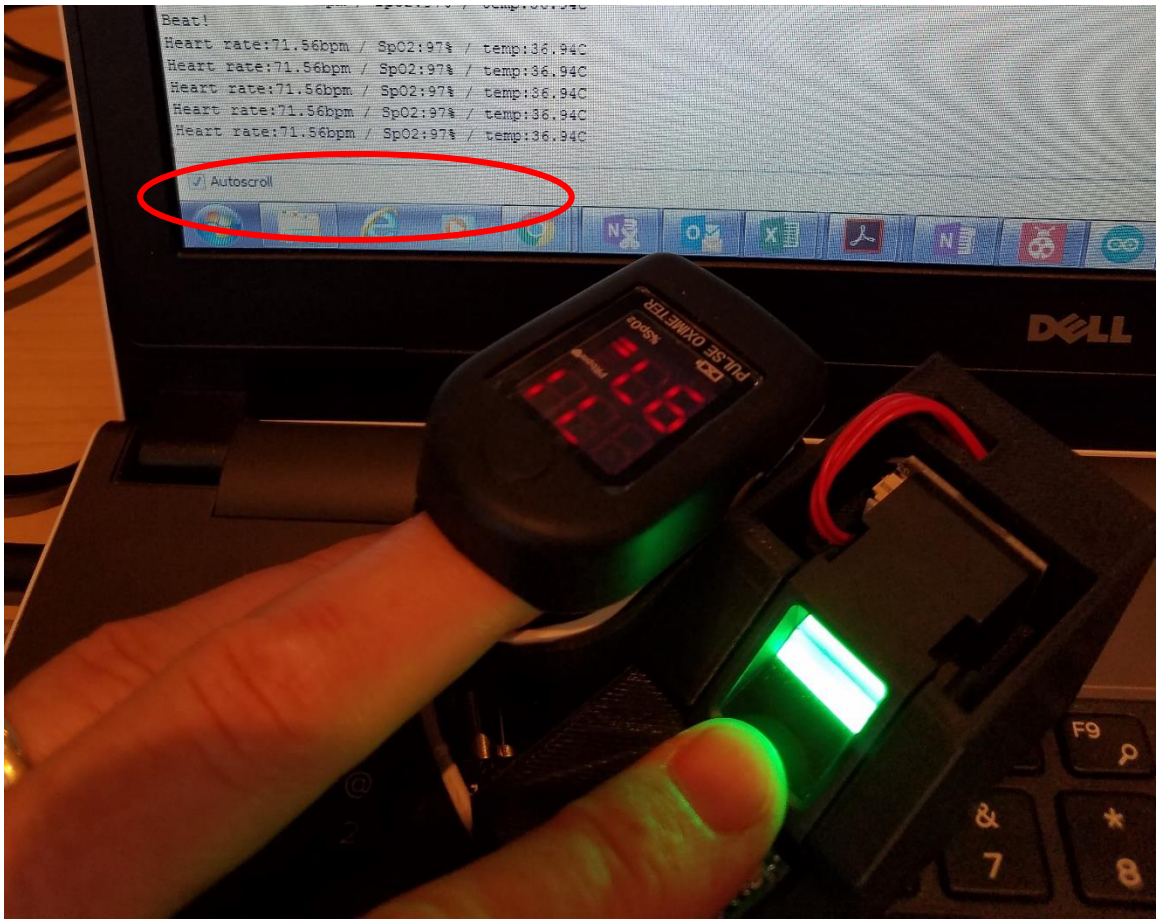

Figure 15. Picture of Pulse and SpO2 Validation Testing of the Pulse Oximeter

Recommended Design Improvements

The recommendation for changes to this point of departure prototype would be using different hardware components. As the electrical system gets more refined, the physical overall design needs to evolve to device that is more “familiar feeling” of a pulse oximeter device that is currently out on the market.

Table 3. Features and Specification for the ZFM1020 Fingerprint Capacitive Sensor

Features

- GROVE Compatible Interface
- FPC1020 CMOS fingerprint sensor
- Best in class imaging quality with 256 true grey scale values in every pixel
- Robust protective coating capable of more than 10 million finger placements
- Full ESD protection to more than ±30kV
- 200 byte fingerprint template
- 1:N Identification (One-to-Many); 1:1 Verification (One-to-One)
- Auto-learning function (Automatically updating the fingerprint features)
- Security level setting; TTL serial interface

Specifications

- Resolutions: 508 DPI
- Fingerprint store capacity: 100 fingerprints
- Verification time: < 0.45 sec
- Identification time: < 0.45 sec
- False accept rate (FAR): < 0.0001%
- False reject rate (FRR): < 0.01%
- Baud rate: 9600, 19200, 38400, 57600, 115200 bps
- Working current: < 50mA; Standby current: < 10µA
- Supply voltage: DC 5V;
  Digital I/O voltage: 2.8V ~ 5V DC
- Operating temperature: - 20℃ ~ 60℃;
  Operating humidity: 20% ~ 80%

One hardware change would be to change the fingerprint sensor to a capacitive sensing sensor. This change would be done for two reasons. One is it would allow for the overall size of the final devise to be reduced dramatically by changing from an optical sensor to a capacitive sensor. The second reason is with the capacitive sensor able to read wet, dirty, scraped up fingers while not needing to maintain a clean sensing surface. One such capacitive sensor fingerprint module is the FPC1020. In Table 3 above, the features and specification for the FPC1020 are given.

A second hardware change would be with the wireless communication by adding Ultra-Wide Band (UWB) as a secondary method of wireless communication which used in wireless networking to achieve high bandwidth connections with low power utilization. UWB can send short signal pulses over a broad spectrum and can operate at data rates of 480 Mbps to 1.6 Gbps over a few meters. UWB radios transmit data by generating a radio frequency (RF) energy at specific time intervals over a large bandwidth enabling pulse-position or time modulation. The information can be modulated on UWB signals (pulses) by encoding the polarity of the pulse, its amplitude, and/or by using orthogonal pulses. UWB pulses can be sent sporadically at relatively low pulse rates to support time or position modulation, but can also be sent at rates up to the inverse of the UWB pulse bandwidth. Pulse-UWB systems have been demonstrated at channel pulse rates in excess of 1.3 giga-pulses per second using a continuous stream of UWB pulses (Continuous Pulse UWB or C-UWB), supporting forward error correction encoded data rates in excess of 675 Mbit/s (Contributors 2003).

Figure 16. decaWave's DWM1000 Module (decaWave 2013)

One option could be decaWave's DW1000-UWB module which is shown in Figure 16. This a complete, single-chip CMOS comes with integrated antenna, power

management, and clock control simplifies design integration. It has communications range of up to 300 m, with a data communications rate up to 6.8 Mb/s, and 6 frequency bands supported with center frequencies from 3.5 GHz to 6.5 GHz (decaWave 2013).

Another improvement that would benefit further version of this device would to incorporate a way to internally recharging the Lithium-Ion battery. The initial thoughts are in favor of inductive charging to provide one less opening to the future device. Further development and research will need to be done into how small the transmitting coils can be without further increasing the charging time. The incoming supply voltage from the inductive coil or USB port will be feed through the Microchip's MCP7331 Li-Ion Charge Management Controller to safely charge the Lithium-Ion battery.

As part of recommendation for the next version of the pulse-oximeter, and schematic (shown in Figure 17) and Bill of Material (Table 4) was created.

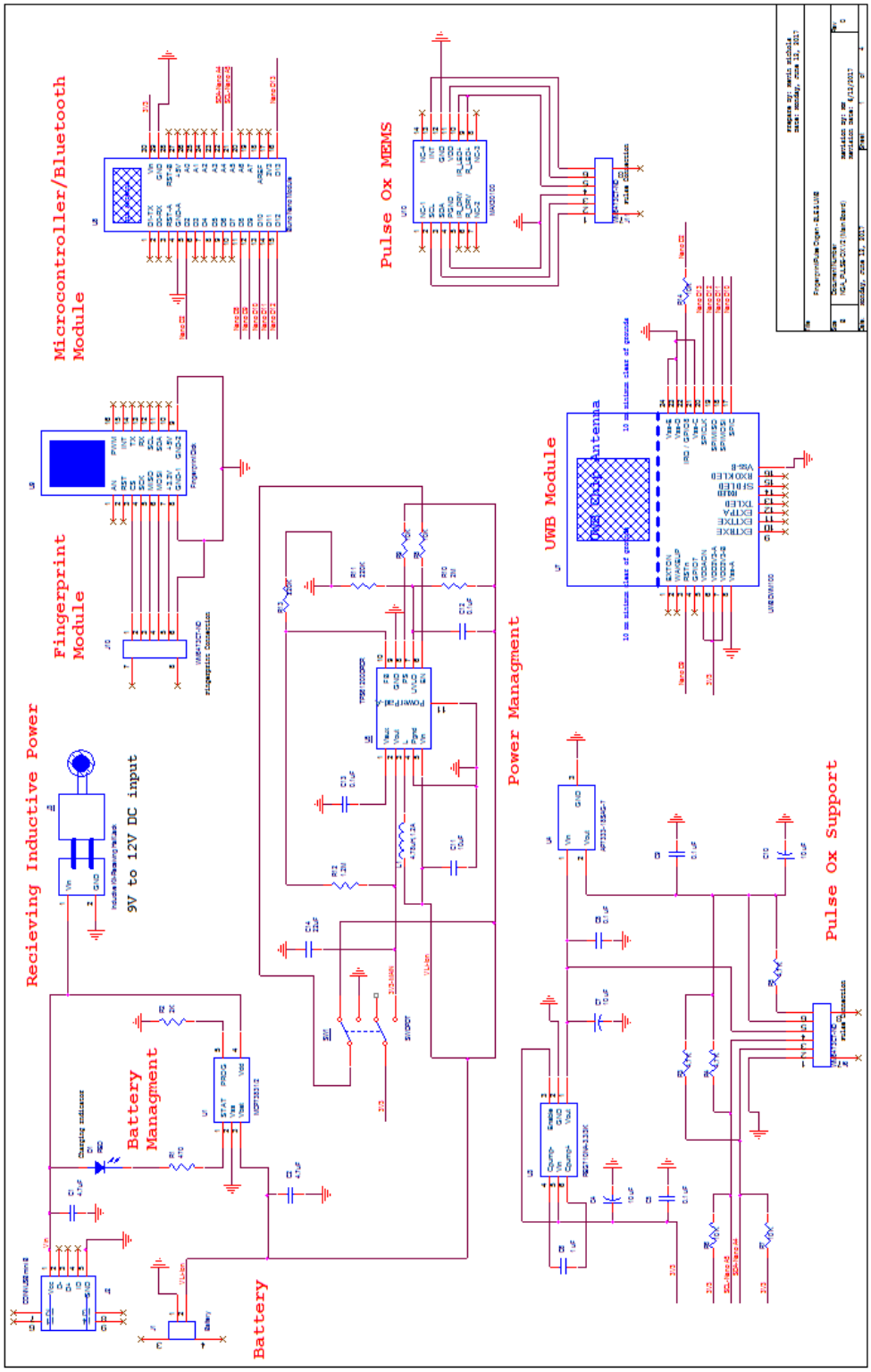

Figure 17. Recommended Reversion Schematic for the Pulse-Oximeter Device

Table 4. Bill of Material for Proposed Pulse Oximeter Revision

Bill of Material

Item #	Section Grouping	Part Name/Description	Unit Quantity	Unit Cost	Total Cost	Manufacturer	Schematic Reference
	Battery Recharing						
1	Battery Recharing	4.7 uF Ceramic Capacitor 10V (0402)	3	$0.380	$1.14	TDK Corporation	C1, C2, C3
2	Battery Recharing	470 ohm Resistor, 1/4W (0603)	1	$0.148	$0.15	Vishay Dale	R1
3	Battery Recharing	2K ohm Resistor, 1/4W (0603)	1	$0.149	$0.15	Vishay Dale	R2
4	Battery Recharing	Red LED Indication, 2.2V (0603)	1	$0.500	$0.50	Kingbright	D1
5	Battery Recharing	IC CONTROLLR LI-ION 4.2V (SOT23-5)	1	$0.580	$0.58	Microchip Technology	U1
6	Battery Recharing	JST 2 pin Connector	1	$0.580	$0.58	JST Sales America Inc.	J1
7	Battery Recharing	USB - mini B, Connector 5 Position, Surface Mount, Right Angle	1	$1.030	$1.03	Molex, LLC	J2
8	Battery Recharing	Boost Switching Regulator IC Positive Adjustable 1.8V 1 Output 1.2A (Switch) 10-VFDFN Exposed Pad	1	$2.460	$2.46	Texas Instruments	U5
9	Battery Recharing	10k Ohm ±5% 0.25W, 1/4W Chip Resistor (0603), Automotive AEC-Q200, Pulse Withstanding Thick Film	2	$0.148	$0.30	Vishay Dale	R8, R9
10	Battery Recharing	2M Ohm ±1% 0.1W, 1/10W Chip Resistor (0603), Automotive AEC-Q200 Thick Film	1	$0.035	$0.04	Vishay Dale	R10
11	Battery Recharing	220k Ohm ±5% 0.25W, 1/4W Chip Resistor (0603), Automotive AEC-Q200, Pulse Withstanding Thick Film	2	$0.148	$0.30	Vishay Dale	R11, R13
12	Battery Recharing	1.2M Ohm ±5% 0.1W, 1/10W Chip Resistor (0603), Automotive AEC-Q200 Thick Film	1	$0.026	$0.03	Vishay Dale	R12
13	Battery Recharing	10µF ±10% Molded Tantalum Capacitors 16V (1206)	1	$0.312	$0.31	KEMET	C11
14	Battery Recharing	0.1µF ±10% 16V Ceramic Capacitor X7R (0603)	3	$0.025	$0.08	KEMET	C12, C13
13	Battery Recharing	22µF ±10% 6.3V Ceramic Capacitor X5R (0805)	1	$0.310	$0.31	KEMET	C14
14	Battery Recharing	4.7µH Shielded Inductor 1.2A 140 mOhm Max Nonstandard	1	$1.090	$1.09	Sumida America Components Inc	L1
15	Battery Recharing	Toggle Switch, DPDT, Panel Mount, 3A, 120V	1	$3.980	$3.98	TE Connectivity ALCOSWITCH Switches	SW1
	Inductive Charging						
16	Inductive Charging	WIRELESS CHARGING KIT 5V 500MA	1	$9.950	$9.95	Adafruit Industries LLC	n/a
17	Inductive Charging	2 Position Wire to Board Terminal Block Horizontal with Board 0.200" (5.08mm) Through Hole	1	$1.000	$1.00	Phoenix Contact	J3, J4
18	Inductive Charging	Power Barrel Connector Jack 2.00mm ID (0.079"), 5.50mm OD (0.217") Through Hole, Right Angle	1	$0.760	$0.76	CUI Inc.	J5
19	Inductive Charging	AC/DC WALL MOUNT ADAPTER 9V 12W	1	$12.800	$12.80	CUI Inc.	n/a
	Pulse-Oxygen						
20	Pulse-Oxygen	Charge Pump Switching Regulator IC Positive Fixed 3.3V 30mA SOT-23-6	1	$1.280	$1.28	Texas Instruments	U3
21	Pulse-Oxygen	IC SENSOR OXIMETER/HEARTRATE	1	$7.030	$7.03	Maxim Integrated	U2
22	Pulse-Oxygen	Linear Voltage Regulator IC Positive Fixed Output 1.8V 500mA TSOT-23-6	1	$0.430	$0.43	Diodes Incorporated	U4
23	Pulse-Oxygen	10µF ±10% Molded Tantalum Capacitors 16V (1206)	3	$0.312	$0.94	KEMET	C4, C7, C10
24	Pulse-Oxygen	0.1µF ±10% 16V Ceramic Capacitor X7R (0603)	3	$0.025	$0.08	KEMET	C5, C8, C9
25	Pulse-Oxygen	1µF ±10% 16V Ceramic Capacitor X7R (0603)	1	$0.070	$0.07	KEMET	C6
26	Pulse-Oxygen	4.7k Ohm ±5% 0.25W, 1/4W Chip Resistor (0603), Automotive AEC-Q200, Pulse Withstanding Thick Film	3	$0.148	$0.44	Vishay Dale	R3, R4, R5
27	Pulse-Oxygen	10k Ohm ±5% 0.25W, 1/4W Chip Resistor (0603), Automotive AEC-Q200, Pulse Withstanding Thick Film	2	$0.148	$0.30	Vishay Dale	R6, R7
	Fingerprint						
28	Fingerprint	FPC1020 Fingerprint module	1	$56.100	$56.10	MikroElektronika	U6
	UWB						
29	UWB	RF TXRX MODULE 802.15.4 CHIP ANT	1	$25.590	$25.59	Decawave Limited	U7
	Bluetooth/Mircocontroller						
30	Bluetooth/Mircocontroller	ATmega328 Bluno Nano AVR® ATmega MCU 8-Bit AVR Embedded Evaluation Board	1	$33.550	$33.55	DFRobot	U8
	Jumper						
31	Jumper	6 Position FFC, FPC Connector Contacts, Bottom 0.020" (0.50mm) Surface Mount, Right Angle	4	$4.335	$17.34	Molex, LLC	J6, J7, J8, J9
32	Jumper	6 Position FFC Cable 0.020" (0.50mm) 4.000" (101.60mm)	2	$3.060	$6.12	Molex, LLC	n/a
		Running Totals For:	Unit Quantity		Total Cost		
			52		$186.93		

CHAPTER 3

WIRELESS STRAIN TRANSMITTER

Motivation

In this research a multifunctional wireless strain gage data acquisition device was developed. The sponsor presented this project with a concept sketch (shown in Figure 18) and a list of requirements which were used to formulate the Design Criteria (Table 5). The goal was to expand existing repertoire of proven, working data acquisition technologies into Bluetooth communication and inductive recharging while developing a device that can transfer data from the strain gages that are to be monitored. The end result also need to be able to able to transfer small scale production for so desired.

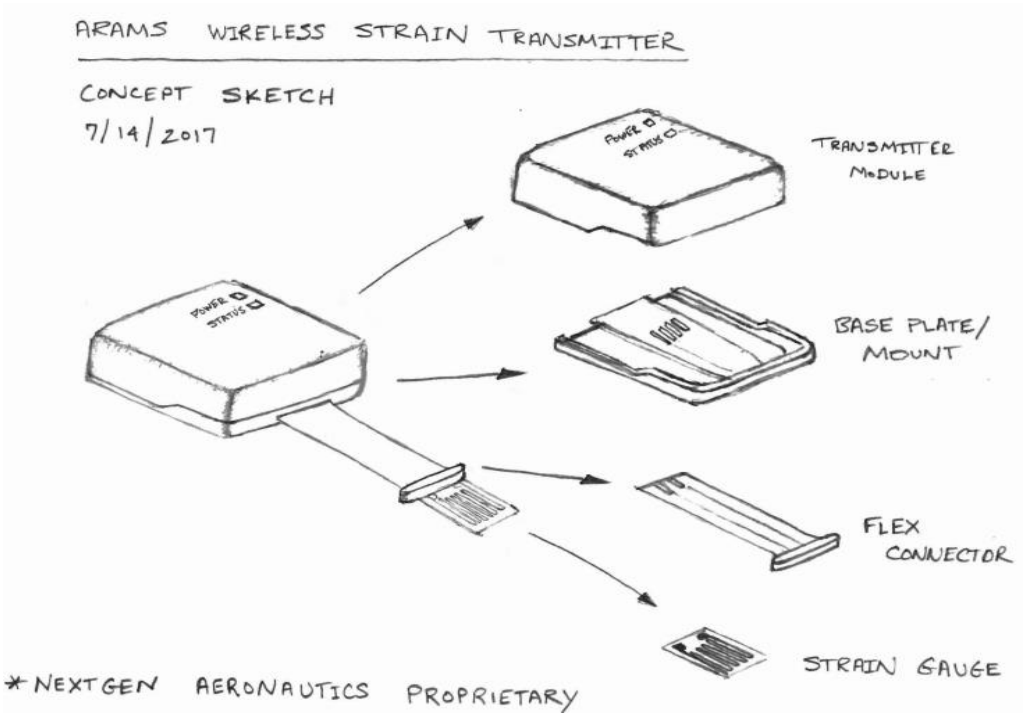

Figure 18. The Presented Proposed Concept Sketch for the Wireless Strain Transmitter Project

Table 5. Design Criteria for Wireless Strain Transmitter

Criteria	Target Goal	Stretch Goal	Rationale
Prototype to be Commercial Scalable	No break-out modules, with part that are readily available	n/a	Want to have the ability to transfer project to low volume production
Rechargeable Battery	Direct connection to recharge Lithium-Ion battery	Recharging Lithium-Ion battery using inductive power	The want to power the system with rechargeable power
Wireless Communication	Bluetooth communication	Bluetooth communication with development GUI inference	The want for wireless communication using Bluetooth technology
Easy Transferring of Transmitter Module	Transmitter that easily attaches to a mounted base and recharging station.	That the different cases involved are ready to transfer to production method of manufacture (i.e. injection modeling).	The device should be able to move the transmitter around to any number of location
Analog Digital Convertor	24 bit ADC	Microcontroller with 24 bit ADC	Quality of reading off the strain gages
Compact in Size	Transmitter under 2 inches square and of minimal height.	Transmitter is 1 ½ inches square and of height ¾ inches.	The device should easily be mounted without having size constants due to a large device
Strain Gage	Able to read two strain gages	Ability to read to read over ten strain gages	The device should be reading and transmitting strain gage data

Operation Methodology of Bluetooth Communication

Bluetooth communication is a global standard for wireless technology that allows devices to communicate with each other over radio frequencies (RF). When released in July of 1999, Bluetooth meant to be a technology that would replace serial data cables cable connection between various devices. Several of the key feature of Bluetooth communication are (Gupta 2013):

- Ad hoc (a decentralized type of wireless network that does not rely on a preexisting infrastructure, such as routers in wired networks or access points in wireless networks like Wi-Fi)
- Small size – easily integrated into smart phones or wearable devices
- Low power – 1mW to 100mW of output power
- Short range – typical range of 10 to 100 meters
- Secure – 128 bit authentication key with configurable encryption key of up to 128 bits
- Does not require direct line of sight
- Can co-exist with other wireless technologies
- Intended to work anywhere in the world since it uses unlicensed band frequency

The Bluetooth communication happens between two Bluetooth IC chips which transmit and receive information. The main task of the Bluetooth chips is to transform digital signals via radio frequency while hold the key protocol data. An illustration of this basic process is shown in Figure 19. The nominal radio frequency Bluetooth operates at is 2.4 GHz which is a regulatory range of 2400 to 2483.5 MHz. When the

Bluetooth device is scanning to discover other Bluetooth devices, it is hopping across 79 RF channels that are separated by 1MHz (Gupta 2013).

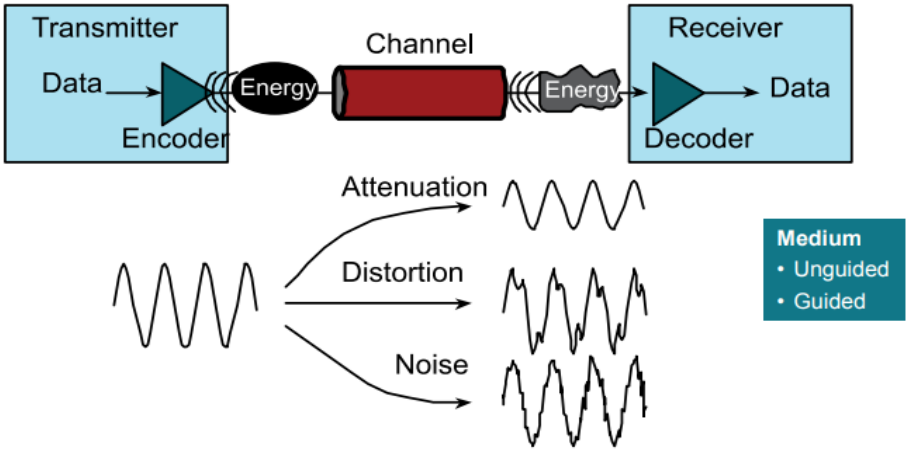

Figure 19. Illustration of Wireless Communication (T. Instruments n.d.)

The processing of pairing to two Bluetooth devices to communicate with each other can be simplified into six steps. The first step is for one of the Bluetooth devices to discover the other device. The second step follows by one of these devices to make an inquiry on the location and necessary information to make connect. The third step is involves the discovered device to allow a connection by being "connectable" which could involve a password or encryption key. If the discovered Bluetooth devise is "connectable," the fourth step is to create a connection between the two units which is offend called "paging". After the connection is made, one of the protocols on the two Bluetooth chips while establish which unit will become a 'Master' while the other becomes the 'Slave' for the fifth step. This connection between the two Bluetooth device will remain connected they are disconnect by code or lose of signal which is the sixth

step in the Bluetooth pairing (Gupta 2013). Figure 20 shows these six step of establishing a Bluetooth connection between two devices.

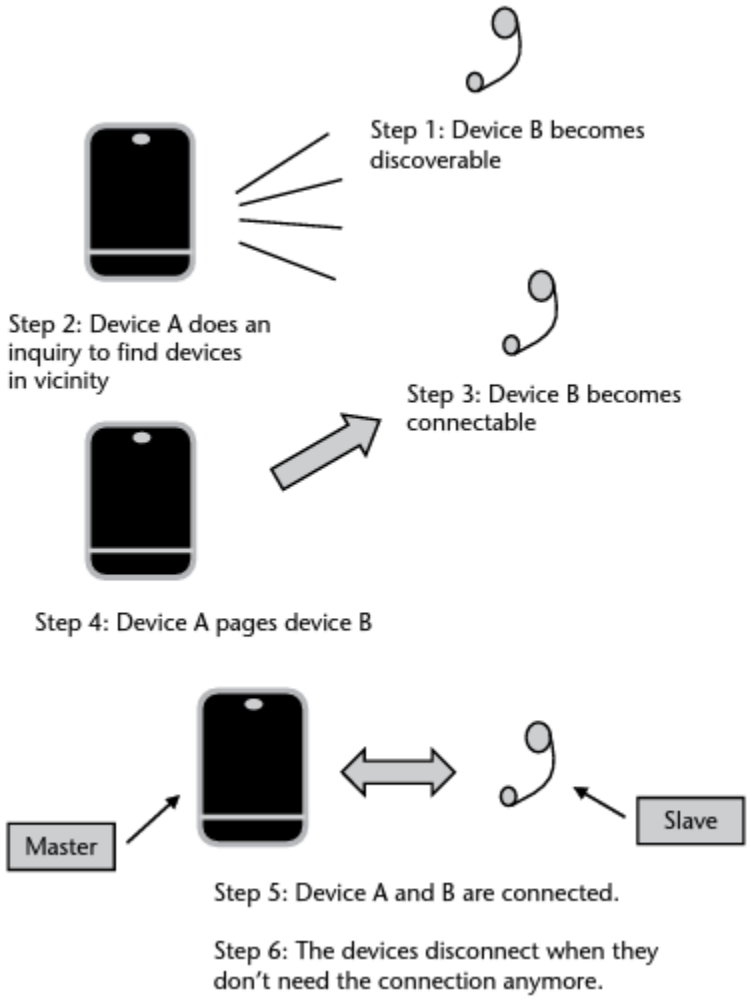

Figure 20. The Six Steps Involved With Bluetooth Pairing (Gupta 2013)

Operation Methodology of Analog-To-Digital Convertor Component

For any analog device to be able to communicate with digital devices, an analog-to-digital convertor (ADC) needs to be used. Temperature sensors, strain gages, light meters, and potentiometer are some of the many different type of analog devices. These sensors need to be connected to a microcontroller which is a digital device. Some

microcontroller have ADC built into their system. An ADC convert the analog signal into a series of binary numbers. The process of conversion begins by the ADC receiving a sample pulse signal and an analog signal. With each pulse of sampling signal, the analog signal is measured. The ADC will then send a grouping, or word, of binary numbers. This binary number is a proportional value of the measured analog voltage to the analog reference voltage. To illustrate this ADC process, the basic principal of a 4-bit ADC is shown in Figure 21. The quality of the resolution of the conversion depends on the number of bits the digital output signal is changed into. For high resolution of continuous monitoring of an analog signal, an ADC with a high bit value needs to be implemented (Scherz and Monk 2013).

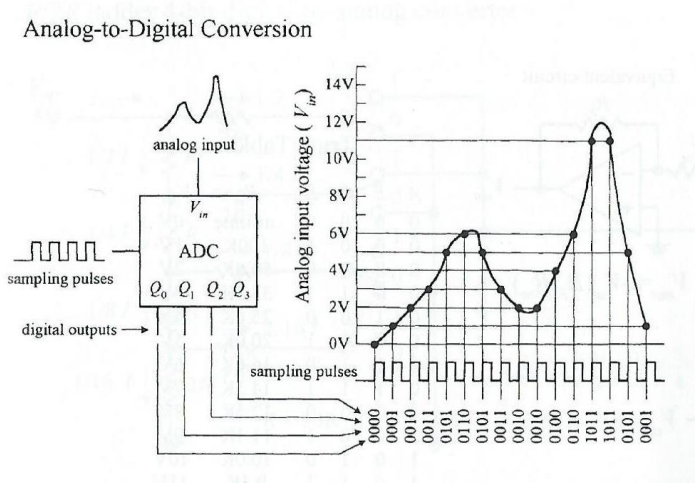

Figure 21. Basic Working Principal Behind a 4-bit Analog-to-Digital Conversion (Scherz and Monk 2013)

Operation Methodology of a Strain Gage Component

The amount of deformation a material experiences due to an applied force is called strain (ε) (N. Instruments, Measuring Strain 2016). The measurement of strain is the fractional amount change in length of an object's body due to a force that has been applied to the object as illustrated below in Figure 22. A strain gage is a commonly used device to measure strain by monitoring the changes in voltage caused by changes in resistance. The resistance of a strain gage varies in proportion to the amount of strain in the device (N. Instruments, NI AN078 1998).

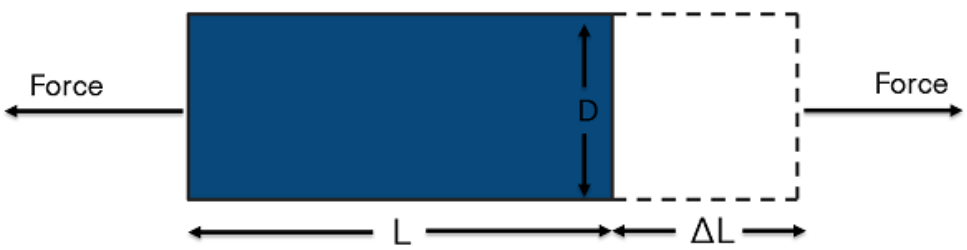

$$\varepsilon = \frac{\Delta L}{L}$$

Figure 22. Illustration of Ratio of How Strain is Calculated (N. Instruments, Measuring Strain 2016)

While there several ways to measure methods of measuring strain, a metallic strain gage is the most common strain sensor. A metallic stain gage consists of metallic foil that has a grid pattern cut into it. A few of these patterns are shown below in Figure 23. The way in which the strain interacts with this grid pattern is what causes the change in resistance through the strain gage. The directional pattern in which it is cut will relate to the direction and type of strain in which the sensor will measure. This metallic grid is

bonded onto a thin carrier which is attached directly to the object that will be measured. An overview of this composition of parts is shown farther down in Figure 24.

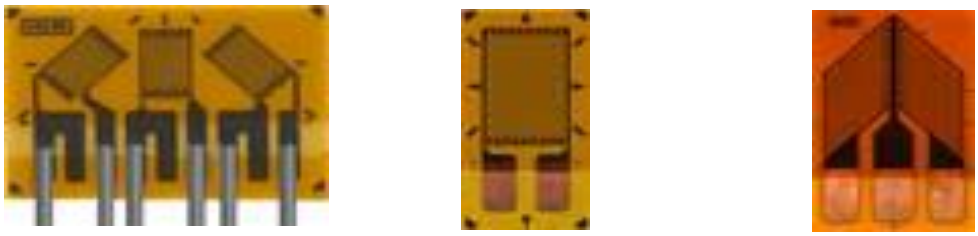

(a) Rectangular (b) Linear (c) Shear/Torque

Figure 23. Three Different Strain Gage Patterns for Different Type of Strain Measurements (Measurements 2017)

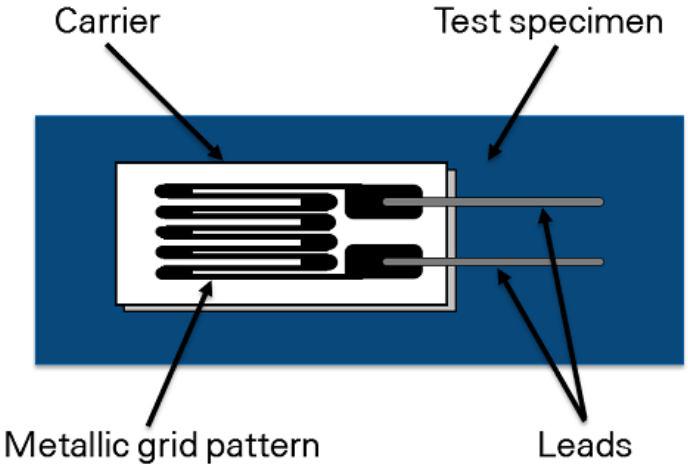

Figure 24. Basic Illustration of Different Element of a Metallic Strain Gage (N. Instruments, Measuring Strain 2016)

Strain gages rarely involve measures that are over a few mill-strain which also means the resistance change is very small. A strain gage with a gage factor of 0.1% electric resistance will only differ by 0.12 Ω in a 120 Ω gage (N. Instruments, Measuring Strain 2016). For this reason, strain gage reading are passed through some level of amplification.

To measure the change in resistance, the strain gage is incorporated into a Wheatstone bridge. A Wheatstone bridge is the electrical equivalence of two parallel voltage dividers that output is the measurement the middle node of the two dividers (N. Instruments, Measuring Strain 2016). There are three different Wheatstone bridge configuration for a strain gage sensor to be incorporated into. One is a Quarter-Bridge which is where one of the four resistor are replaced with a strain gage as shown below in Figure 25 (N. Instruments, NI AN078 1998). In this setup, any change of resistance in the strain gage will change the output voltage.

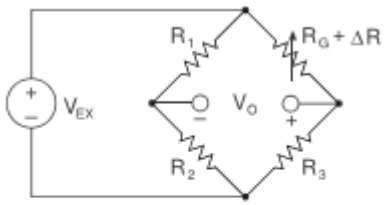

$$\frac{V_O}{V_{EX}} = -\frac{GF \bullet \varepsilon}{4}\left(\frac{1}{1 + GF \bullet \frac{\varepsilon}{2}}\right)$$

Figure 25. Diagram of a Quarter-Bridge Wheatstone Circuit (N. Instruments, NI AN078 1998)

The second Wheatstone bridge configuration is a Half-Bridge. By replacing the resistors that are on both sides of the positive voltage output with strain gauges, the sensitivity doubles so that the compression and tension force are measured. Figure 26 shows how the Half-Bridge circuit looks like and how the strain gage are positioned to get the read these two forces.

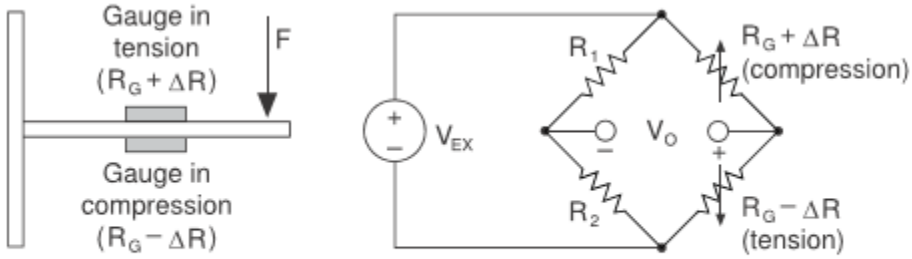

$$\frac{V_O}{V_{EX}} = -\frac{GF \bullet \varepsilon}{2}$$

Figure 26. Diagram of a Half-Bridge Wheatstone Circuit (N. Instruments, NI AN078 1998)

The third Wheatstone bridge configuration for strain gage placement is the Full-Bridge configuration. This increases the sensitivity of the reading of both the tension and compression forces directions. Figure 27 show the full Wheatstone bridge is setup.

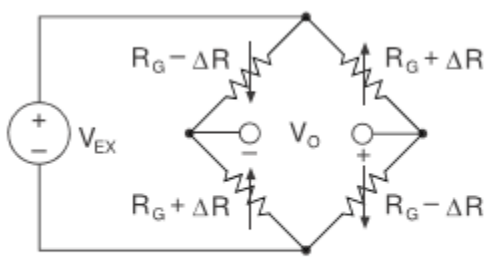

$$\frac{V_O}{V_{EX}} = -GF \bullet \varepsilon$$

Figure 27. Diagram of the Full-Bridge Wheatstone Circuit (N. Instruments, NI AN078 1998)

Reliable measurements from the strain gage requires proper selection and implementation for the design of the bridge configuration, signal conditioning, wires, and data acquisition components are needed. If the bridge is connected wrong, resistor values

are unbalanced, or lack of temperature consideration, the signal from the strain gage(s) will be skewed and have limited obtainable accuracy (N. Instruments, NI AN078 1998). Some other important factors with the signal conditioning that need consideration are the cleanliness of the input power, amplification of the measurement to increase the signals resolution, high-frequency noise filtering, offset nulling, and shut calibration (N. Instruments, Measuring Strain 2016).

Overall System Design

Figure 28. Overview of the Three Units (Recharging Base, Mounting Base, and Transmitter) That Make Up the Complete Wireless Strain Transmitter System

To handle the flexibility in placement of the of the strain gage transmitter module and in battery recharging methods, the Wireless Strain Transmitter system was divided to three units. A picture of these units are shown in Figure 28. They are the Recharging Base Unit which is in the upper left portion of the picture, the Transmitter Unit which is to the right of the picture with the cover off, and the Mounting Base unit. Within these

different units, the system was divided further into five layers. Table 6 is a simplified Bill of Material for the Wireless Strain Transmitter project. The complete Bill of Material has been added to the Appendix D.

Table 6. Simplified Bill of Material for the Wireless Strain Transmitter Project

Section Grouping	Part Name - Description	Part Quantity	Total Cost	Manufacturer
Microcontroller	Linear Voltage Regulator IC Positive Fixed Output, 3.3V, 800mA, SOT-223	1	$1.045	Texas Instruments
Microcontroller	16MHz Ceramic Resonator Built in Capacitor 15pF ±0.3% -20°C ~ 80°C Surface Mount	1	$0.5	Murata Electronics North America
Microcontroller	Atmegea 328P IC MCU 8BIT 32KB FLASH 32VQFN	1	$2.07	Texas Instruments
Battery Recharging	Lithium-Ion Battery Rechargeable (Secondary) 3.7V, 500mAh, Coin, 35.0mm, Wire leads	1	$22.23	Illinois Capacitor
Battery Recharging	4.7µH Shielded Inductor 1.2A 140 mOhm Max Nonstandard	1	$1.09	Sumida America Components Inc
Battery Recharging	IC CONTROLLR LI-ION 4.2V (SOT23-5)	1	$0.58	Microchip Technology
HX711	HX711, SOIC16, 24 bit ADC IC	1	$1.00	Avia Semiconductor
Bluetooth	ANTENNA CHIP 2.4GHZ	1	$0.93	Johanson Technology Inc.
Bluetooth	IC RF TxRx + MCU Bluetooth v4.0 2.4GHz 40-VFQFN Exposed Pad	1	$5.42	Texas Instruments
Inductive Transmitter	Wireless Charging Coils Tx coil 4.95uH 0.03 ohms 50x3mm	1	$7.62	TDK
Inductive Transmitter	Buck Switching Regulator IC Positive Adjustable 0.79V 1 Output 2A 10-WFDFN Exposed Pad	1	$6.93	Linear Technology
Inductive Receiver	1 Coil, 1 Layer 47µH Wireless Charging Coil Receiver 460 mOhm	1	$11.40	Wurth Electronics Inc.
Inductive Receiver	400mA Wireless Synchronous Buck Battery Charger, Lithium-Ion/Polymer, 3mmX3mmQFN16	1	$6.910	Linear Technology

Section Grouping	Part Name - Description	Part Quantity	Total Cost	Manufacturer
Stain Gage Connection	12 Position FFC, FPC Connector Contacts, Top 0.039" (1.00mm) Surface Mount, Right Angle	1	$.85	Amphenol FCI
Total	131 Different Items	265	$175.02	(blank)

Three layers are encase in the Transmitter module which would be able to connect to either the recharging base or mounting base. The layer that is located closest to the bottom of the transmitter module is for battery recharging. The battery recharging was divided out into a separate layer so that the method could be changed by simply switch the board layers between inductive and direct recharging. The middle layer within the transmitter unit is for system processing and communication. The last layer is for the placement of the exterior LED indicator lights.

To support the Lithium-Ion battery recharging, a recharging unit was needed. Within this unit is the system input power control layer. It is designed to support either the inductive or direct recharging method based on the placement of the transmitter module on the recharging base unit.

The remaining unit is the Mounting Unit. It houses the ADC layer would allow the ADC to be close to the strain gage connections and be connected to any transmitter unit. Figure 29 show the Transmitter and Mounting units connected together.

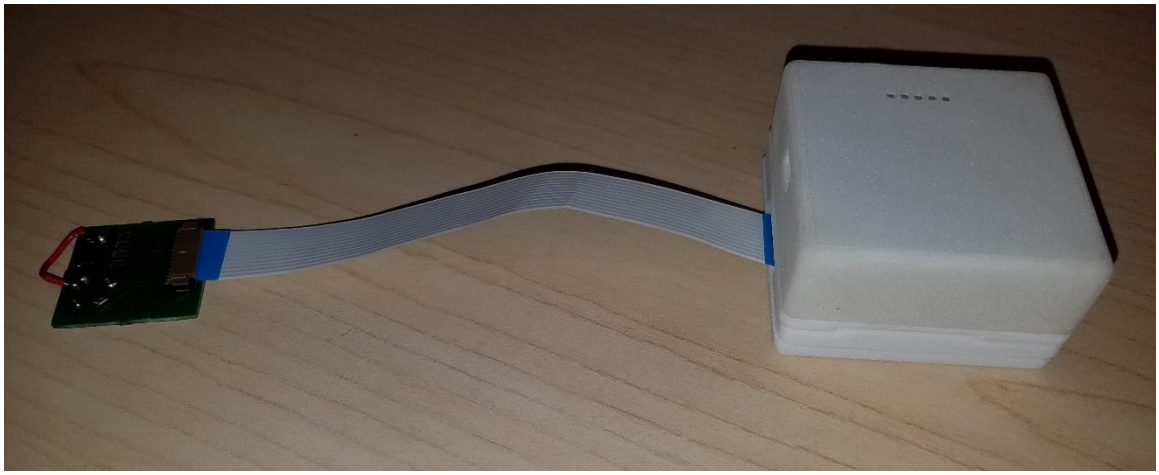

Figure 29. Transmitter Unit Connected on to the Mounting Base and Strain Gages Connector Piece

Wireless Transmitter Module

Inductive Receiver for Battery Recharging

The inductive battery recharging circuit design came from Linear Technology's data sheet and manufacturing application information for their LTC4120 Wireless Power Receiver and Battery Charger IC. The LTC4120 is a constant-current/constant-voltage wireless receiver and battery charger that is suitable for charging Lithium-Ion batteries (L. Technology, Inductive Battery Recharging 2016).

After studying the data sheet and manufacturing application information, a schematic was created. This particular schematic for receiving inductive battery recharging can be seen on the fourth page of the schematic for whole system in the Appendix C. In addition to the components that supports the LTC4120 IC as shown in Figure 30, there were additional components added to provide interconnecting layer connector and power control switch to the inductive battery recharging layer. These connectors are to transfer power and information between the layers and units.

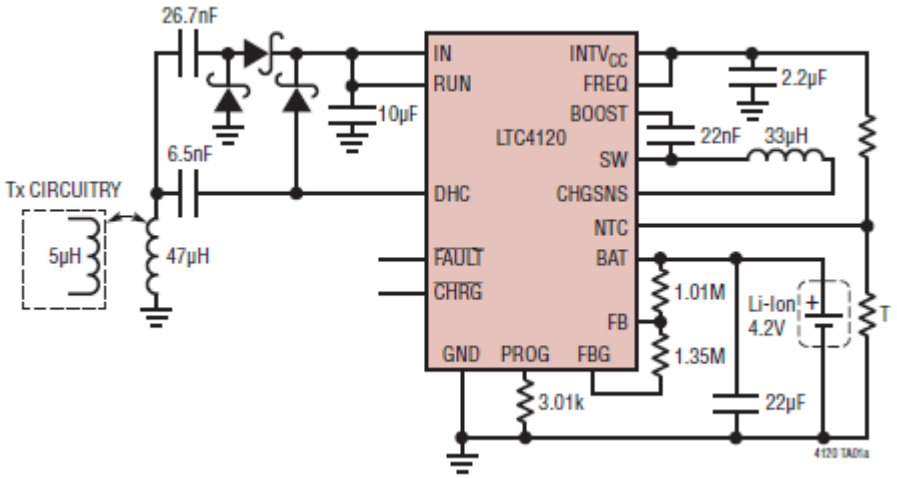

Figure 30. Linear Technology's Simplified Application Schematic for the LTC4120 (L. Technology, Inductive Battery Recharging 2016)

Figure 31 and Figure 32 shown the final populated prototype PCB boards and how most of the PCB board for this layer is occupied by components. Figure 31 shows how the receiver coil and compression pin connector on the bottom face of the inductive receiver layer. The compression pins connector are to complete the connection between the Mounting Base or the Recharging Base unit when the Transmitter Unit is slide into position.

Figure 31. Bottom Face of the Assembled PCB for the Receiving Inductive Battery Recharging

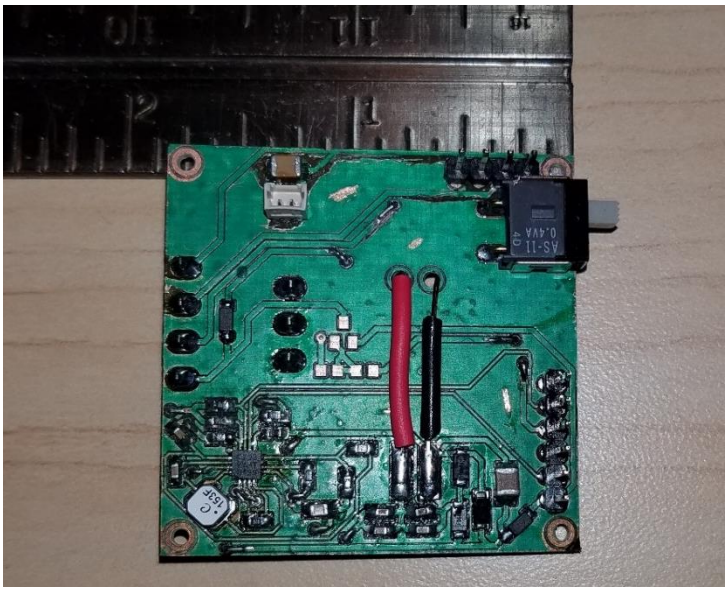

Figure 32. Top Face of the Assembled PCB for the Receiving Inductive Battery Recharging

Direct Power Battery Recharging

The second option for battery recharging is managed by Microchip Technology's MCP7331 controller IC. The MCP73831 device is a highly advanced linear charge management controller whose small physical size and low number of required external components make ideally suited for portable applications as evident in the schematic shown in Figure 33. The MCP73831 employ a constant-current/constant voltage charge algorithm with selectable preconditioning and charge termination (M. Technology 2014).

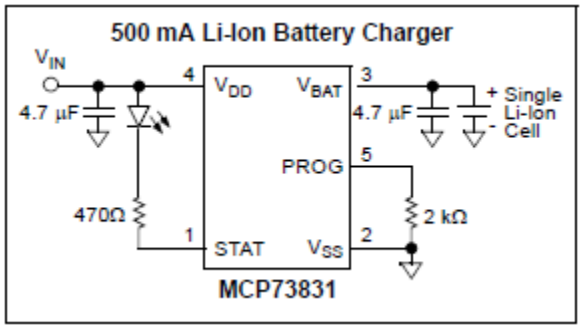

Figure 33. Typical Application Schematic for the MCP73831 Found Within the Datasheets (M. Technology 2014)

Direct power battery recharging was primarily put on a separate layer of because the separate develop of the two Lithium-Ion battery recharging options. Similar to the inductive layer, additional components added to provide interconnecting layer connection and power control. However, the switch for the direct power recharging was changed to a double pole/double throw (DPDT) to alternate how power flows in and out of this layer. Without this switch, it was possible to have circle charging and discharging due to the cross use of pin number one on the compression pin connector. The resulting, populated PCB board for this layer is shown in Figure 34 and Figure 35. The schematic that was

created for direct power recharging can be reviewed on the seventh page of the schematic for whole system which is in Appendix C.

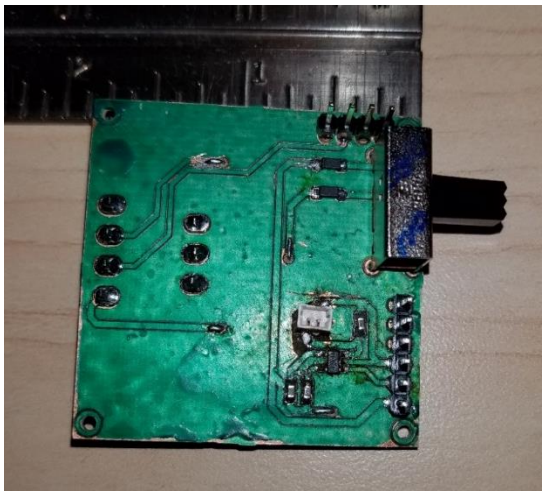

Figure 34. Top Face of the Assembled Direct Power Battery Recharging

Figure 35. Bottom Face of the Assembled Direct Power Battery Recharging

Bluetooth Communication

For the Bluetooth communication, Texas Instruments' CC2540 IC (integrated circuit) was implemented. This chip has lot of development support documentation and application examples available from Texas Instruments to aid in the development

process. It is also the same chip that is used in the different Bluno Bluetooth breakout modules. After comparison of the schematics from Texas Instruments and Bluno Micro found the two to be nearly identical, this meant the firmware coding from the Bluno breakout modules could be used aid in the startup of this chip. The Bluno Micro is the only module in the Bluno series that is without a built-in microcontroller and power regulation.

Outside the Bluetooth chip, the antenna and impedance matching for RF are two design elements that are important to get the Bluetooth communication to work. Within the many Application Note that support the CC2540, there are two that aided in implementing a successful design for this project. One is Application Note AN107 which is on how to simplify and reduce the possible of error in design in impedance matching. It is about Murata Balun filtering component that was specially designed for use with many of Texas Instruments devices to replace nine discrete components (Kervel 2011). Figure 36 and Figure 37 shown how a balun component simplifies the impedance matching.

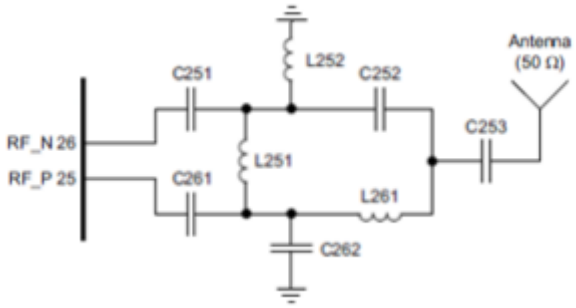

Figure 36. Traditional Reference Design with the Nine Discrete Components for Impedance Matching (Kervel 2011)

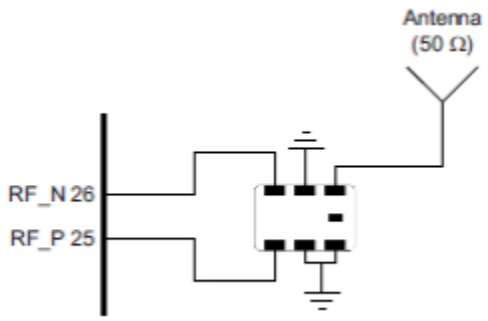

Figure 37. Modified Reference Design after Implementation of Murata Balum (Kervel 2011)

The antenna design was guided by Application Note AN058 from Texas Instruments. Among the many PCB antenna design and chip antenna that are in this application document, there is the Johanson Technologies ceramic chip antenna.

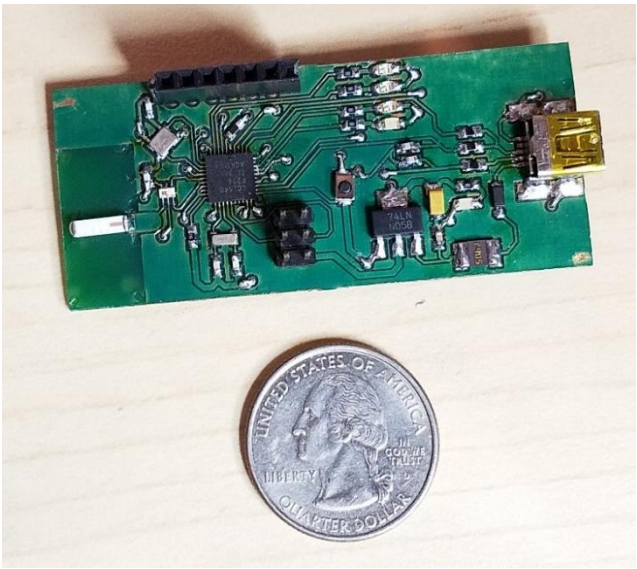

Figure 38. Prototype Breakout Design Testing of the Bluetooth Communication

To test the Bluetooth design before fully implementation into the transmitter module's design, it was built and tested separately as shown in Figure 38. The schematic for the Bluetooth design can be reviewed on the third page of the schematic for whole

system which is in Appendix C. After testing this Bluetooth design, it was fully incorporated into the system processing and communication layer of the transmitter module. The Bluetooth design was on the top face of this PCB layer, as shown in Figure 39, to keep the antenna clear of the many interfering obstacles to the antenna's transmitting performance.

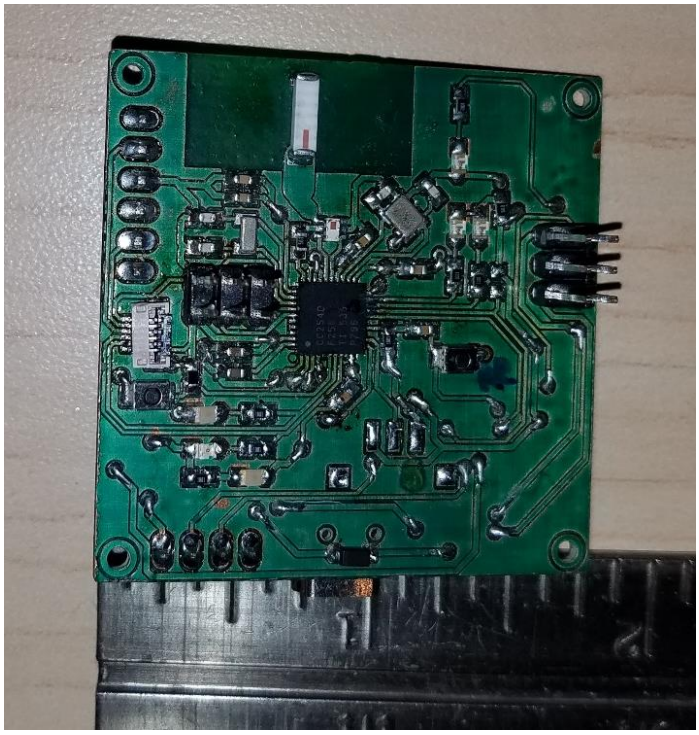

Figure 39. Bluetooth Face of the Assembled PCB for the Microcontroller and Bluetooth

Microcontroller

The overall electrical design revolves around the microcontroller. The selection of the microcontroller will result in establish the systems power requirement and any possible additional support that will be needed to meet the project's criteria. At first, the microcontroller selection for this project focused on five key specifications. There were a

core size of 16-Bits or higher, operation speed of 16 MHz or faster, integrated ADC that has a 24-bit resolution, supported I^2C (Inter-Integrated Circuit) and SPI (Serial Peripheral Interface) communication, and lastly was familiarity with the company's controller. Other key specifications that are normally related to microcontroller selection process, like the number of I/O (Input/Output) pins, peripheral features, program memory size, and ram speed, were noted but accounted for in the initial selection process. After review with client, the key factors behind the microcontroller was familiar and previous success with the microcontroller to eliminate the difficulty of starting up an unfamiliar microcontroller in conjunction with the development of the Bluetooth communication. This resulted in the selection of using an Atmega 328P microcontroller. This meant that an external ADC would need to be implemented to obtain the 24 bit resolution from the strain gage readings and an operating voltage of 3.3 volts. Figure 40 shows the populated bottom face of the system processing and communication layer of the transmitter module. On this side of the PCB board, there is the power regulator and inter-board connectors along with the microcontroller. The schematic for the microcontroller design can be reviewed on the first page of the schematic for whole system which is in Appendix C.

Figure 40. Microcontroller Face of the Assembled PCB for the Microcontroller and Bluetooth Layer

LED Indicators

To provide feedback about the systems status without connecting and congesting the Bluetooth communication signal, exterior indicators are needed. Surface mounted LEDs are small lights that can be used as exterior indicators and does not take up a lots of room. As a flexible and easily way to place these LED indicates close to the top of the transmitter module as shown in Figure 41, a small PCB board with LEDs on the top side and the remaining circuitry resistors and connector for the jumper cable on the bottom side. The schematic for the LED exterior indicators can be reviewed on the sixth page of the schematic for whole system which is in Appendix C.

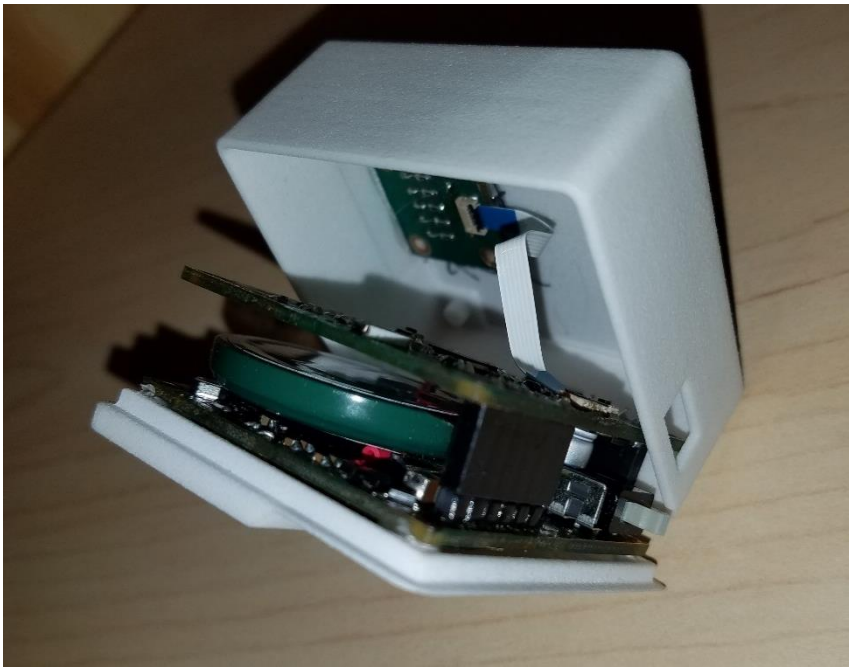

Figure 41. LED Indicator Lights Mounted Inside the Transmitter Top Case Piece

Figure 42 shows the small PCB board with five LEDs on the top side for different important overall system status. One of the LED is used to indicate the systems power status. Another two LEDs are to indicate recharging status of the battery being done charging or error with the battery recharging. The remaining two LEDs are to relay the status related to the Bluetooth connection process. One of the Bluetooth LEDs is indicate if the Bluetooth is attempting to establish a connection. The second Bluetooth LED is to indicate when a pairing of Bluetooth devices has be completed.

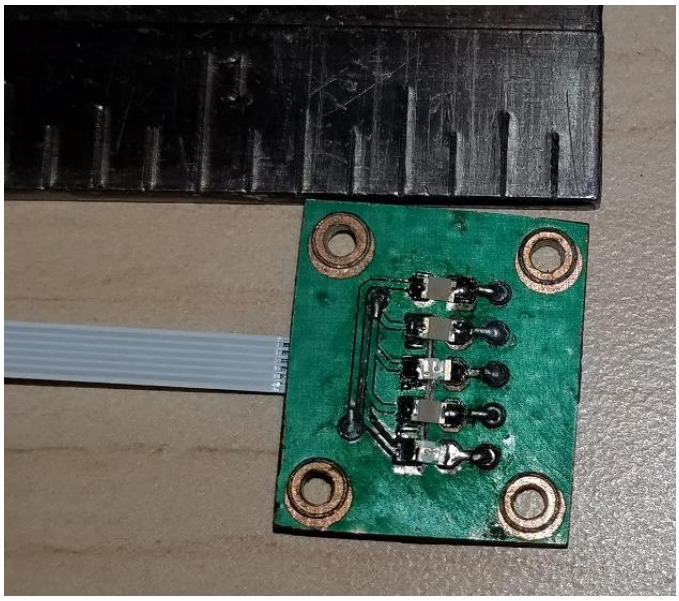

Figure 42. Top Assembled Face of the Exterior LED Indicators

Mounting Module

Figure 43. The Assembled Mounting Base in the 3D Printed Case

The mounting module purpose is to provide a way to physical means of attachment for the transmitter module and way to connect to strain gages. Figure 43 shows the assembled mounting module. In this picture, one can see to top configuration

of stops and dovetails to position the transmitter module. Within the middle of the dovetail there is the mating compression connector plate which is part of the ADC layer of the system. Figure 44 show how the transmitter module fits atop over the mounting base.

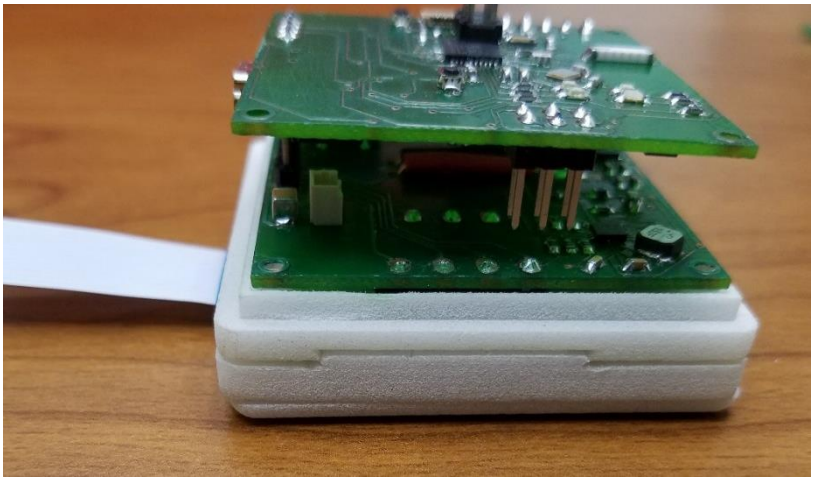

Figure 44. Close Up of the Mounting Base Fitted with the Transmitter Unit in an Inductive Recharging Configuration with the Transmitter Top Case Piece Removed

Analog-To-Digital Convertor

The HX711 analog-to-digital chip was selected to handle the external ADC requirement for the system. Besides have a conversion resolution of 24-bit, the HX711 overall application design is to interface directly with a bridge sensor. It has a two channel input with programmable gain amplification. There is also an internal power supply regulator for the analog sensors and ADC (Semiconductor n.d.).

The top side of the PCB board only has the mating female compression connector which was shown earlier in Figure 43. The bottom side of the PCB board shown in Figure 45 has the HX711 IC along with the supporting discrete components and

connection point to the strain gages. The schematic for the HX711 design can be reviewed on the second page of the schematic for whole system which is in the Appendix C.

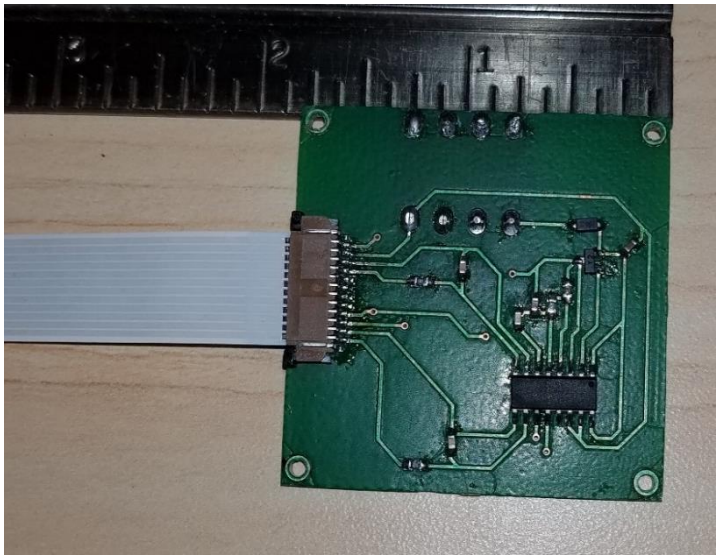

Figure 45. Bottom Face of the Assembled Mounting Base PCB with the HX711

Strain Gage Connection

To provide a simple way of connection to strain gages for testing to the system, a strain gage connector PBC board was made (Figure 46). This allowed for a Quarter-Wheatstone bridge setup of a strain gage and/or connection point for any other strain gage setup.

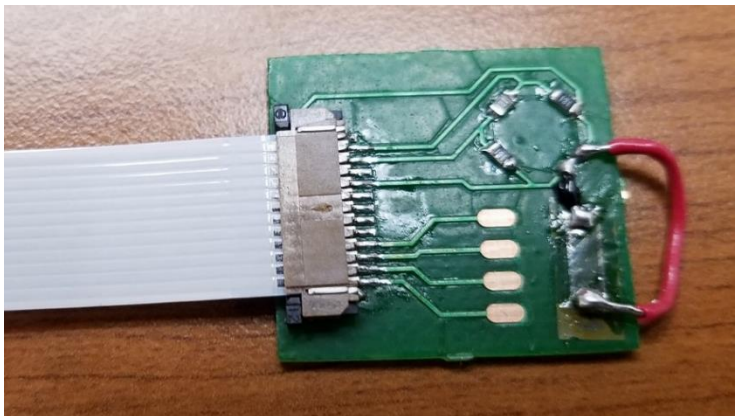

Figure 46. Strain Gage Interface PCB Board Where a Strain Gage can be Connected Up to the System

Recharging Base

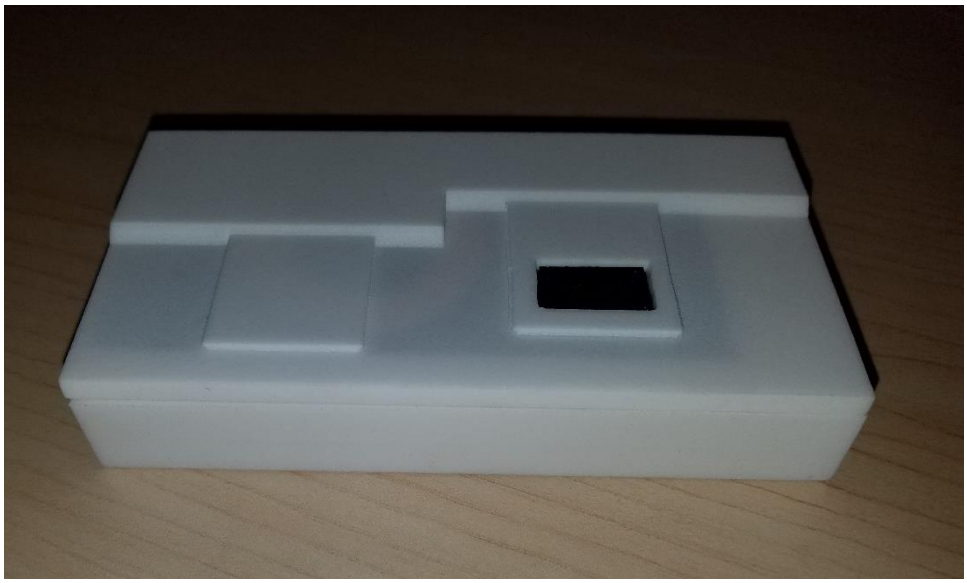

Figure 47. The Assembled Recharging Base Unit for either Inductive Recharging or Direct Recharging

The recharging base was created to complete to support primarily the inductive recharging method. The secondary reason was to begin a docking station design for the direct battery recharging method. This prototyped recharging station for a single

transmitter module is shown in Figure 47. Fitted inside the recharging base unit is the recharging PCB layer. The top face of this board, shown in Figure 48, has the transmitting inductive coil and the mating female compression connector.

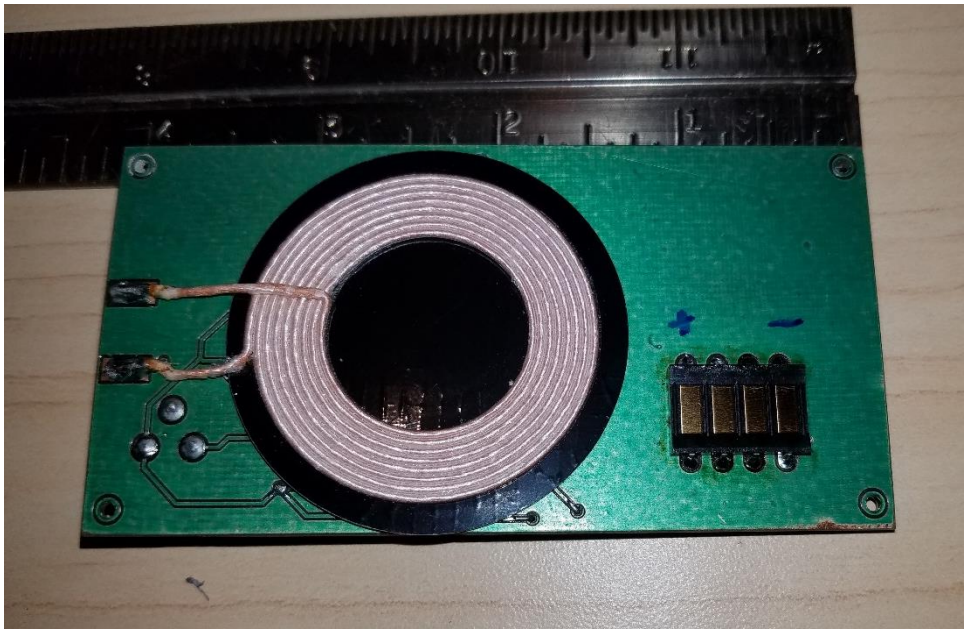

Figure 48. Top Face of the Assembled PCB for the Charging Base

The bottom face of the recharging PCB board has everything else need to take a DC power source and send it out to the appropriate recharging method. When you look at this recharging PCB board bottom side shown in Figure 50, it appears to be divided into two sections. Left side of PCB board is the inductive transmitting circuitry. This is "divided" by the trace that runs down the middle to the power indicator LED. The right side is the five volt power regulator circuity to directly power the direct power recharging. The design for the inductive transmitting circuitry came the supporting and demo board DC2181A schematic (Figure 49) that Linear Technology has for their LT4120 wireless battery recharging. The schematic for the inductive transmitting design

can be reviewed on the fifth page of the schematic for whole system which is in the Appendix C.

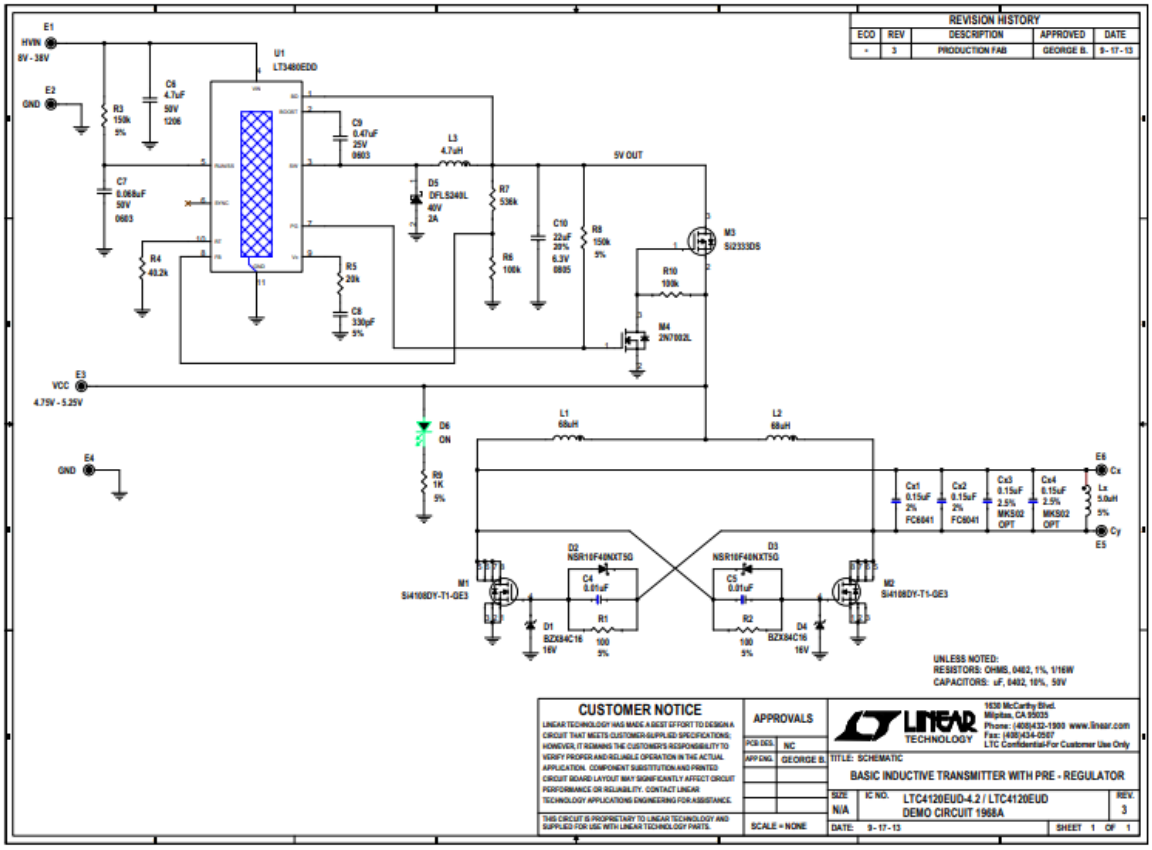

Figure 49. Transmitter Demo Schematic from Linear Technology (L. Technology, Inductive Demo Manual 2013)

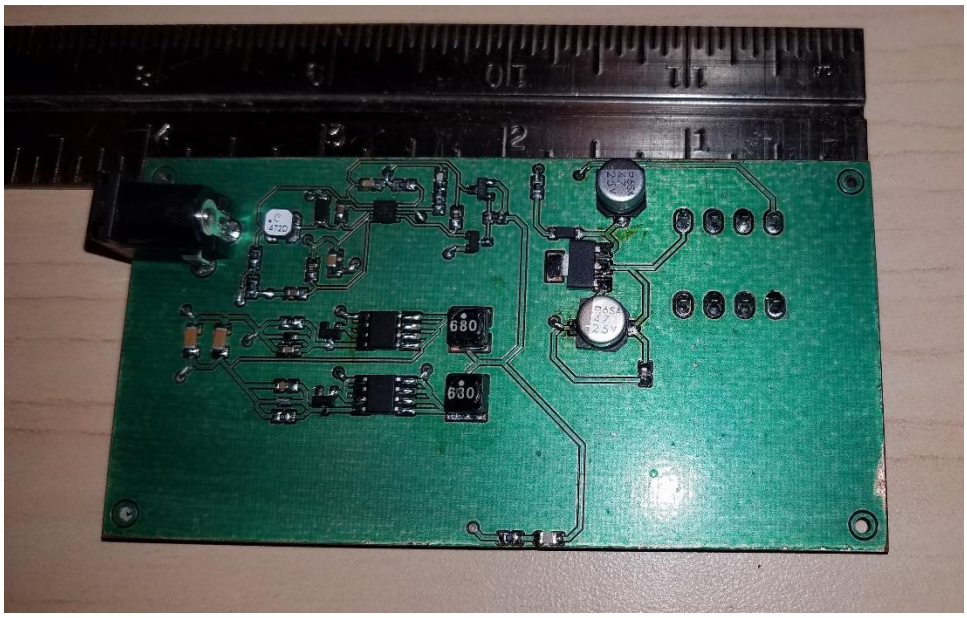

Figure 50. Bottom Face of the Assembled PCB for the Charging Base

Design Validation Testing

To validate that this design is fully functional and meeting the project's criteria, validation testing was broken into two main types of testing. The first type of validation testing was voltage measurements at different points within the system. The second type of validation testing involved the wireless communication and system's performance. Outside of these two main validation testing types, there were several small test which was more done to check how the startup and coding was progressing. Some of these minor tests including flashing an LED after starting up the microcontroller, checking continuity at connectors, and reading changing sensed at the strain gage to check the HX711 ADC functionality.

For the measurement validation testing, pivotal points in the system had the voltage check with a multimeter. This was done to verify that the system was receiving

and managing the different voltage in the expected manor. Table 7 list the points of interest that are located throughout the system and the expected resulting measurements. Figure 51 and Figure 52 are pictures of two of these points being measured. Figure 51 shows the measuring of the inductive received input power. Figure 52 shows the resulting measurement of the battery output.

Table 7. Table Listing the Critical Points the Voltage Level was Validated and the Expected Resulting Voltage Measurement for the Wireless Strain Transmitter Project

Point of Measurement (location)	Expected DC Voltage Measurement
DC Power Jack	Inputed Power Level
Input power at voltage regulator at Recharging Base (pin #3 @ U3)	≈ Inputed Power Level
Output power at voltage regulator at Recharging Base (pin #2 @ U3)	5 volts
Received Inductive power (pin #1 @ J11)	≈ Inputed Power Level
Battery Recharging via Inductive Power (pin #2 @ J12)	4.2 volts
Received Direct Power (pin #1 @ J15)	5 volts
Battery Recharging via Direct Power (pin #2 @ J16)	4.2 volts
Battery Output Voltage (pin #2 @ J12 & J16)	3.7 volts
USB input power (pin #1 @ J4 or pin #2 @D1)	5 volts
Output power at system's voltage regulator (pin #2 or tab @ U4)	3.3 volts

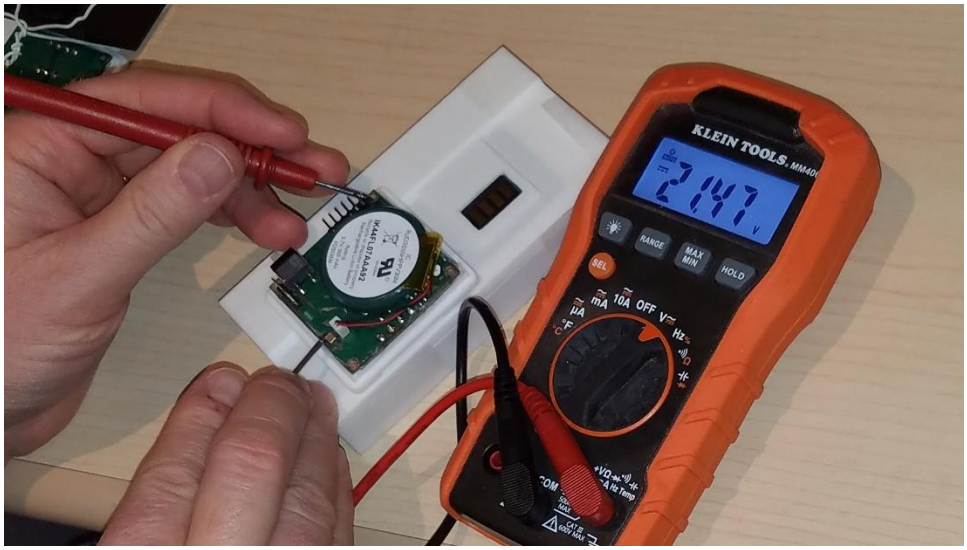

Figure 51. Validation Testing of the Incoming Power for Inductive Battery Recharging

Figure 52. Validation Testing of the Battery Power for Inductive Battery Recharging

As previously stated, the second type of validation testing involved the wireless communication and system's performance. This was completed by pairing the system with a smartphone. After pairing the two devices, the message received on the smartphone provide wireless feedback about reading the system had collected or received

instruction which potentially could change the flow through the program. Since most communication with the client involved teleconferences, a video of the working prototype was filmed to easily share the results of the project. It was from this video that Figure 53 through Figure 57 were clipped from.

Figure 53. Clipped Image from the Demo Video of the Power Indicator LED Being On After System Was Switched On

The system's performance and communication testing began by switching on the power and observing the extrior power indicator as shown in Figure 53. With the power on, a Bluetooth line of communication between a smartphone and the system was established as indicated by the pairing LED being on in Figure 54. Additional, validation of the two devices being paired together is change in displayed meassage on the smartphone after the letter 'Y' was sent out from the smartphone as shown in Figure 55. The message changes from request of acknowledgement of pairing which was a way to pause the coding to allow the Bluetooth pairing to occur, to instruction of what code to send.

Figure 54. Clipped Image from the Demo Video of the Pairing Indicator LED the Connection Was Established With a Smartphone

After the system has been made aware of the established Bluetooth connection, there is a calibration process the system going through. Once the user has completed the two steps for calibrating the system, weights or forces can be applied to the strain gage setup and the system will transmit the amount of force sensed. Figure 56 show a known weight of 1003 grams being applied to the strain gage setup used in this test and Figure 57 shows the system response to the load. While the load reading is above the know weight, it is well within the ten percent margin (902 to 1103 grams). This validation testing also include change the system to strain reading to dual, only channel ‘B’, and back to only channel ‘A.’

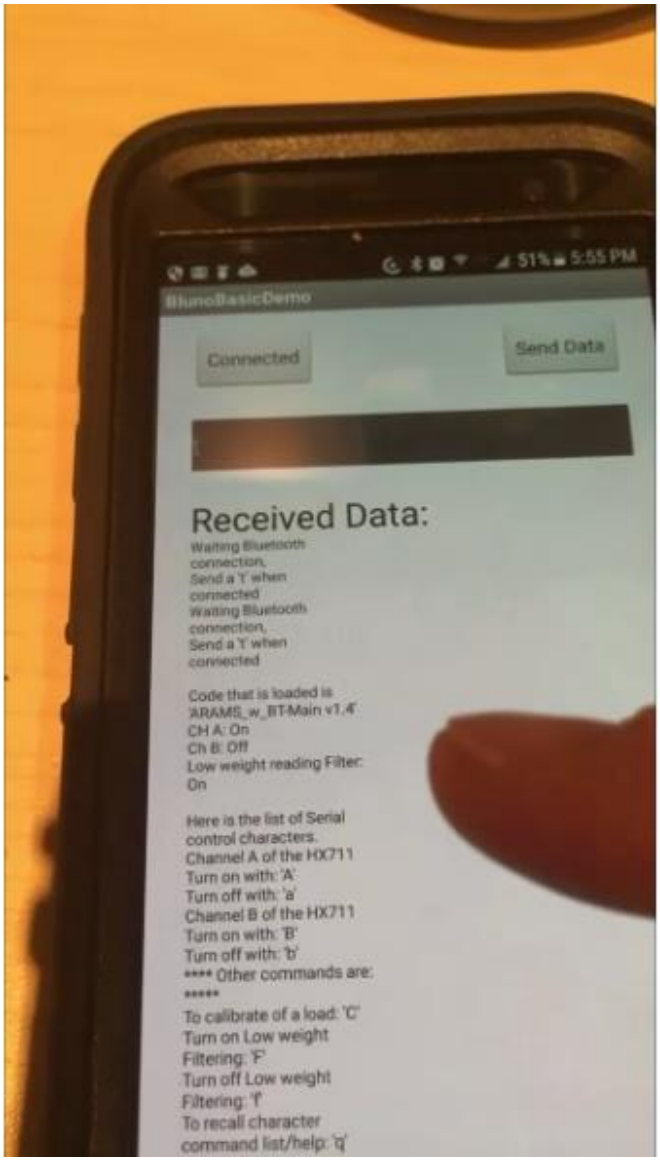

Figure 55. Clipped Image from the Demo Video of the Initial Response Sent From the Transmitter to the Smartphone

Figure 56. Clipped Image from the Demo Video of a Known Weight of 1003 Grams Being Applied to Full-Bridge Strain Gage Setup on an Aluminum Rod

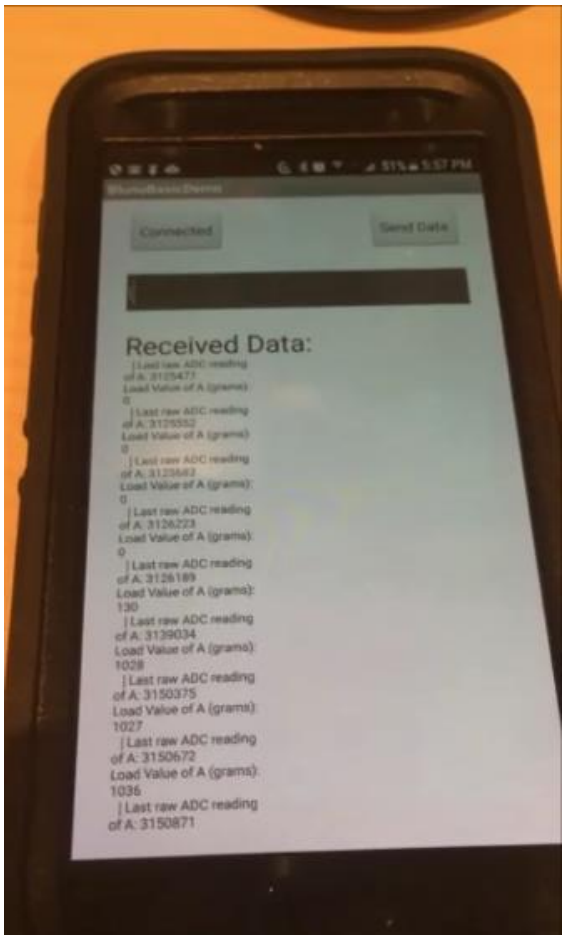

Figure 57. Clipped Image from the Demo Video of the Resulting Transmitted Strain Reading of the 1003 Gram Load to the Smartphone

CHAPTER 4

FLEXABLE SENSOR MODULES

Motivation

With a wearable sensor, the comfort of the device when worn is an important aspect in the wearable device's design. Biometric wearable sensors are becoming a highly research area. For that reason, there appeared a Department of Defence need to examine sensor circuitry that are built on flexible PCB boards as a means of providing comfort to the end user of a wearable biometric device. By having the wearable device's circuit on a flexible broad, a wearer will experience a significant level of comfort compared to a nonconforming rigid device. For that reason, four point-of-departure biometric devices that are on flexible PCB board were developed as proof of concept and feasibility. The four point-of-departure biometric devices that were selected to develop on the flexible PCB boards were a pulse-oximeter device, heart rate monitor device, air quality devise, and 9 degree of freedom Inertial Measurement Unit (IMU).

Design

The design for three of biometric device were taken from open source schematic repository to expedite the process of developing these point-of-departure biometric devices. The schematic for the pulse-oximeter device was based on the design presented in chapter two. The heart rate monitor device is from Sparkfun's breakout board number SEN-12650 which can measure the electric actives of the heart to chart Electrocardiogram (ECG). The air quality device is another Sparkfun breakout board (number CCS811) which can be used as a gas sensor that senses a wide range of Total

Volatile Organic Compounds which can be used to monitor a person's breathing. The last device, the 9 degree of freedom device, is the multipurpose Inertial Measure Unit from Sparkfun (number SEN-14001). This last device can be programmed to monitor motion or used as a pedometer with Lithium-Ion battery charger, micro-SD card socket and microcontroller.

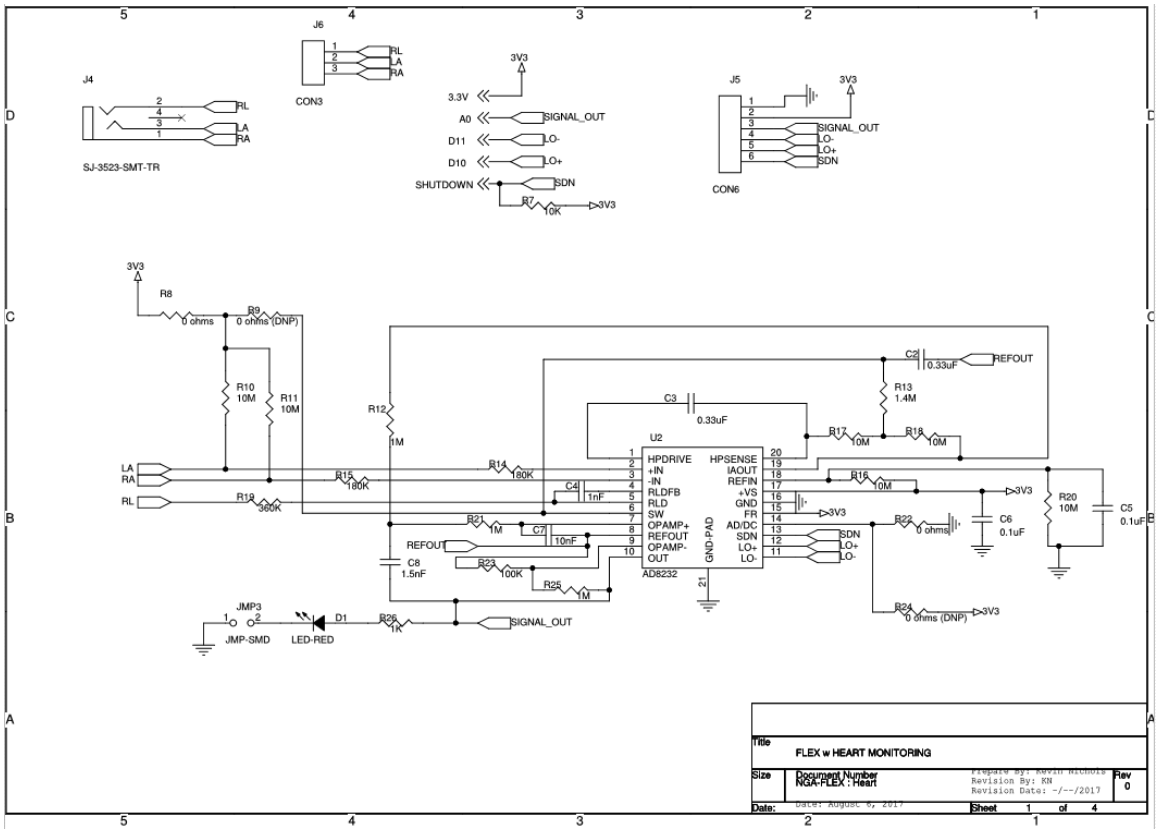

Figure 58. Schematic Created for Heart Monitoring Flex Breakout Device

For each of these device, a schematic was created separately like the one for the Heart Monitoring device shown in Figure 58. The schematic for all four devices have been included in the Appendix F. After the completion of the schematics, a Bill-of-Material for this project was created. Below in Table 8 is a condensed version of the full Bill-of-Material which has been included in the Appendix G. As a way to save on the

PCB board fabrication cost, all four designs were combined together on a single flexible board which could then be later be cut into separate devices after the board has been made. Figure 59 shows this layout with the heart monitor device in the upper left corner. From here, moving clockwise around the board layout, is the nine degree of freedom device, pulse-oximeter, and ends at the air quality device.

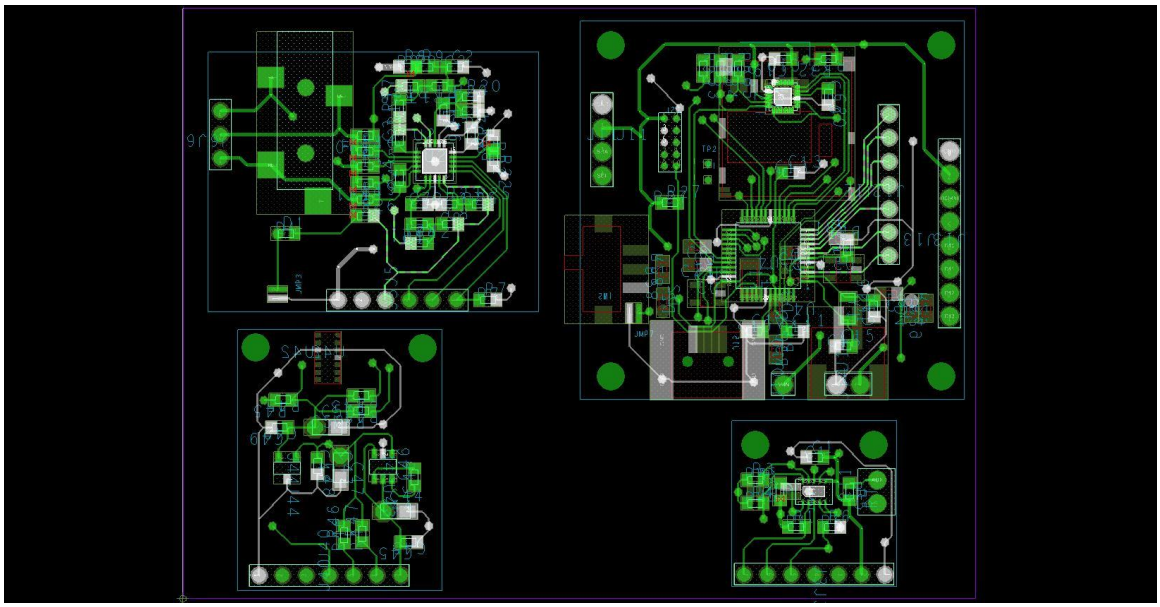

Figure 59. The Top Layer of the PCB Layout for the Flexible Sensors That Was Created In Cadence's Allegro

Table 8. Simplified Bill-of-Material for the Flex Sensor Modules Project

Section Grouping	Part Name - Description	Part Quantity	Total Cost	Manufacturer
Air Quality	Air Quality Sensor I²C	1	$12.42	ams
Air Quality	NTC THERMISTOR 10K OHM 3% BEAD	1	$0.90	Vishay BC Components
Heart Monitor	AD8232 IC, ECG Front End IC Heart Rate Monitoring, 20-LFCSP-WQ (4x4)	1	$3.96	Analog Devices Inc.
Heart Monitor	SENSOR CABLE - ELECTRODE PADS	1	$5.00	SparkFun Electronics
Heart Monitor	BIOMEDICAL SENSOR PAD	1	$7.95	SparkFun Electronics
Heart Monitor	CONN JACK, 3.50mm (0.141", 1/8", Mini Plug) - Headphone Phone Jack Stereo Connector Solder, SMD, R/A	1	$1.02	CUI Inc.
Pulse-Oximeter	IC SENSOR OXIMETER/HEARTRATE	1	$7.03	Maxim Integrated
Pulse-Oximeter	Charge Pump Switching Regulator IC Positive Fixed 3.3V 30mA SOT-23-6	1	$1.28	Texas Instruments
9 DoF-Razor IMU	Accelerometer, Gyroscope, Magnetometer, 3 Axis Sensor I²C, SPI Output, 24QFN	1	$9.32	TDK InvenSense
9 DoF-Razor IMU	ARM® Cortex®-M0+ SAM D21G Microcontroller IC 32-Bit 48MHz 256KB (256K x 8) FLASH 48-TQFP (7x7)	1	$3.22	Microchip Technology
9 DoF-Razor IMU	IC CONTROLLR LI-ION 4.2V (SOT23-5)	1	$0.58	Microchip Technology
9 DoF-Razor IMU	8 Position Card Connector microSD™ Surface Mount, Right Angle Gold-Palladium	1	$4.28	TE Connectivity AMP Connectors
9 DoF-Razor IMU	USB - mini B USB 2.0 OTG Receptacle Connector 5 Position Surface Mount, Right Angle	1	$1.03	Molex, LLC
Total	60 Different Items	91	$69.40	(blank)

The Gerber files for the combined flex sensors PCB board layout was sent out to a PCB board manufacture to be made. The resulting flexible PCB board is shown in Figure 60. From here the different sensor modules were separated and populated.

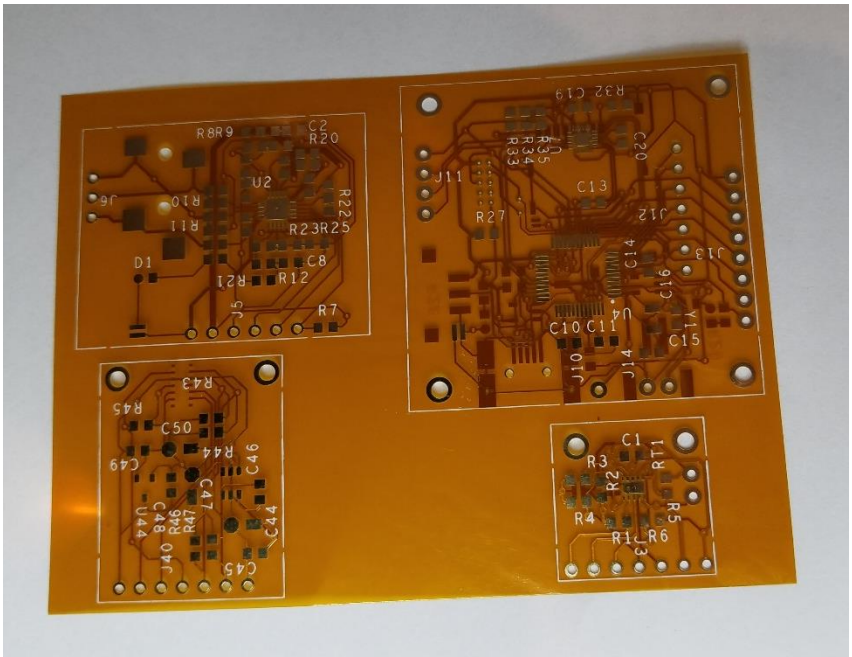

Figure 60. The Flexible PCB Board with All Four Sensor On One Board Layout

The assembled pulse-oximeter device is shown in Figure 61. In this picture, it is clear to see how small this test device was initial made. One design change to this layout is the pulse oximeter IC sensor is on one side by its self to allow it to be placed next to the skin with the other component exposed to be touched.

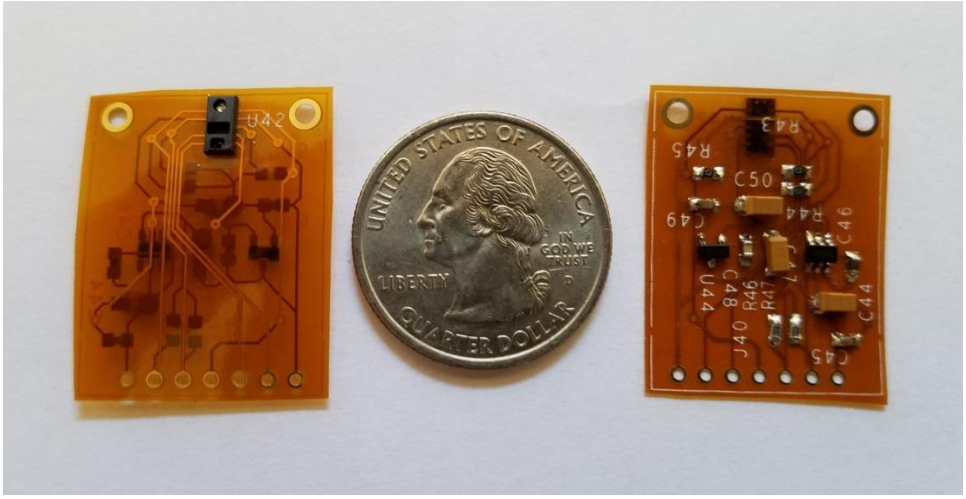

Figure 61. Top and Bottom Side of the Pulse-Oximeter Device after Being Populated With Its Components

The assembled heart rate monitor device is shown in Figure 62. In this picture you can see that if the headphone stereo phone jack was removed, the biometric sensor device could be made even smaller.

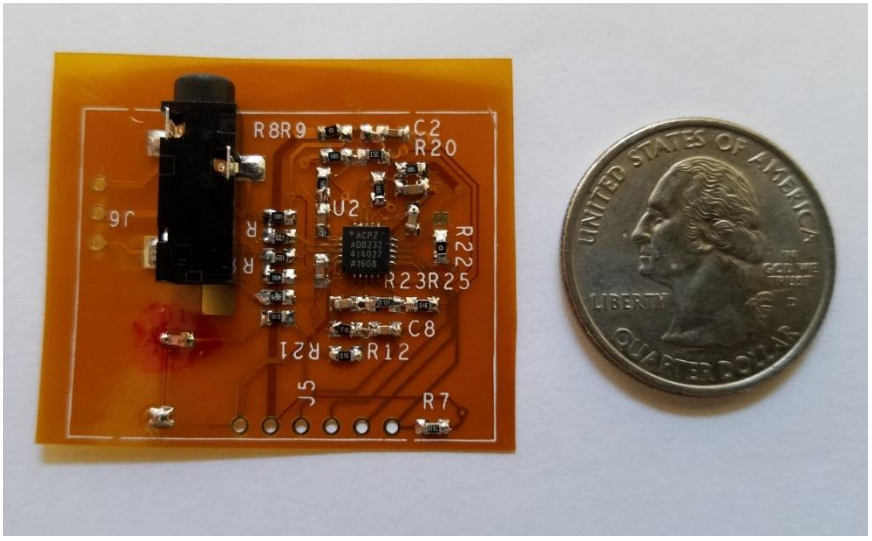

Figure 62. Top Face of the Heart Rate Monitor Sensor after Being Populated With Its Components

The assembled air quality devise is shown in Figure 63.

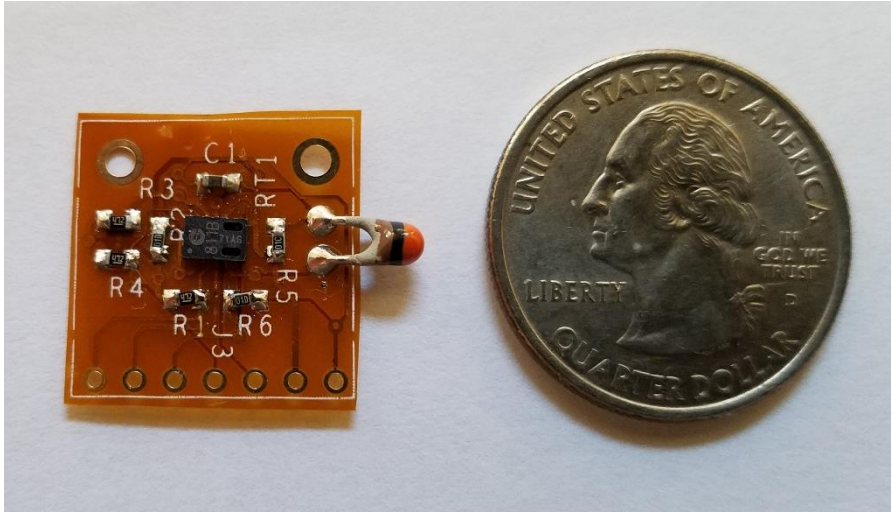

Figure 63. Top Face of the Air Quality Sensor after Being Populated With Its Components

The assembled nine degree-of-freedom devise is shown in Figure 64. During the assembly of this sensor module, it became even more obvious that assembling a flexible PCB boards present some unique challenges. One such challenge is that as more small components are mounted, it becomes increasingly more difficult to hand solder larger components. One also needs to take care in how large components are mounted to the PCB broad is need to avoid unnecessary curling of the board. With these flexible PCB boards being so thin, appropriate measures were needed to avoid losing solder connection on one side while soldering on the other.

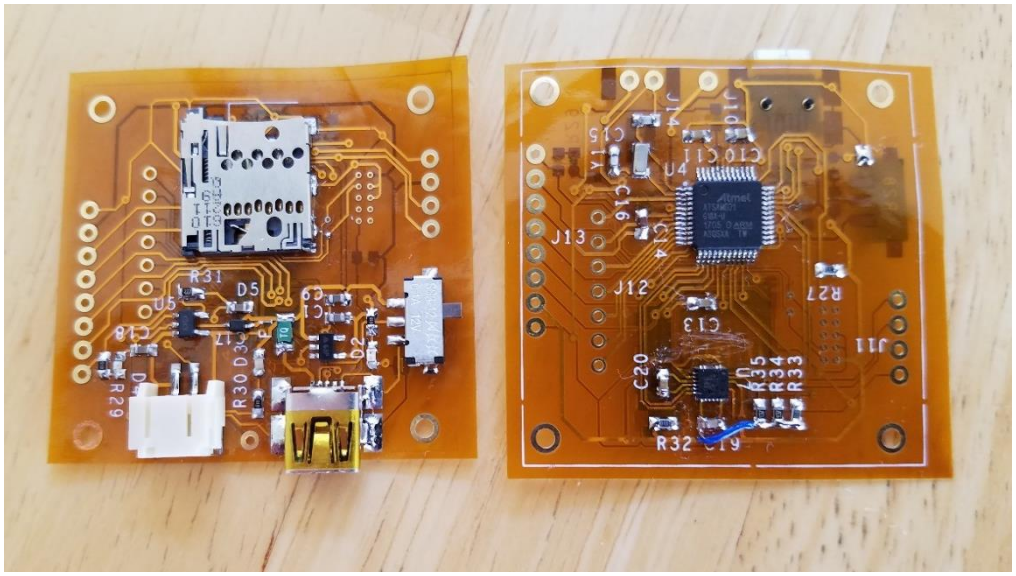

Figure 64. Top and Bottom Side of the 9-Degrees-Of-Freedom Module after Being Populated With Its Components

Design Validation Testing

Validation testing for the pulse oximeter was involved running the code through the device and checking the resulting output. Figure 65 show the serial out reading off the pulse oximeter device. The device does get good readings if the finger does not move around.

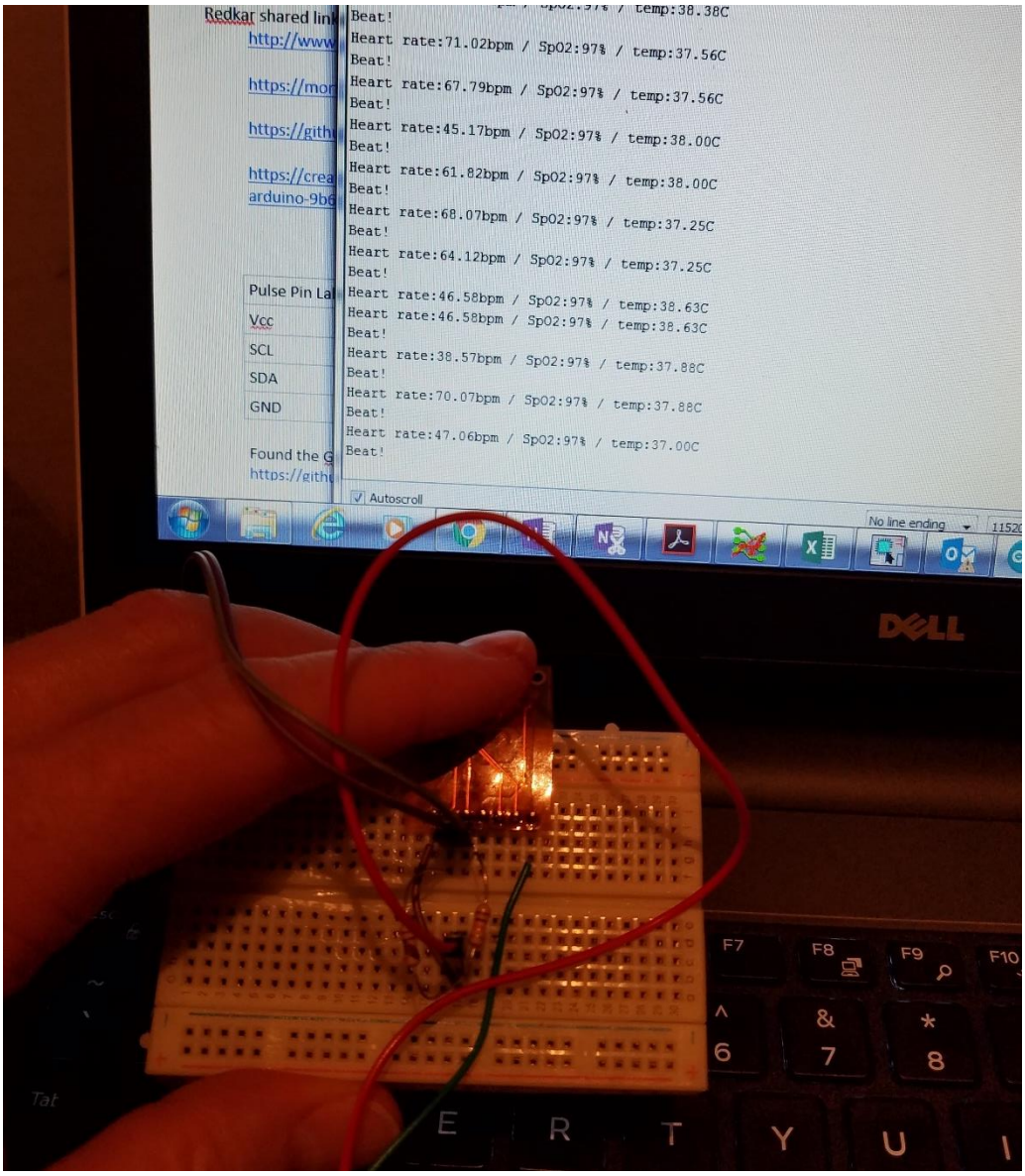

Figure 65. Testing the Pulse-Oximeter Sensor

For testing in the heart monitoring device, code that would produce an Electrocardiogram chart was implemented. This code was taken directly from the support documentation that Sparkfun's porvides for their heart monitoring breakout sensor module. Figure 66 shows the results of the heart monitor device working after the sensor probes were attached to my body.

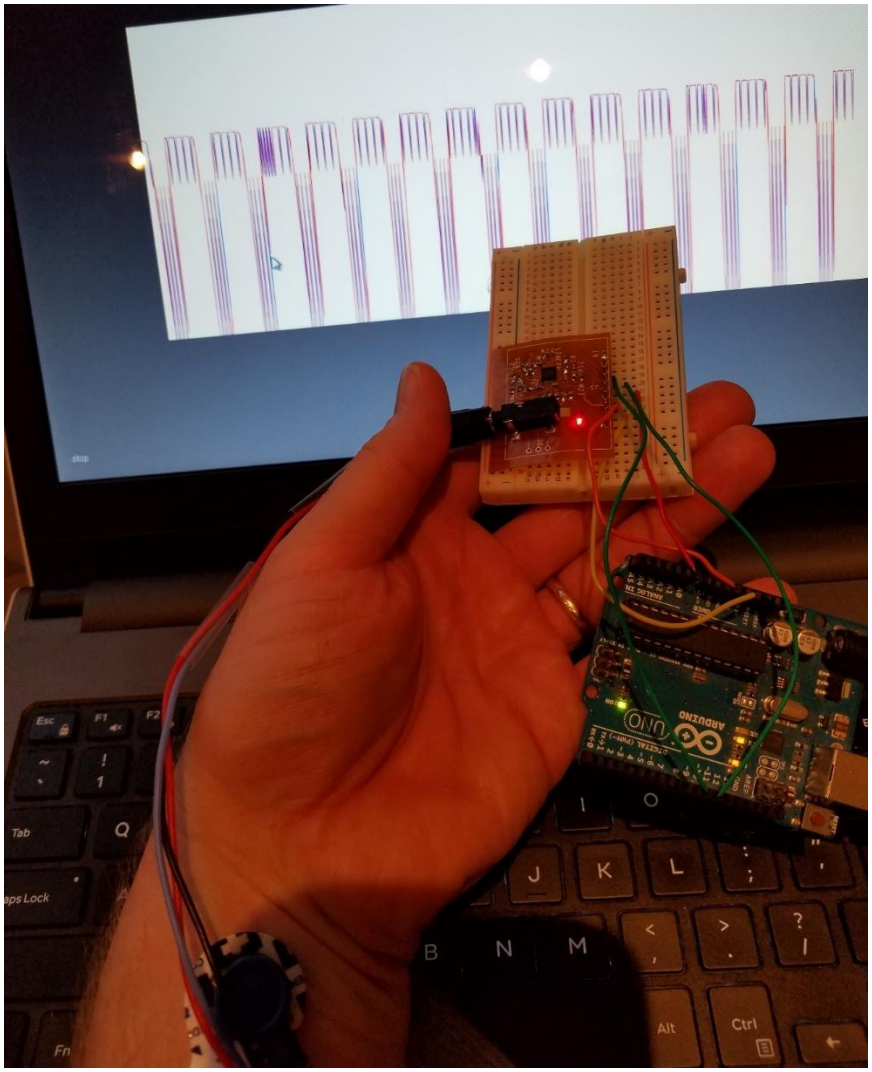

Figure 66. Testing the Heart Monitor Device to Evaluate If It Works As an ECG Device

The validation testing for the air quality sensor followed many of the same steps that the heart monitor sensor went through. Sample code for getting CO2 level, room temperature, and humidity values was taken directly from the support documentation that Sparkfun's provides for their air quality breakout sensor module. Figure 67 shows the results this code was producing from the air quality IC sensor device.

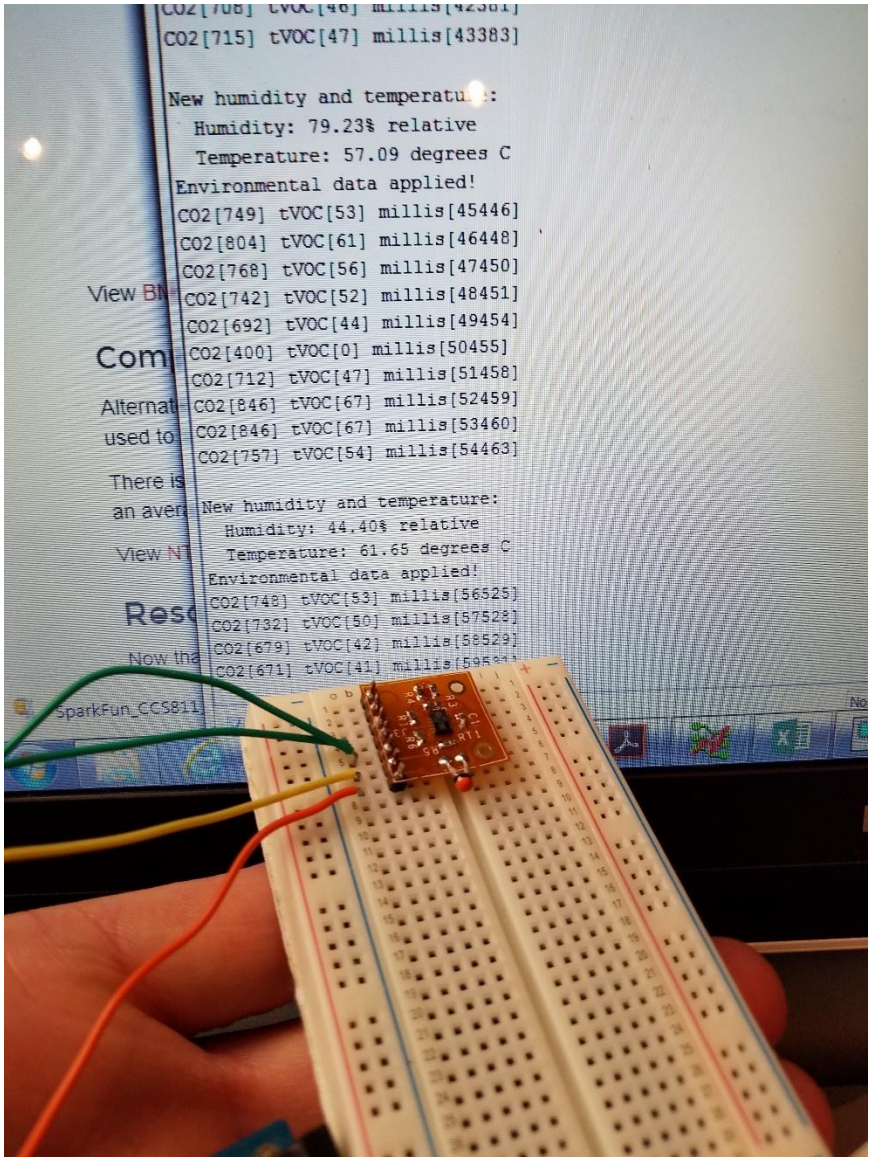

Figure 67. Testing the Air-Quality Device

The nine degree-of-freedom sensor device was similarly tested and efforts are underway to improve the design.

Recommended Design Improvements

Since these devices were developed as a point-of-departure on flexible PCB boards, there are only a few recommended improvements for these sensors modules. Due

to the challenges of implementing the 9 degree-of-freedom sensor on a flexible PCB, one recommendation would be to use a more rigid flexible PCB board when component that have large footprints, like the micro SD slot or IC packages similar to a TQFP (7 mm x 7 mm) are to be used. Another recommendation would be to do medical device comparison testing before further implementation of these devices. The last recommendation would be to look what other connector can be used to interface with these sensors.

CHAPTER 5

CONCLUSION

In this research, some novel sensors for physiological and environment monitoring were developed. The research began from identifying the requirements, understanding the specifications, developing the electrical circuit and schematic and finally prototype building and testing. The wireless pulse ox sensor with fingerprinting was conceived from a Department of Defense requirement of rapid assessment and screening of combat casualty. The functional prototype was built and successfully tested.

The second sensor was developed with rapid reconfiguration capability where the sensors can be hot-swapped. This system can acquire data from variety of sensors but strain gages were chosen to demonstrate its applicability for environmental monitoring. This system is capable of induction/wireless charging and communicates via Bluetooth Low Energy protocol with the host computer. The user also has an option of capturing data via a smart phone app.

The third sensor suite comprised of sensors on flexible substrates. The rigid circuits developed previously were transferred on to a flexible conformal PCB. The sensors developed on flexible substrate can potentially be integrated into a garment that user can wear from continuous physiological sensor monitoring. In this effort, pulse-ox sensor, air quality sensor and EKG sensor were developed and tested. The efforts are underway to integrate these sensors into a base layer that can potentially be used to control “iron-man” type exoskeleton.

REFERENCES

Adafruit. 2012. *Fingerprint Sensor, product ID: 751.* November. Accessed May 2017. https://www.adafruit.com/product/751.

Bajpai, Ayushi, Gaurav Shukla, and Rachna Singh. 2016. *Sensor Market-Report.* Market Report, Portland: Allied Market Research. Accessed March 2018. https://www.alliedmarketresearch.com/sensor-market.

Chan, Vincent, and Steve Underwood. 2005. *A Single-Chip Pulsoximeter Design Using the MSP430.* Application Report, Texas Instruments. Accessed Feb 2018. http://www.ti.com/lit/an/slaa274b/slaa274b.pdf.

Contributors, Wikipedia. 2003. *Ultra-wideband.* Wikipedia, The Free Encyclopedia. January. Accessed June 2017. https://en.wikipedia.org/w/index.php?title=Ultra-wideband&oldid=823041491.

decaWave. 2013. "ScenSor DWM1000 Module." *decaWave.* decaWave. Accessed June 2017. https://www.decawave.com/products/dwm1000-module.

Gupta, Naresh. 2013. "Background of Bluetooth." Chap. 2 in *Inside Bluetooth Low Energy*, 15-32. Boston: Artech House. Accessed March 8, 2018. https://ebookcentral-proquest-com.ezproxy1.lib.asu.edu/lib/asulib-ebooks/detail.action?docID=3002030.

Instruments, National. 2016. *Measuring Strain with Strain Gages.* White Paper, National Instruments. Accessed October 2017. http://www.ni.com/white-paper/3642/en/.

Instruments, National. 1998. *Strain Gauge Measurement - A Tutorial.* Application Note, National Instruments. Accessed December 2017. http://elektron.pol.lublin.pl/elekp/ap_notes/NI_AN078_Strain_Gauge_Meas.pdf.

Instruments, Texas. n.d. "Bluetooth Low Energy Lecture." *Texas Instruments.* Accessed March 7, 2018. http://www.ti.com/lit/ml/swrp221/swrp221.pdf.

Integrated, Maxim. 2014. *Pulse Oximeter and Heart-Rate Sensor IC for Wearable Health.* Data Sheet, Maxim Integrated. Accessed June 2017. https://datasheets.maximintegrated.com/en/ds/MAX30100.pdf.

John. 2011. *Working of Fingerprint Scanner.* Circuit Today. November 15. Accessed February 2018. http://www.circuitstoday.com/working-of-fingerprint-scanner-2.

Kervel, Fredrik. 2011. *Murata Balun for CC253x and CC254x LFB182G45BG2D280.* Application Note, Texas Instruments. Accessed June 22, 2017. http://www.ti.com/lit/an/swra380a/swra380a.pdf.

Lemay, Mathieu, Mattia Bertschi, Josep Sola, Philippe Renevey, Jakub Parak, and Ilkka Korhonen. 2014. "Application of Optical Heart Rate Monitoring." Chap. 2.3 in *Wearable Sensors : Fundamentals, Implementation and Applications*, by Edward Sazonov and Michael Neuman, 105-113. Burlington: Academic Press. Accessed March 2018.

Maltoni, David, Dario Maio, Anil K Jain, and Salil Prabhakar. 2003. "Handbook of Fingerprint Recognition." Chap. 2.4 in *Handbook of Fingerprint Recognition*, 58-66. New York: Springer. Accessed February 2018.

Measurements, Micro. 2017. *Stress Analysis Strain Gages.* Micro Measurements-A VPG Brand. Accessed March 2018. http://www.vishaypg.com/micro-measurements/stress-analysis-strain-gages/.

Nokia. 2017. "Withings Pulse - What does SpO2 mean? What is a normal SpO2 level?" *Nokia | Health.* Noki: Health. Accessed March 2018. https://support.health.nokia.com/hc/en-us/articles/201494667-Withings-Pulse-What-does-SpO2-mean-What-is-a-normal-SpO2-level-.

Poon, Carmen C.Y. , Yali Zheng, Ningqi Luo, Xiaorong Ding, and Yuan Ting Zhang. 2014. "Wearing Sensors Inside and Outside of the Human Body for the Early Detection of Diseases." Chap. 7.2 in *Wearable Sensors : Fundamentals, Implementation and Applications*, by Edward Sazonov and Michael R Neuman, 543-561. San Diego, California: Academic Press. Accessed March 2018.

Scherz, Paul, and Simon Monk. 2013. "Analog-to-Digital and Digital-to-Analog Conversion." Chap. 2 in *Practical Electronic for Inventors*, 820-821. New York: McGraw-Hill Education. Accessed March 2018.

Semiconductor, Avia. n.d. *24-Bit Analog-to-Digital Convert (ADC) for Weigh Scales.* Data Sheet, Avia Semiconductor. Accessed June 2017. https://cdn.sparkfun.com/datasheets/Sensors/ForceFlex/hx711_english.pdf.

Staff, National Research Council Staff. 1995. *Expanding the Vision of Sensor Materials.* Washington, D.C.: National Academy Press. Accessed March 2018. doi:10.17226/4782.

Strogonovs, Raivis. 2017. "Implementing pulse oximeter using MAX30100." *Morf Coding and Engineering.* Web. March 8. Accessed May 2017. https://morf.lv/implementing-pulse-oximeter-using-max30100.

Technology, Linear. 2013. *Demo Manual DC2181A-A/B, Wireless Power Receiver and 400mA Buck Battery Charger.* Manual, Linear Technology. Accessed June 2017. http://cds.linear.com/docs/en/demo-board-manual/DC2181AFB.PDF.

Technology, Linear. 2016. *Wireless Power Receiver and 400mA Buck Battery Charger.* Data Sheet, Milpitas, California: Linear Technology. Accessed June 2017. http://cds.linear.com/docs/en/datasheet/4120ff.pdf.

Technology, Microchip. 2014. *Miniature Single-Cell, Fully Integrated Li-Ion,.* Data Sheet, Microchip Technology Inc. Accessed June 2017. http://ww1.microchip.com/downloads/en/DeviceDoc/20001984g.pdf.

Technology, Security. 2010. *ZFM-20, Fingerprint identification module.* Manual, ZhianTec. Accessed May 2017.

ZhianTec. 2008. *ZFM-20 Series Fingerprint Identification Module.* Manual, ZhianTec. Accessed May 2017.

APPENDIX A

BASIC MECHANICAL DRAWING FOR WIRELESS PULSE OXIMETER WITH A FINGERPRINT SENSOR

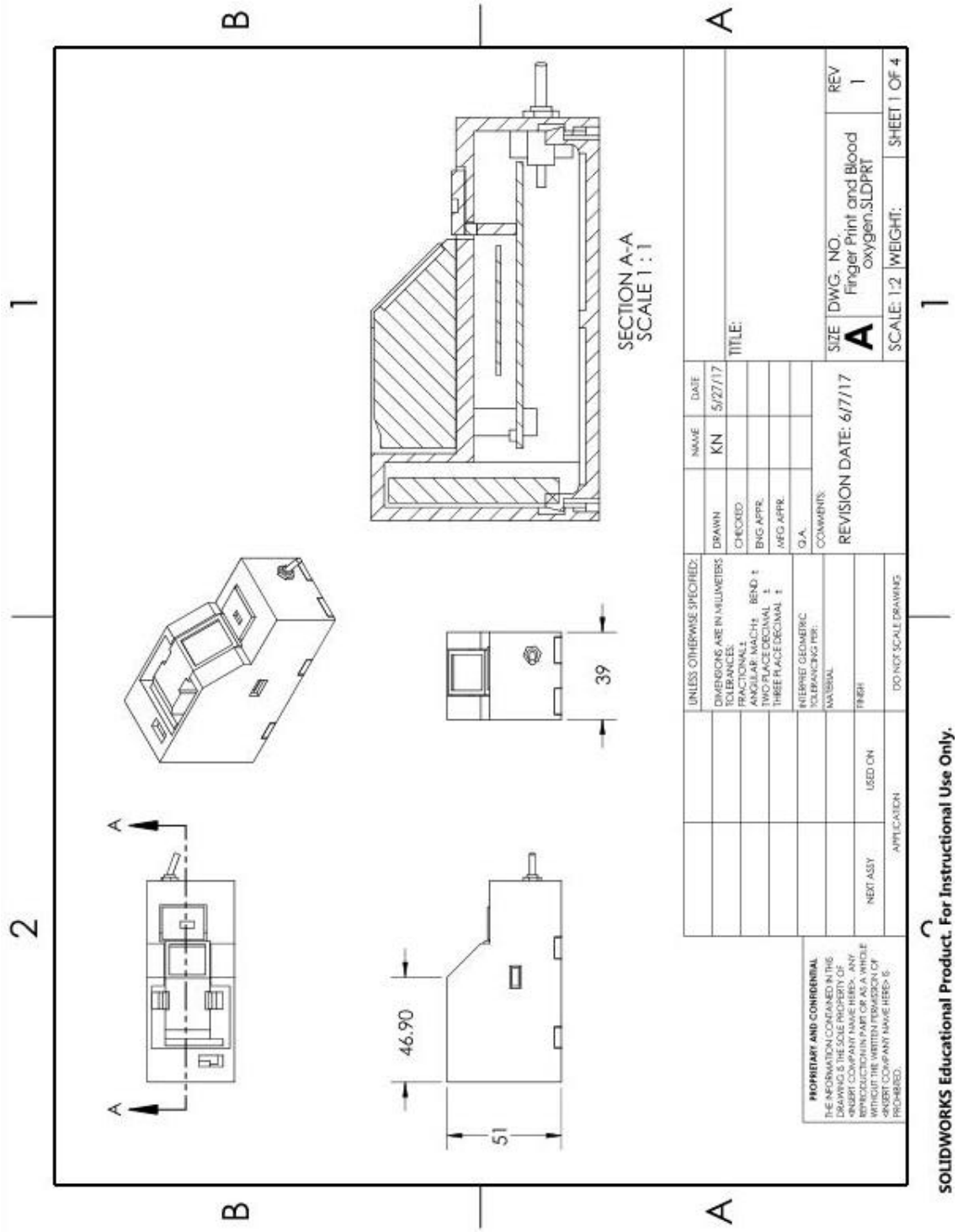
SECTION A-A
SCALE 1 : 1
39
46.90
51
A
A
UNLESS OTHERWISE SPECIFIED:
DIMENSIONS ARE IN MILLIMETERS
TOLERANCES:
FRACTIONAL ±
ANGULAR: MACH ± BEND ±
TWO PLACE DECIMAL ±
THREE PLACE DECIMAL ±
INTERPRET GEOMETRIC TOLERANCING PER:
MATERIAL
FINISH
DO NOT SCALE DRAWING
NEXT ASSY
USED ON
APPLICATION
PROPRIETARY AND CONFIDENTIAL
THE INFORMATION CONTAINED IN THIS DRAWING IS THE SOLE PROPERTY OF <INSERT COMPANY NAME HERE>. ANY REPRODUCTION IN PART OR AS A WHOLE WITHOUT THE WRITTEN PERMISSION OF <INSERT COMPANY NAME HERE> IS PROHIBITED.
NAME
DATE
DRAWN
KN
5/27/17
CHECKED
ENG APPR.
MFG APPR.
Q.A.
COMMENTS:
REVISION DATE: 6/7/17
TITLE:
SIZE
A
DWG. NO.
Finger Print and Blood oxygen.SLDPRT
REV
1
SCALE: 1:2
WEIGHT:
SHEET 1 OF 4
SOLIDWORKS Educational Product. For Instructional Use Only.

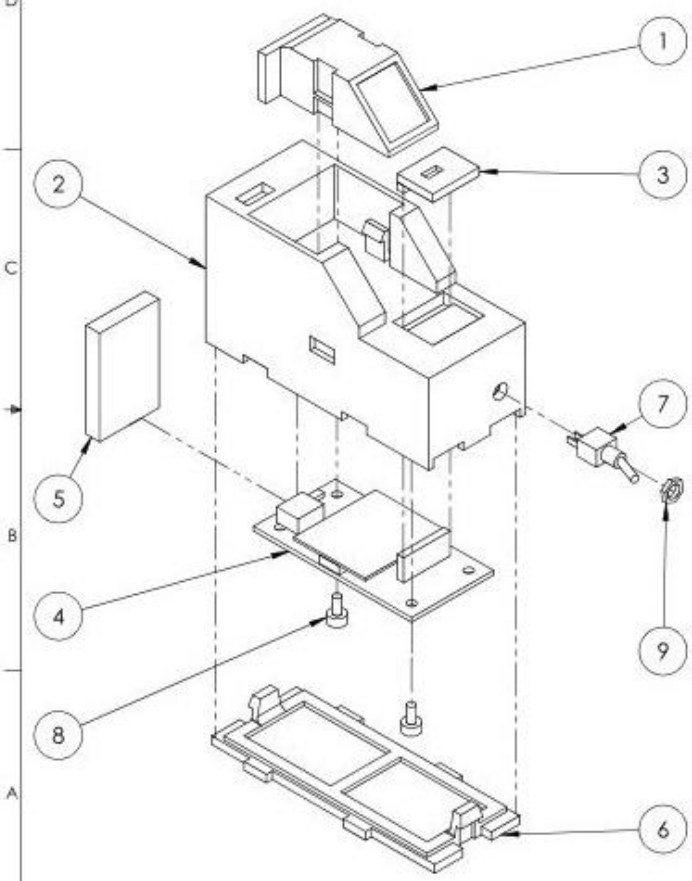

ITEM NO.	PART NUMBER	DESCRIPTION	QTY.
1	Finger Reader Module		1
2	Upper Finger House		1
3	Pusle Module		1
4	Board		1
5	Battery		1
6	Housing Bottom Plate		1
7	Switch		1
8	Board Locking Button		2
9	Switch Locking Nut		1

SIZE	DWG. NO.	REV.
A	Finger Print and Blood oxygen.SLDPRT	1
SCALE	CAD FILE:	SHEET 2 OF 4

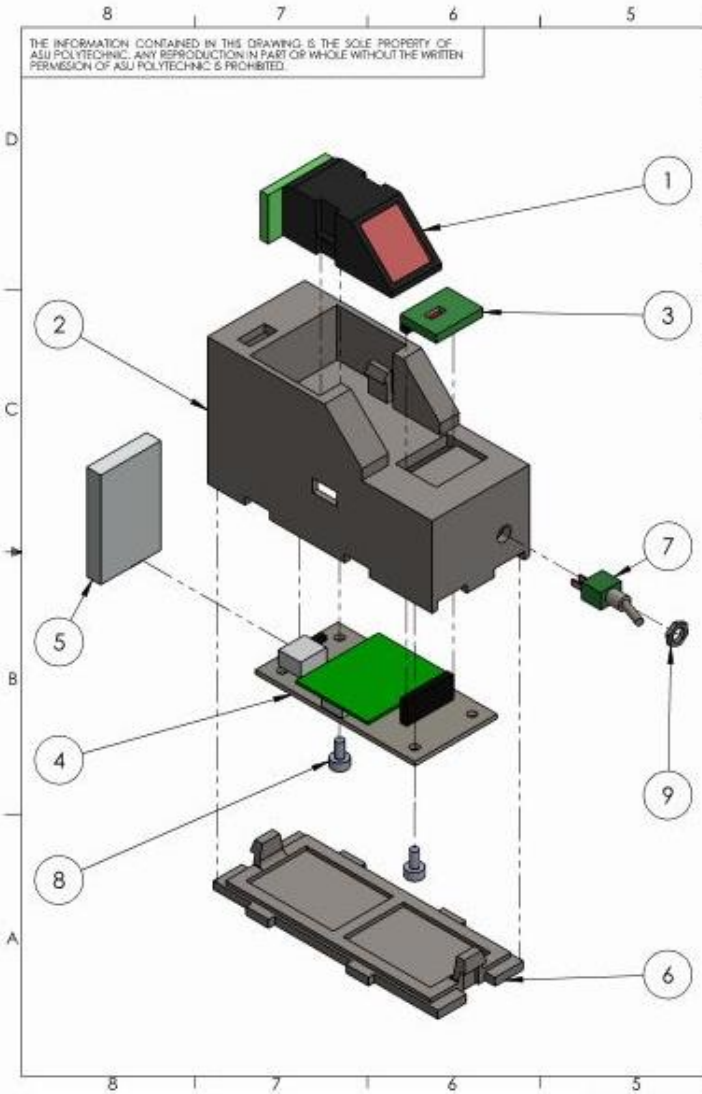

ITEM NO.	PART NUMBER	DESCRIPTION	QTY.
1	Finger Reader Module		1
2	Upper Finger House		1
3	Pusle Module		1
4	Board		1
5	Battery		1
6	Housing Bottom Plate		1
7	Switch		1
8	Board Locking Button		2
9	Switch Locking Nut		1

SIZE A | DWG. NO. Finger Print and Blood oxygen.SLDPRT | REV. 1
SCALE | CAD FILE | SHEET 3 OF 4

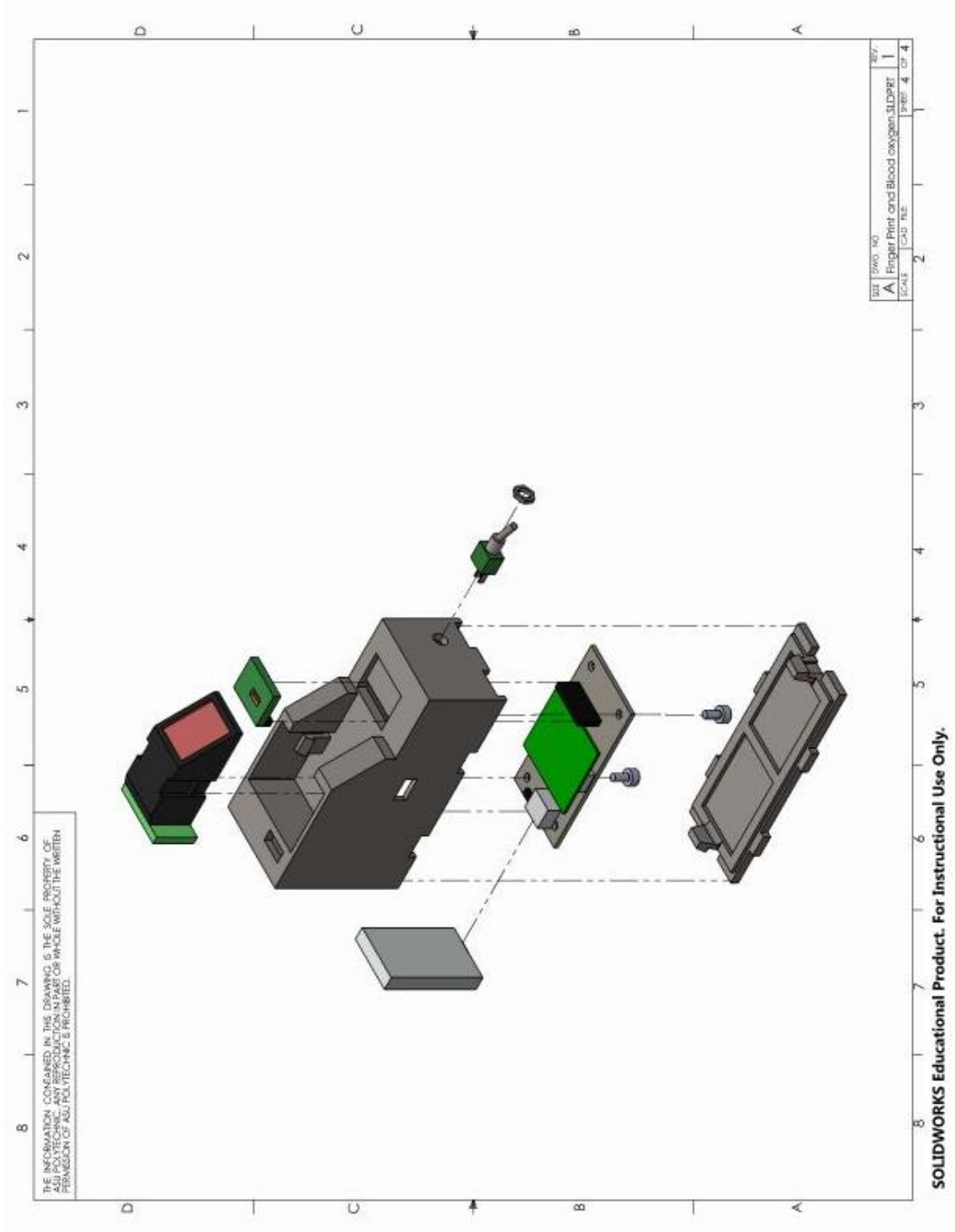
THE INFORMATION CONTAINED IN THIS DRAWING IS THE SOLE PROPERTY OF
ASU POLYTECHNIC. ANY REPRODUCTION IN PART OR WHOLE WITHOUT THE WRITTEN
PERMISSION OF ASU POLYTECHNIC IS PROHIBITED.
SIZE
A
DWG. NO.
Finger Print and Blood oxygen.SLDPRT
REV.
1
SCALE:
CAD FILE:
SHEET 4 OF 4
SOLIDWORKS Educational Product. For Instructional Use Only.

APPENDIX B

CODE FOR WIRELESS PULSE OXIMETER WITH A FINGERPRINT SENSOR

Arduino code file name: “Fingure-SpO2_Prog1_v1.ino”

```
/*
Arduino-MAX30100 oximetry / heart rate integrated sensor library
Copyright (C) 2016  OXullo Intersecans <x@brainrapers.org>

This program is free software: you can redistribute it and/or modify
it under the terms of the GNU General Public License as published by
the Free Software Foundation, either version 3 of the License, or
(at your option) any later version.

This program is distributed in the hope that it will be useful,
but WITHOUT ANY WARRANTY; without even the implied warranty of
MERCHANTABILITY or FITNESS FOR A PARTICULAR PURPOSE.  See the
GNU General Public License for more details.

You should have received a copy of the GNU General Public License
along with this program.  If not, see <http://www.gnu.org/licenses/>.
*/
/***************************************************
  This is an example sketch for our optical Fingerprint sensor

  Designed specifically to work with the Adafruit BMP085 Breakout
  ----> http://www.adafruit.com/products/751

  These displays use TTL Serial to communicate, 2 pins are required to
  interface
  Adafruit invests time and resources providing this open source code,
  please support Adafruit and open-source hardware by purchasing
  products from Adafruit!

  Written by Limor Fried/Ladyada for Adafruit Industries.
  BSD license, all text above must be included in any redistribution
 ****************************************************/

#include <Wire.h>
#include "MAX30100_PulseOximeter.h"
#include <Adafruit_Fingerprint.h>
#include <SoftwareSerial.h>

int getFingerprintIDez();

// pin #2 is IN from sensor (GREEN wire)
// pin #3 is OUT from arduino  (WHITE wire)
SoftwareSerial mySerial(2, 3);
```

```
Adafruit_Fingerprint finger = Adafruit_Fingerprint(&mySerial);

#define REPORTING_PERIOD_MS     100

// PulseOximeter is the higher level interface to the sensor
// it offers:
//  * beat detection reporting
//  * heart rate calculation
//  * SpO2 (oxidation level) calculation
PulseOximeter pox;

uint32_t tsLastReport = 0;

// Callback (registered below) fired when a pulse is detected
void onBeatDetected()
{
    Serial.println("Beat!");
}

void setup()
{
    //Fingure Print setup
  Serial.println("Adafruit finger detect test");

  // set the data rate for the sensor serial port
    finger.begin(57600);

  if (finger.verifyPassword()) {
    Serial.println("Found fingerprint sensor!");
  } else {
    Serial.println("Did not find fingerprint sensor :(");
    while (1);
  }
  Serial.println("Waiting for valid finger...");

  // Pulse SpO2 Setup
  Serial.begin(115200);

    Serial.print("Initializing pulse oximeter..");

    // Initialize the PulseOximeter instance
    // Failures are generally due to an improper I2C wiring, missing power supply
    // or wrong target chip
    if (!pox.begin()) {
        Serial.println("FAILED");
```

```
        for(;;);
    } else {
        Serial.println("SUCCESS");
    }

    // The default current for the IR LED is 50mA and it could be changed
    //   by uncommenting the one of the following line.

    //     pox.setIRLedCurrent(MAX30100_LED_CURR_0MA);
    //     pox.setIRLedCurrent(MAX30100_LED_CURR_4_4MA);
         pox.setIRLedCurrent(MAX30100_LED_CURR_7_6MA);//Best
    //     pox.setIRLedCurrent(MAX30100_LED_CURR_11MA);
    //     pox.setIRLedCurrent(MAX30100_LED_CURR_14_2MA);
    //     pox.setIRLedCurrent(MAX30100_LED_CURR_17_4MA);
    //     pox.setIRLedCurrent(MAX30100_LED_CURR_20_8MA);
    //     pox.setIRLedCurrent(MAX30100_LED_CURR_24MA);
    //     pox.setIRLedCurrent(MAX30100_LED_CURR_27_1MA);
    //     pox.setIRLedCurrent(MAX30100_LED_CURR_30_6MA);
    //     pox.setIRLedCurrent(MAX30100_LED_CURR_33_8MA);
    //     pox.setIRLedCurrent(MAX30100_LED_CURR_37MA);
    //     pox.setIRLedCurrent(MAX30100_LED_CURR_40_2MA);
    //     pox.setIRLedCurrent(MAX30100_LED_CURR_43_6MA);
    //     pox.setIRLedCurrent(MAX30100_LED_CURR_46_8MA);
    //     pox.setIRLedCurrent(MAX30100_LED_CURR_50MA);

    // Register a callback for the beat detection
    pox.setOnBeatDetectedCallback(onBeatDetected);
}

void loop()
{
    getFingerprintIDez();
    // Make sure to call update as fast as possible
    pox.update();
    // Asynchronously dump heart rate and oxidation levels to the serial
    // For both, a value of 0 means "invalid"
    if (millis() - tsLastReport > REPORTING_PERIOD_MS) {
        Serial.print("Heart rate:");
        Serial.print(pox.getHeartRate());
        Serial.print("bpm / SpO2:");
        Serial.print(pox.getSpO2());
        Serial.print("% / temp:");
        Serial.print(pox.getTemperature());
        Serial.println("C");
```

```
      tsLastReport = millis();
    }
}

//Different option for the fingure print scan
uint8_t getFingerprintID() {
  uint8_t p = finger.getImage();
  switch (p) {
    case FINGERPRINT_OK:
      Serial.println("Image taken");
      break;
    case FINGERPRINT_NOFINGER:
      Serial.println("No finger detected");
      return p;
    case FINGERPRINT_PACKETRECIEVEERR:
      Serial.println("Communication error");
      return p;
    case FINGERPRINT_IMAGEFAIL:
      Serial.println("Imaging error");
      return p;
    default:
      Serial.println("Unknown error");
      return p;
  }

  // OK success!

  p = finger.image2Tz();
  switch (p) {
    case FINGERPRINT_OK:
      Serial.println("Image converted");
      break;
    case FINGERPRINT_IMAGEMESS:
      Serial.println("Image too messy");
      return p;
    case FINGERPRINT_PACKETRECIEVEERR:
      Serial.println("Communication error");
      return p;
    case FINGERPRINT_FEATUREFAIL:
      Serial.println("Could not find fingerprint features");
      return p;
    case FINGERPRINT_INVALIDIMAGE:
      Serial.println("Could not find fingerprint features");
      return p;
    default:
```

```
    Serial.println("Unknown error");
    return p;
  }

// OK converted!
  p = finger.fingerFastSearch();
  if (p == FINGERPRINT_OK) {
    Serial.println("Found a print match!");
  } else if (p == FINGERPRINT_PACKETRECIEVEERR) {
    Serial.println("Communication error");
    return p;
  } else if (p == FINGERPRINT_NOTFOUND) {
    Serial.println("Did not find a match");
    return p;
  } else {
    Serial.println("Unknown error");
    return p;
  }

  // found a match!
  Serial.print("Found ID #"); Serial.print(finger.fingerID);
  Serial.print(" with confidence of "); Serial.println(finger.confidence);
}

// returns -1 if failed, otherwise returns ID #
int getFingerprintIDez() {
  uint8_t p = finger.getImage();
  if (p != FINGERPRINT_OK)  return -1;
  p = finger.image2Tz();
  if (p != FINGERPRINT_OK)  return -1;
  p = finger.fingerFastSearch();
  if (p != FINGERPRINT_OK)  return -1;
  // found a match!
  Serial.print("Found ID #"); Serial.print(finger.fingerID);
  Serial.print(" with confidence of "); Serial.println(finger.confidence);
  return finger.fingerID;
}
```

APPENDIX C

SCHEMATIC FOR THE WIRELESS STRAIN TRANSMITTER

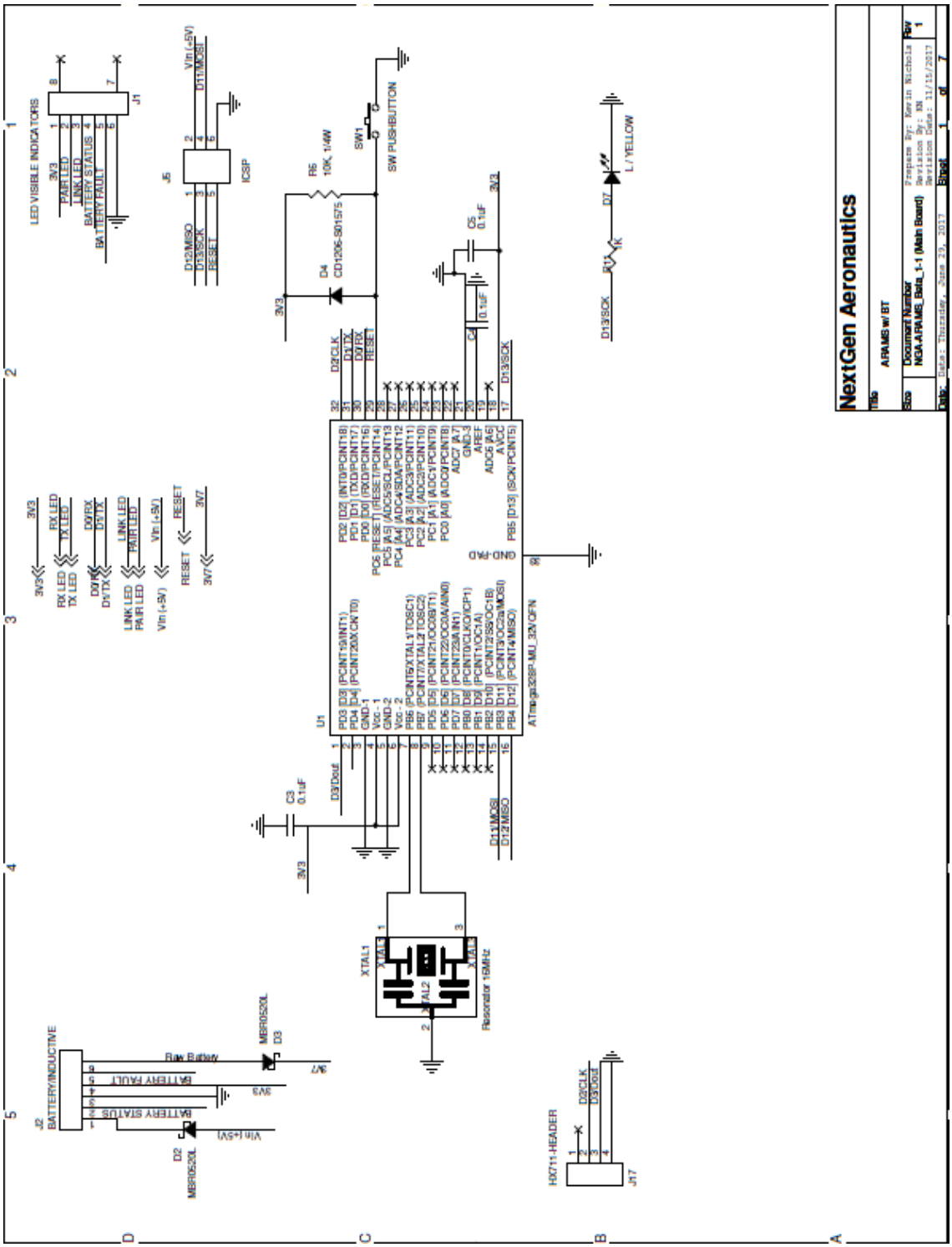
NextGen Aeronautics
AFRAMS w/ BT
Document Number
NGA-AFRAMS_Beta_1-1 (Main Board)
Rev
1
Date: Thursday, June 29, 2017
Sheet 1 of 7
LED VISIBLE INDICATORS
J1
J5
ICSP
SW1
SW PUSHBUTTON
R5
10K, 1/4W
D4
CD1206-S01575
C5
0.1uF
C4
0.1uF
D7
L / YELLOW
R13
U1
ATmega328P-MU_32VQFN
C3
0.1uF
XTAL1
Resonator 16MHz
J2
BATTERY/INDUCTIVE
Raw Battery
MBR0520L
D3
D2
MBR0520L
HX711-HEADER
J17

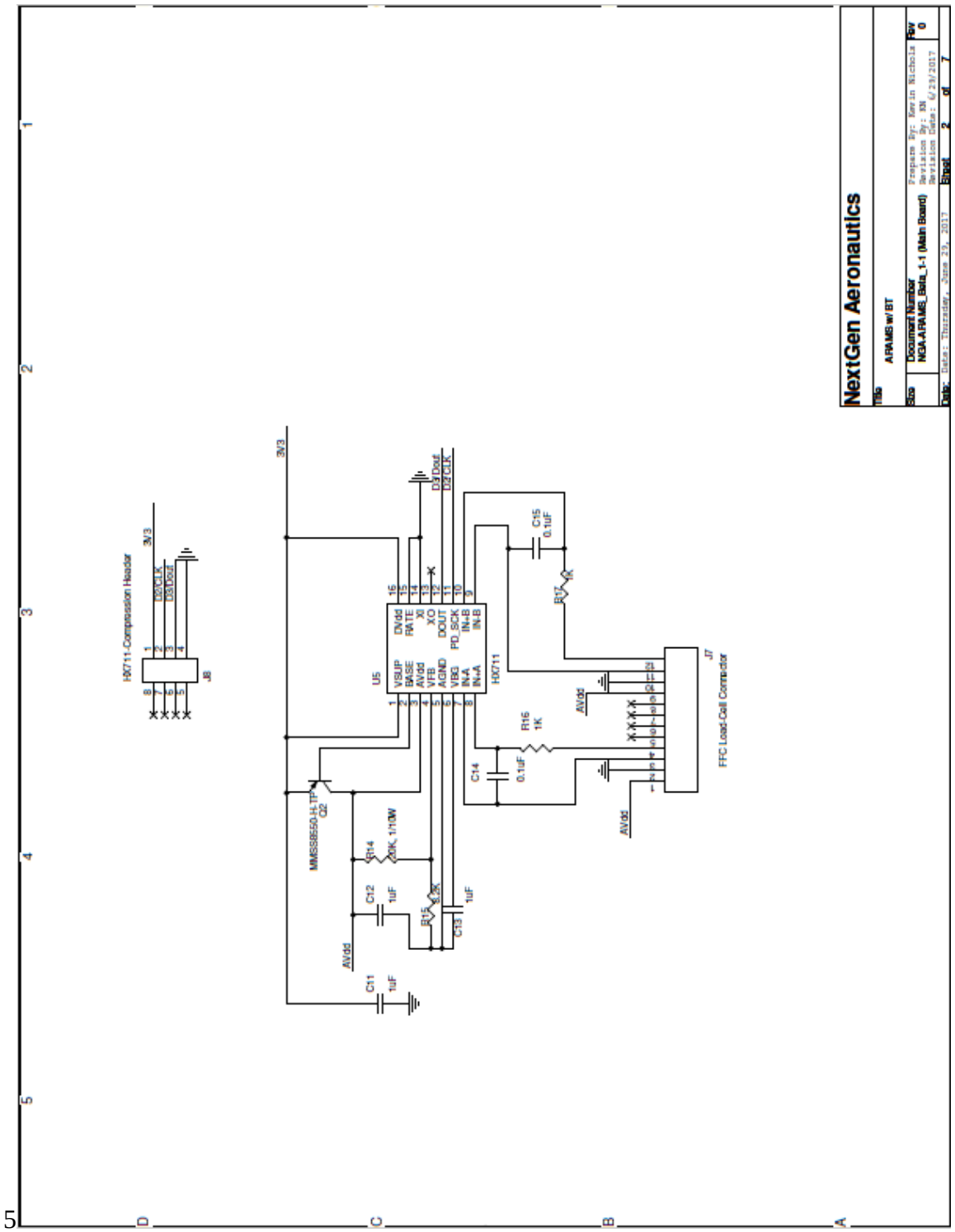
NextGen Aeronautics
Title
ARAMS w/ BT
Size
Document Number
NGA-ARAMS_Beta_1-1 (Main Board)
Rev
0
Date: Thursday, June 29, 2017
Sheet 2 of 7
H0711-Compensation Header
J8
3V3
D2/CLK
D3/Dout
U5
H0711
DVdd
RATE
XI
XO
DOUT
PD_SCK
IN+B
IN-B
VSUP
BASE
AVdd
VFB
AGND
VBG
IN+A
IN-A
D3/Dout
D2/CLK
C15
0.1uF
R17
1K
AVdd
R16
1K
C14
0.1uF
J7
FFC Load-Cell Connector
MMBS8550-H,TF
Q2
R14
20K, 1/10W
C12
1uF
R15
6.2K
C13
1uF
C11
1uF

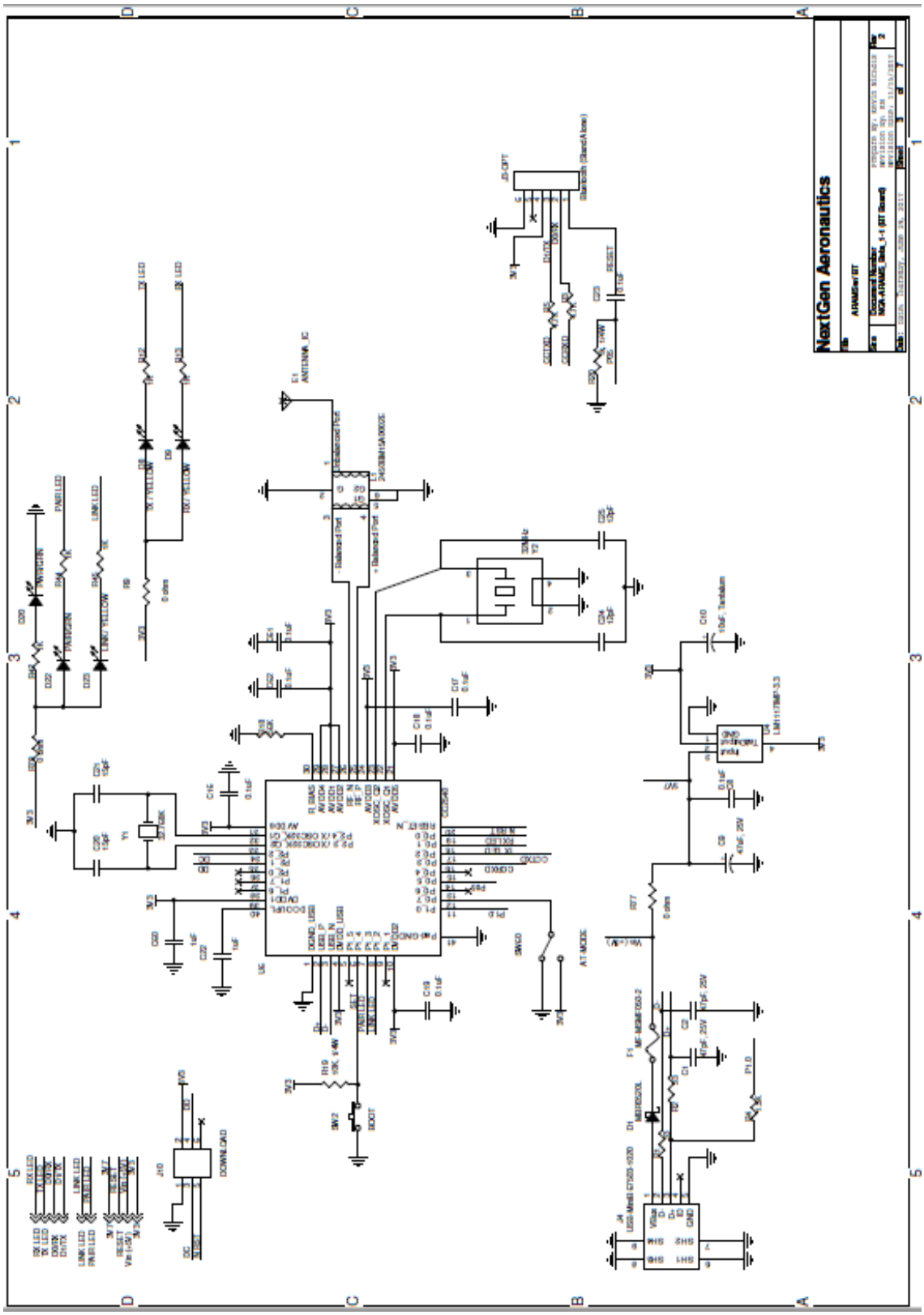
NextGen Aeronautics
ANTENNA_IC
Bluetooth (Stand Alone)
DOWNLOAD
BOOT
AT-MODE
A
B
C
D
1
2
3
4
5

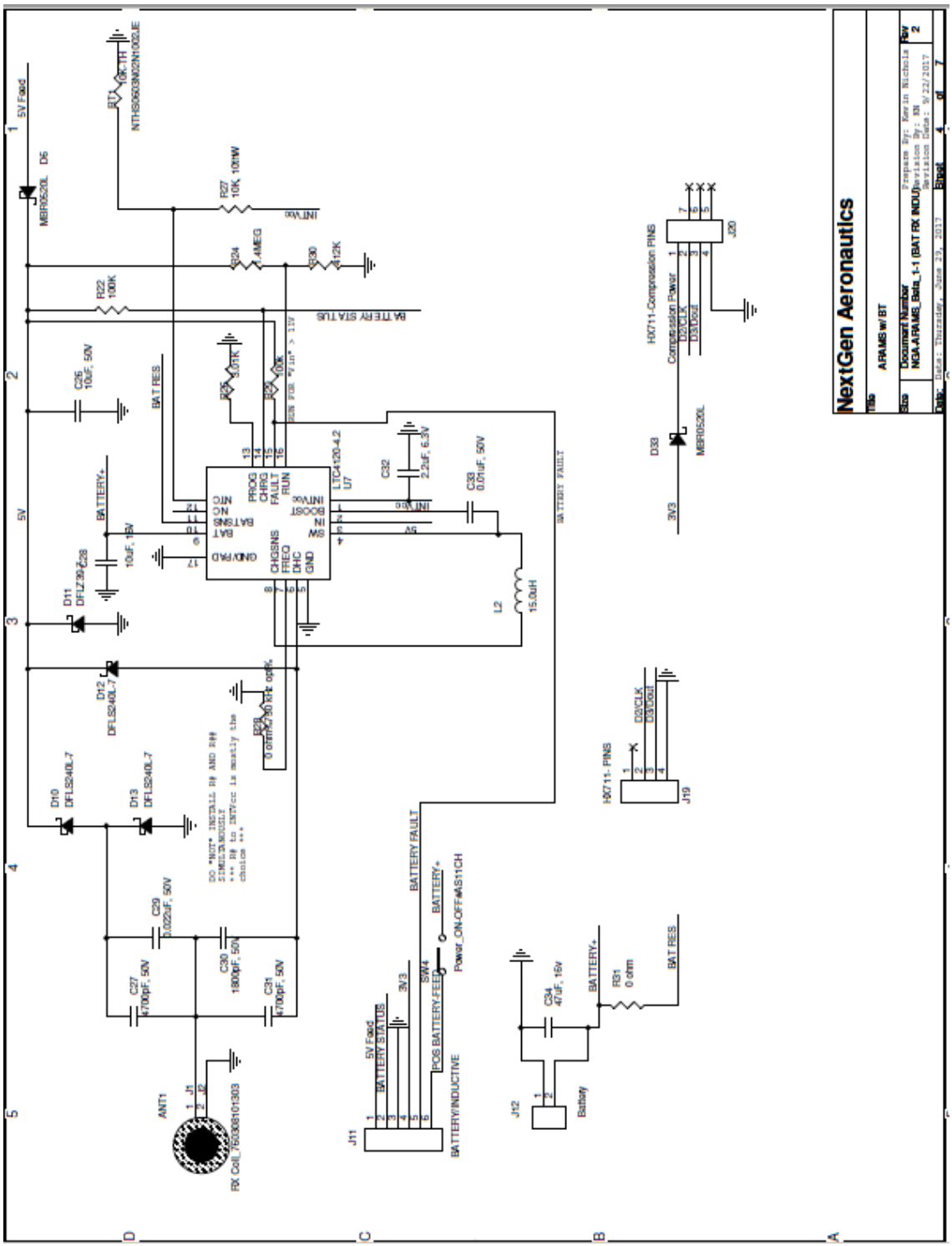
NextGen Aeronautics
AFAIMS w/ BT
Document Number
NGA-AFAIMS_Batt_1-1 (BAT RX INDU)
Revision By: BN
Revision Date: 9/22/2017
Prepare By: Kevin Nichols
Date: Thursday, June 29, 2017
Sheet 4 of 7
Rev 2
LTC4120-4.2
U7
PROG
CHRG
FAULT
RUN
INTVcc
BOOST
IN
SW
BAT
BATSNS
NC
NC
GND/PAD
CHGSNS
FREQ
DHC
GND
BATTERY+
BAT RES
BATTERY STATUS
BATTERY FAULT
BATTERY/INDUCTIVE
POS BATTERY FEED
Power_ON-OFF#MS11CH
SW4
J11
J12
J19
J20
ANT1
RX Coil_7533610130 3
H-X711-PINS
H-X711-Compression PINS
Compression Power
D2/CLK
D3/DOUT
MBR0520L
D5
D33
D11
DFLZ39V
D12
DFLS240L-7
D10
DFLS240L-7
D13
DFLS240L-7
L2
15.0uH
C32
2.2uF, 6.3V
C33
0.01uF, 50V
C25
10uF, 50V
C28
10uF, 16V
C29
0.022uF, 50V
C27
4700pF, 50V
C30
1800pF, 50V
C31
4700pF, 50V
C34
47uF, 16V
R27
10K, 1%1W
R24
4.MEG
R30
412K
R22
100K
R23
10K
R25
3.01K
R31
0 ohm
5V Feed
3V3
INTVcc
BATTERY FAULT
BATTERY STATUS
DO *NOT* INSTALL R9 AND R8
SIMULTANEOUSLY
*** R9 to INTVcc is mostly the
choice ***

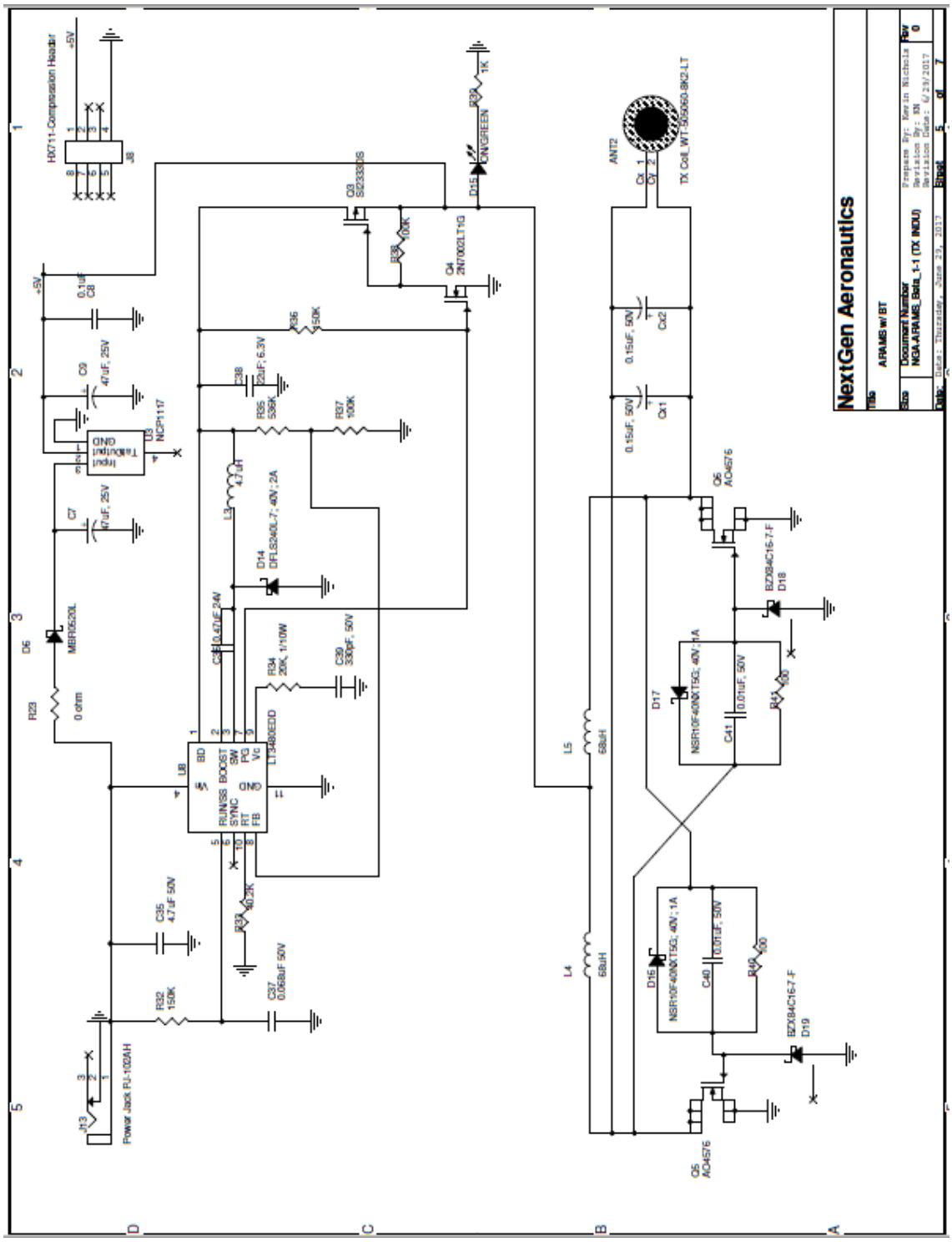
NextGen Aeronautics
ARAMS w/ BT
Document Number
NGA-ARAMS_Beta_1-1 (TX INDU)
Rev
0
Sheet
5
of
7
H0711-Compression Header
J8
+5V
0.1uF
C8
C9
47uF, 25V
U3
NCP1117
Input
Tab/Output
GND
C7
47uF, 25V
D6
MBR0520L
R23
0 ohm
R13
Power Jack PJ-102AH
C35
4.7uF 50V
R32
150K
C37
0.068uF 50V
U8
LT3480EDD
BID
BOOST
SW
PG
Vc
GND
RUN/SS
SYNC
RT
FB
R33
40.2K
C38
0.47uF, 24V
L3
4.7uH
D14
DFLS240L-7; 40V; 2A
R35
536K
C36
22uF; 6.3V
R36
50K
R37
100K
R34
20K, 1/10W
C39
330pF, 50V
Q3
SI2333DS
R38
100K
Q4
2N7002LT1G
D15
ON/GREEN
R39
1K
ANT2
TX Coil_WT-505060-8K2-LT
Cx 1
Cy 2
Cx1
0.15uF, 50V
Cx2
0.15uF, 50V
Q6
AO4576
BZX84C16-7-F
D18
D17
NSR10F40NXT5G; 40V; 1A
C41
0.01uF, 50V
R41
100
L5
68uH
L4
68uH
D16
NSR10F40NXT5G; 40V; 1A
C40
0.01uF, 50V
R40
100
BZX84C16-7-F
D19
Q5
AO4576

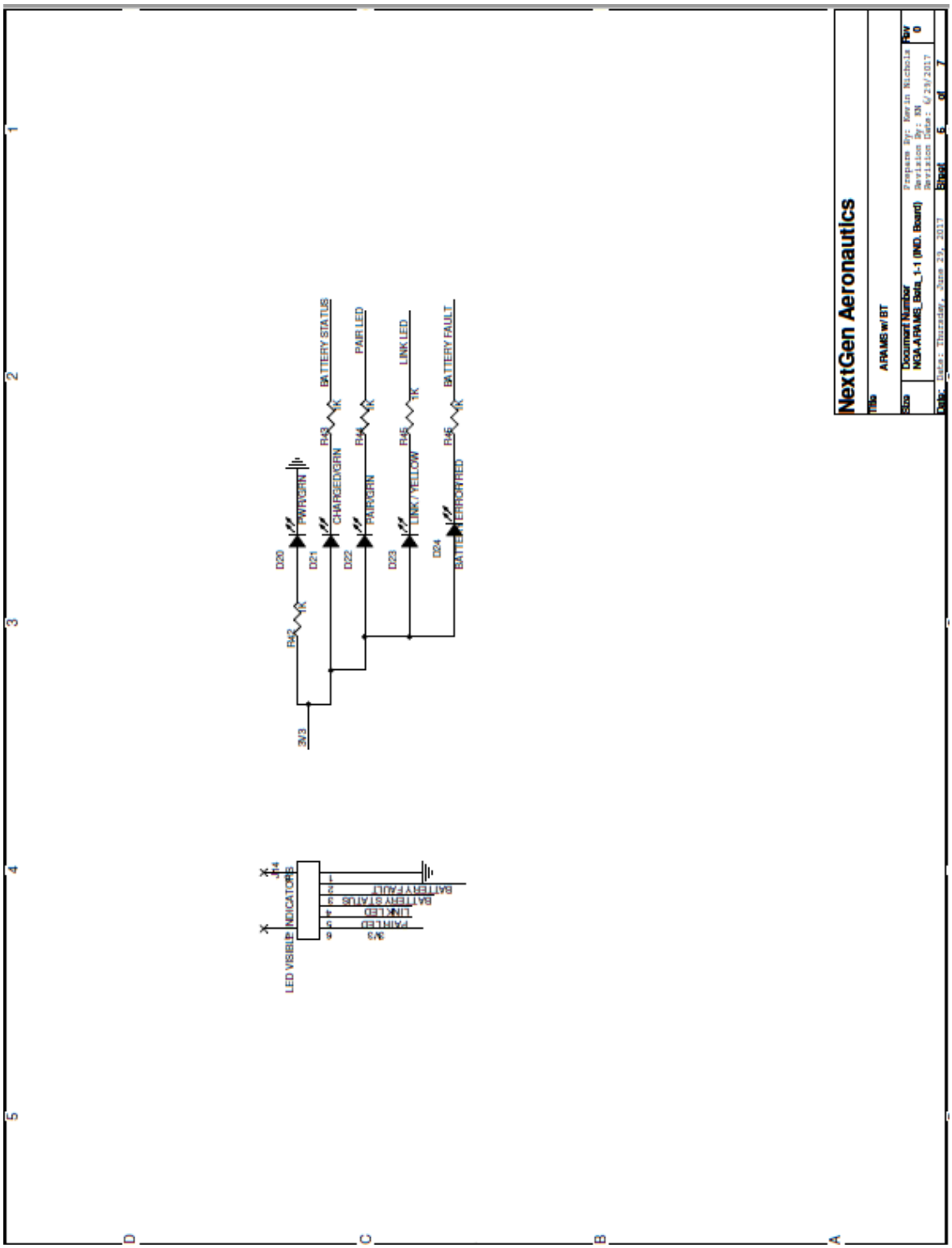
NextGen Aeronautics
Title
ARAMS w/ BT
Size
Document Number
NGA-ARAMS_Batt_1-1 (IND. Board)
Rev
0
Date: Date: Thursday, June 29, 2017
Sheet 5 of 7
LED VISIBLE INDICATORS
J14
3V3
PAIR LED
LINK LED
BATTERY STATUS
BATTERY FAULT
D20
D21
D22
D23
D24
PWR/GRN
CHARGED/GRN
PAIR/GRN
LINK/YELLOW
BATTERY/RED
R42
R43
R44
R45
R46
1K
BATTERY STATUS
PAIR LED
LINK LED
BATTERY FAULT

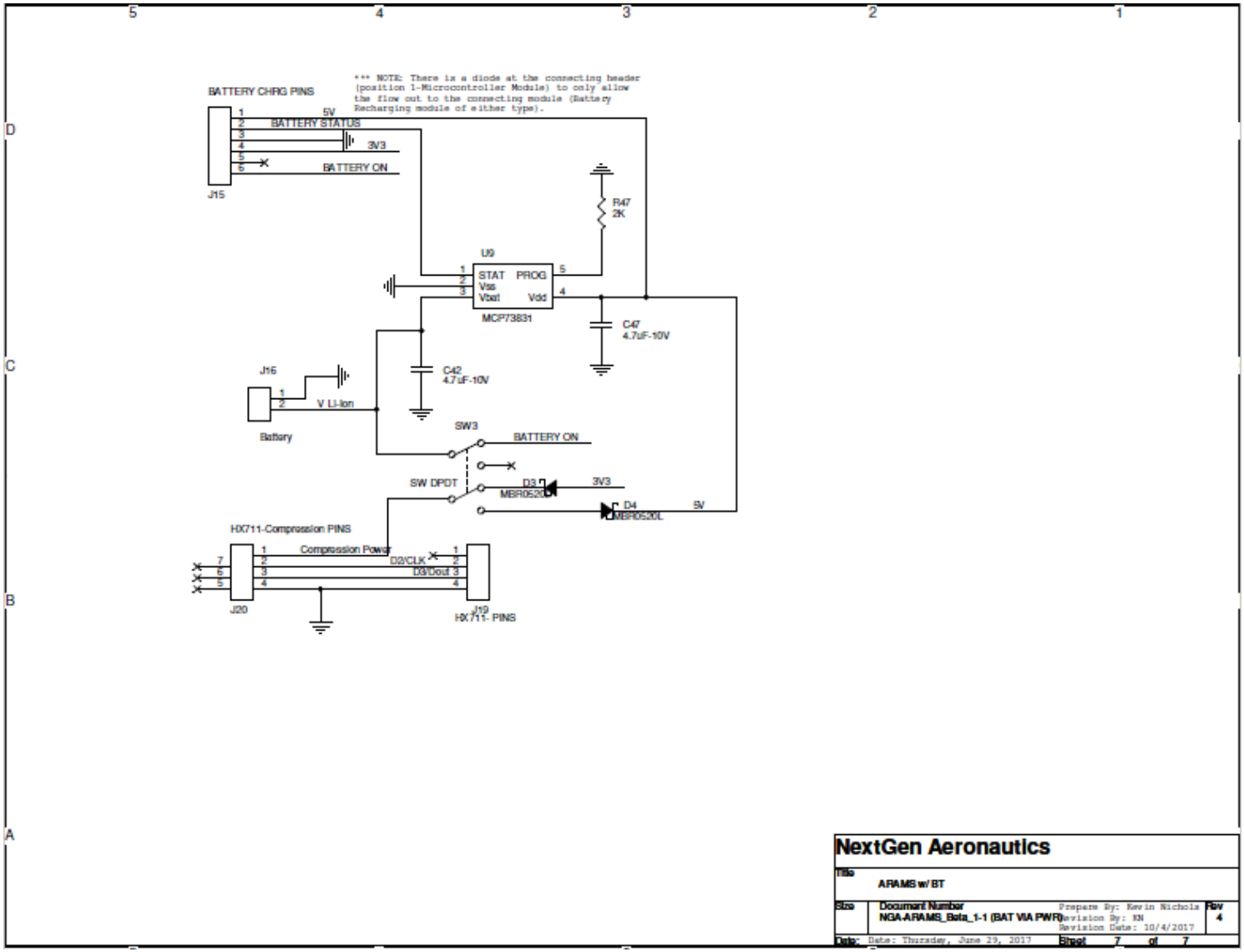
*** NOTE: There is a diode at the connecting header (position 1-Microcontroller Module) to only allow the flow out to the connecting module (Battery Recharging module of either type).
BATTERY CHRG PINS
5V
BATTERY STATUS
3V3
BATTERY ON
J15
R47
2K
U9
STAT
PROG
Vss
Vbat
Vdd
MCP73831
C47
4.7uF-10V
C42
4.7uF-10V
J16
V Li-ion
Battery
SW3
BATTERY ON
SW DPDT
D3
MBR0520L
3V3
D4
MBR0520L
5V
HX711-Compression PINS
Compression Power
D2/CLK
D3/Dout
J20
J19
HX711- PINS
NextGen Aeronautics
Title
ARAMS w/ BT
Size
Document Number
NGA-ARAMS_Bota_1-1 (BAT VIA PWR)
Prepare By: Kevin Nichols
Revision By: KN
Revision Date: 10/4/2017
Rev
4
Date: Date: Thursday, June 29, 2017
Sheet 7 of 7

APPENDIX D

BILL-OF-MATERIAL FOR THE WIRELESS STRAIN TRANSMITTER

		Project Name:	NGA-Wireless Strain Transmitter Project															
		Prepared By:	Kevin Nichols															
		Version Number:	Beta 1.3								**Prototype Quantity:**		**5**					
		Version Date:	9/7/2017								**Production Qty:**		**200**					
		Bill of Material																
sort ref	**Item #**	**Section Grouping**	**Part Name/Description**	**Unit Quantity**	**Unit Cost**	**Total Cost**	**Unit Production Cost**	**Total Production Cost**	**Manufacturer**	**Manufacturer Part #**	**Supplier**	**Supplier Part #**	**Qty Ordered**	**Total Order Cost**	**Qty Received**	**Qty Used**	**Surplus Qty**	**Schematic Reference**
A		**10-Load-Cell Connection**																
J-12pos-FFC	1	10-Load-Cell Connection	12 Position FFC, FPC Connector Contacts, Top 0.039" (1.00mm) Surface Mount, Right Angle	1	$0.850	$0.85	$0.641	$128.22	Amphenol FCI	SFW12R-2STE1LF	Digi-Key	609-1901-1-ND	5	$4.25	5	2	3	J41
R-Match	2	10-Load-Cell Connection	Resistors to match resistance of stain gauge, 0603 (1608 Metric) or 0805 (2012 Metric)	3		$0.00		$0.00						$0.00		0	0	R40, R41, R42
Z	2	**10-Load-Cell Connection Section End**				$0.85		$128.22						$4.25				
A		**1-Microcontroller**																
C-0.1uF	3	1-Microcontroller	0.1µF ±10% 16V Ceramic Capacitor X7R (0603)	5	$0.025	$0.13	$0.011	$11.20	KEMET	C0603C104K4RACTU	Digi-Key	399-1096-1-ND	35	$0.88	35	10	25	C3, C4, C5, C6
C-10uF	4	1-Microcontroller	10µF ±20% Molded Tantalum Capacitors 4V (1206) 6 Ohm	1	$0.254	$0.25	$0.152	$30.42	KEMET	T491A106M004AT	Digi-Key	495-2174-1-ND	5	$1.27	5	3	2	C10
C-47pF	5	1-Microcontroller	47pF ±5% 25V Ceramic Capacitor C0G, NP0 (0603)	2	$0.063	$0.13	$0.028	$11.16	KEMET	C0603C470J3GACTU	Digi-Key	399-9083-1-ND	10	$0.63	10	6	4	C1, C2
C-47uF	6	1-Microcontroller	47µF 25V Aluminum Electrolytic Capacitors Radial, Can - SMD 2000 Hrs @ 85°C	2	$0.380	$0.76	$0.159	$63.76	United Chemi-Con	EMVA250ADA470MF55G	Digi-Key	565-2103-1-ND	10	$3.80	10	3	7	C7, C9
D-100V	7	1-Microcontroller	Diode Standard 100V 150mA Surface Mount (1206)	1	$0.149	$0.15	$0.057	$11.46	Bourns Inc.	CD1206-S01575	Digi-Key	CD1206-S01575CT-ND	5	$0.75	5	2	3	D4
D-20V	8	1-Microcontroller	Diode Schottky 20V 500mA Surface Mount SOD-123	5	$0.295	$1.48	$0.103	$103.00	Fairchild/ON Semiconductor	MBR0520L	Digi-Key	MBR0520LCT-ND	20	$5.90	20	9	11	D1, D2, D3, D6, D6*
D-G	9	1-Microcontroller	Green 570nm LED Indication - Discrete 2.2V (0805)	1	$0.180	$0.18	$0.095	$18.96	OSRAM Opto Semiconductors Inc.	LG R971-KN-1	Digi-Key	475-1410-1-ND	5	$0.90	5	1	4	D5
D-Y	10	1-Microcontroller	Yellow 588nm LED Indication - Discrete 2.1V (0805)	3	$0.282	$0.85	$0.089	$53.46	Kingbright	APT2012YC	Digi-Key	754-1135-1-ND	15	$4.23	15	8	7	D7, D8, D9
F	11	1-Microcontroller	PTC Resettable Fuse 15V Ih Surface Mount (1812)	1	$0.220	$0.22	$0.175	$35.04	Bourns Inc.	MF-MSMF050-2	Digi-Key	MF-MSMF050-2CT-ND	5	$1.10	5	3	2	F1
J-6pos	12	1-Microcontroller	6 Positions Header Connector 0.100" (2.54mm) Through Hole Tin	1	$0.258	$0.26	$0.155	$30.91	Amphenol FCI	67996-406HLF	Digi-Key	609-3218-ND	5	$1.29	5	3	2	J5
J-usb	13	1-Microcontroller	USB - mini B USB 2.0 OTG Receptacle Connector 5 Position Surface Mount, Right Angle	1	$1.030	$1.03	$0.778	$155.66	Molex, LLC	0675031020	Digi-Key	WM5461CT-ND	5	$5.15	5	3	2	J4
R-1.5K	14	1-Microcontroller	1.5k Ohm ±1% 0.25W, 1/4W Chip Resistor (0603), Automotive AEC-Q200, Pulse Withstanding Thick Film	1	$0.146	$0.15	$0.056	$11.26	Vishay Dale	RCS06031K50FKEA	Digi-Key	541-2789-1-ND	5	$0.73	5	3	2	R4
R-10K	15	1-Microcontroller	10k Ohm ±1% 0.25W, 1/4W Chip Resistor (0603), Automotive AEC-Q200, Pulse Withstanding Thick Film	1	$0.146	$0.15	$0.025	$4.95	Vishay Dale	RCS06031K0FKEA	Digi-Key	541-2795-1-ND	30	$4.38	30	2	28	R6
R-1K	16	1-Microcontroller	1k Ohm ±1% 0.1W, 1/10W Chip Resistor (0603), Automotive AEC-Q200, Thick Film	4	$0.035	$0.14	$0.006	$5.07	Vishay Dale	CRCW06031K00FKTA	Mouser	71-CRCW0603-1.0K	22	$0.77	30	9	21	R11, R12, R13
R-33	17	1-Microcontroller	33 Ohm ±1% 0.25W, 1/4W Chip Resistor (0603), Automotive AEC-Q200, Pulse Withstanding Thick Film	2	$0.146	$0.29	$0.056	$22.52	Vishay Dale	RCS060333R0FKEA	Digi-Key	541-2782-1-ND	10	$1.46	10	6	4	R1, R2
R-4.7K	18	1-Microcontroller	4.7k Ohm ±5% 0.25W, 1/4W Chip Resistor (0603), Automotive AEC-Q200, Pulse Withstanding Thick Film	2	$0.100	$0.20	$0.034	$13.60	Panasonic Electronic Components	ERJ-PA3J472V	Digi-Key	P4.7KBZCT-ND	10	$1.00	10	6	4	R3, R5
SW-PB	19	1-Microcontroller	Tactile Switch SPST-NO Top Actuated Surface Mount	1	$1.000	$1.00	$0.725	$145.02	Omron Electronics Inc-EMC Div	B3U-1000P	Digi-Key	SW1020CT-ND	5	$5.00	5	2	3	SW1
U-3V3	20	1-Microcontroller	Linear Voltage Regulator IC Positive Fixed Output, 3.3V, 800mA, SOT-223	1	$1.040	$1.04	$0.723	$144.50	Texas Instruments	LM1117IMP-3.3/NOPB	Digi-Key	LM1117IMP-3.3/NOPBCT-ND	10	$10.40	10	3	7	U4
U-5V	21	1-Microcontroller	Linear Voltage Regulator IC Positive Fixed Output, 5V, 1A, SOT-223	1	$0.500	$0.50	$0.321	$64.22	ON Semiconductor	NCP1117ST50T3G	Digi-Key	NCP1117ST50T3GOSCT-ND	5	$2.50	5	1	4	U3
U-C	22	1-Microcontroller	Atmegea 328P IC MCU 8BIT 32KB FLASH 32VQFN	1	$2.070	$2.07	$1.720	$344.02	Microchip Technology	ATMEGA328P-MU	Digi-Key	ATMEGA328P-MU-ND	5	$10.35	5	2	3	U1
U-Op	23	1-Microcontroller	IC OPAMP GP 1MHZ RRO 8VSSOP	1	$0.770	$0.77	$0.521	$104.24	Texas Instruments	LMV358IDGKR	Digi-Key	296-13455-1-ND	5	$3.85	5	2	3	U2
Y-16MHz	24	1-Microcontroller	16MHz Ceramic Resonator Built in Capacitor 15pF ±0.3% -20°C ~ 80°C Surface Mount	1	$0.500	$0.50	$0.336	$67.14	Murata Electronics North America	CSTCE16M0V53-R0	Digi-Key	490-1198-1-ND	5	$2.50	5	2	3	XTAL1
Z	22	**1-Microcontroller Section End**				$12.23		$1,451.58						$68.83				
A		**2-Battery Recharging**																

sort ref	Item #	Section Grouping	Part Name/Description	Unit Quantity	Unit Cost	Total Cost	Unit Production Cost	Total Production Cost	Manufacturer	Manufacturer Part #	Supplier	Supplier Part #	Qty Ordered	Total Order Cost	Qty Received	Qty Used	Surplus Qty	Schematic Reference
Bat	25	2-Battery Recharging	Lithium-Ion Battery Rechargeable (Secondary) 3.7V, 500mAh, Coin, 35.0mm, Wire leads	1	$22.230	$22.23	$16.960	$3,392.00	Illinois Capacitor	RJD3555HPPV30M	Mouser Digi-Key (more $)	598-RJD3555HPPV30M 1572-1627-ND	2	$44.46	2	0	2	n/a
C-0.1uF	26	2-Battery Recharging	0.1µF ±10% 16V Ceramic Capacitor X7R (0603)	2	$0.025	$0.05	$0.011	$4.48	KEMET	C0603C104K4RACTU	Digi-Key	399-1096-1-ND	15	$0.38	15	4	11	C44, C45
C-10uF	27	2-Battery Recharging	10µF ±10% Molded Tantalum Capacitors 16V (1206)	1	$0.312	$0.31	$0.187	$37.46	KEMET	T491A106K016AT	Digi-Key	399-8269-1-ND	5	$1.56	5	2	3	C46
C-22uF	28	2-Battery Recharging	22µF ±10% 6.3V Ceramic Capacitor X5R (0805)	1	$0.310	$0.31	$0.186	$37.20	KEMET	C0805C226K9PAC7800	Digi-Key	399-11661-1-ND	5	$1.55	5	2	3	C43
C-4.7uF	29	2-Battery Recharging	4.7µF ±10% 10V Ceramic Capacitor X5R (0603)	2	$0.197	$0.39	$0.118	$47.20	KEMET	C0603C475K8PACTU	Digi-Key	399-5503-1-ND	10	$1.97	10	4	6	C42, C47
I-4.7uH	30	2-Battery Recharging	4.7µH Shielded Inductor 1.2A 140 mOhm Max Nonstandard	1	$1.090	$1.09	$0.730	$145.94	Sumida America Components Inc	CDRH2D18/HPNP-4R7NC	Digi-Key	308-2297-1-ND	5	$5.45	5	2	3	L7
J-4Pos-Male	31	2-Battery Recharging	4 Position Spring Compression Contact, Male Connector Through Hole	1	$1.860	$1.86	$1.446	$289.18	Bourns Inc.	70ADH-4-ML0	Digi-Key	70ADH-4-M-ND	10	$18.60	10	1	9	J20
J-4Pos-Pin	32	2-Battery Recharging	4 Position,Through Hole	1		$0.00		$0.00			Digi-Key		10	$0.00	10	1	9	J19
J-6Pos-Pin	33	2-Battery Recharging	6 Position,Through Hole	1		$0.00		$0.00			Digi-Key		10	$0.00	10	1	9	J15
J-Bat	34	2-Battery Recharging	2 Positions Header Connector 0.049" (1.25mm) Through Hole Tin	1	$0.320	$0.32	$0.020	$4.02	Molex, LLC	530470210	Digi-Key	WM1731-ND	5	$1.60	5	4	1	J16
R-1.2M	35	2-Battery Recharging	1.2M Ohm ±5% 0.1W, 1/10W Chip Resistor (0603), Automotive AEC-Q200 Thick Film	1	$0.026	$0.03	$0.010	$2.08	Vishay Dale	CRCW06031M20JNEA	Digi-Key	541-1.2MGCT-ND	10	$0.26	10	2	8	R49
R-220K	37	2-Battery Recharging	220k Ohm ±5% 0.25W, 1/4W Chip Resistor (0603), Automotive AEC-Q200, Pulse Withstanding Thick Film	2	$0.148	$0.30	$0.057	$22.76	Vishay Dale	RCS0603220KJNEA	Digi-Key	541-2821-1-ND	10	$1.48	10	4	6	R48, R50
R-2K	38	2-Battery Recharging	2K ohm Resistor, 1/4W (0603)	1	$0.149	$0.15	$0.058	$11.64	Vishay Dale	CRCW06032K00JNEAHP	Digi-Key	541-2.0KSACT-ND	5	$0.75	5	2	3	R47
R-2M	39	2-Battery Recharging	2M Ohm ±1% 0.1W, 1/10W Chip Resistor (0603), Automotive AEC-Q200 Thick Film	1	$0.035	$0.04	$0.014	$2.84	Vishay Dale	CRCW06032M00FKEA	Digi-Key	541-2.00MHCT-ND	10	$0.35	10	2	8	R53
SW-DPDT	40	2-Battery Recharging	Slide Switch DPDT Through Hole, Right Angle, 300mA, 125V	1	$2.310	$2.31	$1.836	$367.10	TE Connectivity ALCOSWITCH Switches	1571630-2	Digi-Key	450-1590-ND	5	$11.55	5	2	3	SW3
U-1V8	41	2-Battery Recharging	Boost Switching Regulator IC Positive Adjustable 1.8V 1 Output 1.2A (Switch) 10-VFDFN Exposed Pad	1	$2.460	$2.46	$1.777	$355.42	Texas Instruments	TPS61200DRCR	Digi-Key	296-27017-1-ND	5	$12.30	5	2	3	U10
U-Bat	42	2-Battery Recharging	IC CONTROLLR LI-ION 4.2V (SOT23-5)	1	$0.580	$0.58	$0.433	$86.52	Microchip Technology	MCP73831T-2ACI/OT	Digi-Key	MCP73831T-2ACI/OTCT-ND	5	$2.90	5	2	3	U9
Z	17	**2-Battery Recharging Section End**		20		$32.42		$4,805.84						$105.15				
A		**3-HX711**																
C-0.1uF	43	3-HX711	0.1µF ±10% 16V Ceramic Capacitor X7R (0603)	2	$0.025	$0.05	$0.008	$3.18	KEMET	C0603C104K4RACTU	Digi-Key	399-1096-1-ND	15	$0.38	15	2	13	C14, C15
C-1uF	44	3-HX711	1µF ±10% 6.3V Ceramic Capacitor X5R (0603)	3	$0.042	$0.13	$0.019	$11.16	Murata Electronics North America	GRM188R60J105KA01D	Digi-Key	490-1550-1-ND	50	$2.10	50	3	47	C11, C12, C13
D-20V	45	3-HX711	Diode Schottky 20V 500mA Surface Mount SOD-123	1	$0.295	$0.30	$0.103	$20.60	Fairchild/ON Semiconductor	MBR0520L	Digi-Key	MBR0520LCT-ND	0	$0.00	0	0	0	D6
J-12pos-FFC	46	3-HX711	12 Position FFC, FPC Connector Contacts, Top 0.039" (1.00mm) Surface Mount, Right Angle	1	$0.850	$0.85	$0.641	$128.22	Amphenol FCI	SFW12R-2STE1LF	Digi-Key	609-1901-1-ND	5	$4.25	5	1	4	J7
J-4Pos-Fem	47	3-HX711	4 Position Spring Compression Contact, Female Connector Through Hole	1	$1.680	$1.68	$1.303	$260.62	Bourns Inc.	70ADH-4-FL0	Digi-Key	70ADH-4-F-ND	10	$16.80	10	go	#VALUE!	J8
Q-PNP	48	3-HX711	Bipolar (BJT) Transistor PNP 25V 1.5A 100MHz 625mW Surface Mount SOT-23	1	$0.210	$0.21	$0.125	$24.92	Micro Commercial Co	MMSS8550-H-TP	Digi-Key	MMSS8550-H-TPMSCT-ND	5	$1.05	5	1	0	Q2
R-1K	49	3-HX711	1k Ohm ±1% 0.1W, 1/10W Chip Resistor (0603), Automotive AEC-Q200, Thick Film	2	$0.035	$0.07	$0.006	$2.53	Vishay Dale	CRCW06031K00FKTA	Mouser	71-CRCW0603-1.0K	12	$0.42	20	2	18	R16, R17
R20K	50	3-HX711	20k Ohm ±1% 0.063W, 1/16W Chip Resistor (0603) Thin Film	1	$0.162	$0.16	$0.063	$12.68	TE Connectivity Passive Product	CPF0603F20KC1	Digi-Key	A102237CT-ND	5	$0.81	5	1	4	R14
R-8.2K	51	3-HX711	8.2k Ohm ±1% 0.25W, 1/4W Chip Resistor (0603), Automotive AEC-Q200, Pulse Withstanding Thick Film	1	$0.163	$0.16	$0.064	$12.72	Vishay Dale	CRCW06038K20FKEAHP	Digi-Key	541-8.20KSCT-ND	5	$0.82	5	1	0	R15
U-HX	52	3-HX711	HX711, SOIC16, 24 bit ADC IC for Load Cell http://www.sunrom.com/m/4872	1	$1.000	$1.00	$0.900	$180.00	Avia Semiconductor	HX711	SunRom	4872	10	$10.00	10	1	9	U5
WIRE	53	3-HX711	FFC / FPC Jumper Cables FFC 1.00 Type A 12 ckts lgt 127	1	$1.000	$1.00	$0.900	$180.00	Molex	15167-0275	Mouser	538-15167-0275	10	$10.00	10	0	10	U5
Z	11	**3-HX711 Section End**		15		$5.61		$836.64						$25.00				
A		**4-BT**																
C-0.1uF	54	4-BT	0.1µF ±10% 16V Ceramic Capacitor X7R (0603)	8	$0.025	$0.20	$0.008	$12.74	KEMET	C0603C104K4RACTU	Digi-Key	399-1096-1-ND	35	$0.88	35	25	10	C8, C16, C17, C18, C19, C23, C61, C62

sort ref	Item #	Section Grouping	Part Name/Description	Unit Quantity	Unit Cost	Total Cost	Unit Production Cost	Total Production Cost	Manufacturer	Manufacturer Part #	Supplier	Supplier Part #	Qty Ordered	Total Order Cost	Qty Received	Qty Used	Surplus Qty	Schematic Reference
C-12pF	55	4-BT	12pF ±5% 25V Ceramic Capacitor C0G, NP0 (0603)	2	$0.199	$0.40	$0.101	$40.36	KEMET	C0603C120J3GAC7867	Digi-Key	399-14483-1-ND	20	$3.98	20	8	12	C24, C25
C-15pF	56	4-BT	15pF ±20% 10V Ceramic Capacitor C0G, NP0 (0603)	2	$0.063	$0.13	$0.028	$11.16	KEMET	C0603C150M8GACTU	Digi-Key	399-9005-1-ND	20	$1.26	20	8	12	C20, C21
C-1uF	57	4-BT	1µF ±10% 6.3V Ceramic Capacitor X5R (0603)	2	$0.042	$0.08	$0.019	$7.44	Murata Electronics North America	GRM188R60J105KA01D	Digi-Key	490-1550-1-ND	50	$2.10	50	6	44	C22, C60
E	58	4-BT	ANTENNA CHIP 2.4GHZ	1	$0.930	$0.93	$0.626	$125.14	Johanson Technology Inc.	2450AT43A100E	Digi-Key	712-1009-1-ND	7	$6.51	7	4	3	E1
J-6pos	59	4-BT	6 Positions Header Connector 0.100" (2.54mm) Through Hole Tin	1	$0.258	$0.26	$0.180	$36.06	Amphenol FCI	67996-406HLF	Digi-Key	609-3218-ND	5	$1.29	5	3	2	J10
L	60	4-BT	RF Balun 2.4GHz ~ 2.5GHz 50 / - Ohm (0805)	1	$0.839	$0.84	$0.444	$88.82	Johanson Technology Inc.	2450BM15A0002E	Digi-Key	712-1536-1-ND	7	$5.87	7	4	3	L1
D-G	61	4-BT	Green 570nm LED Indication - Discrete 2.2V (0805)	2	$0.180	$0.36	$0.095	$37.92	OSRAM Opto Semiconductors Inc.	LG R971-KN-1	Digi-Key	475-1410-1-ND	5	$0.90	5	2	3	D20, D22
D-Y	62	4-BT	Yellow 588nm LED Indication - Discrete 2.1V (0805)	1	$0.282	$0.28	$0.089	$17.82	Kingbright	APT2012YC	Digi-Key	754-1135-1-ND	15	$4.23	15	1	14	D23
R-0	63	4-BT	0.0 Ohm Jumper 0.1W, 1/10W Chip Resistor (0603), Automotive AEC-Q200, Thick Film	3	$0.022	$0.07	$0.007	$4.15	Vishay Dale	CRCW06030000ZSTA	Mouser	71-CRCW0603-0	50	$1.10	50	4	46	R9, R77, R78
R-1K	64	4-BT	1k Ohm ±1% 0.1W, 1/10W Chip Resistor (0603), Automotive AEC-Q200, Thick Film	4	$0.035	$0.14	$0.006	$5.07	Vishay Dale	CRCW06031K00FKTA	Mouser	71-CRCW0603-1.0K	22	$0.77	20	4	16	R20, R42, R44, R45
R-10K	65	4-BT	10k Ohm ±1% 0.25W, 1/4W Chip Resistor (0603), Automotive AEC-Q200, Pulse Withstanding Thick Film	1	$0.146	$0.15	$0.056	$11.26	Vishay Dale	RCS060310K0FKEA	Digi-Key	541-2795-1-ND	40	$5.84	40	13	27	R19
R-56K	66	4-BT	56k Ohm ±5% 0.25W, 1/4W Chip Resistor (0603), Automotive AEC-Q200, Pulse Withstanding Thick Film	1	$0.149	$0.15	$0.058	$11.64	Vishay Dale	CRCW060356K0JNEAHP	Digi-Key	541-56KSACT-ND	5	$0.75	5	4	1	R18
SW-SPST	66	4-BT	Tactile Switch SPST-NO Top Actuated Surface Mount	1	$0.961	$0.96	$0.725	$145.02	Omron Electronics Inc-EMC Div	B3U-1000P	Digi-Key	SW1020CT-ND	5	$4.81	5	4	1	SW2
SW-SPDT	67	4-BT	Slide Switch SPDT Surface Mount, Right Angle	1	$3.020	$3.02	$2.394	$478.80	NKK Switches	SS312SAH4	Digi-Key	360-3250-ND	4	$12.08	4	2	2	SW60
U-Blue	68	4-BT	IC RF TxRx + MCU Bluetooth v4.0 2.4GHz 40-VFQFN Exposed Pad	1	$5.420	$5.42	$3.965	$792.98	Texas Instruments	CC2540F256RHAT	Digi-Key	296-27922-1-ND	5	$27.10	5	2	3	U6
Y-32.768	69	4-BT	32.768kHz ±20ppm Crystal 12.5pF 70 kOhm -40°C ~ 125°C AEC-Q200 Surface Mount 2-SMD, No Lead	1	$1.030	$1.03	$0.752	$150.48	NDK America, Inc.	NX3215SA-32.768K-STD-MUS-2	Digi-Key	644-1159-1-ND	7	$7.21	7	4	3	Y1
Y-32MHz	70	4-BT	32MHz ±10ppm Crystal 16pF 50 Ohm -30°C ~ 85°C Surface Mount 4-SMD, No Lead	1	$0.760	$0.76	$0.554	$110.78	NDK America, Inc.	NX3225SA-32M-EXS00A-02994	Digi-Key	644-1251-1-ND	7	$5.32	7	4	3	Y2
Z	18	4-BT Section End				$15.17		$2,087.64						$91.99				
A		5-BT Module						$0.00										
U	-	5-BT Module	(BLE Micro-Super Compact)	0	$9.900				DFRobot	TEL0084	Digi-Key	1738-1045-ND	0	$0.00	0	0	0	
U	71	5-BT Module	USB Bluetooth 4.0 Dongle RF Transceiver 2.4GHz Bluetooth v4.0, Low Energy (BLE) USB 1Mbps	1	$9.900	$9.90			DFRobot	TEL0087	Digi-Key	1738-1180-ND	2	$19.80	2	0	2	n/a
Z		5-BT Module				$9.90								$19.80				
A		6-Board Interconnection																
J-12pos	72	6-Board Interconnection	CON12	2	$1.149	$2.30		$0.00	Samtec Inc.	SSA-112-S-T	Digi-Key	SAM1122-12-ND	8	$9.19	8	0	8	J3, J9
J-12pos	73	6-Board Interconnection	CON 12-TEST	2	$1.149	$2.30		$0.00	Samtec Inc.	SSA-112-S-T	Digi-Key	SAM1122-12-ND	10	$11.49	10	0	10	J-TEST-OPT1, J-TEST-OPT2
J-4Pos	74	6-Board Interconnection	CON 4	1	$1.149	$1.15		$0.00	Samtec Inc.	SSA-112-S-T	Digi-Key	SAM1122-12-ND	4	$4.60	4	0	4	J15, J17
J-6Pos	75	6-Board Interconnection	CON 6	1	$1.149	$1.15		$0.00	Samtec Inc.	SSA-112-S-T	Digi-Key	SAM1122-12-ND	8	$9.19	8	0	8	J2, J11
Z	4	6-Board Interconnection Section End				$6.89		$0.00						$34.47				
A		7-LED Indicators																
D-G	76	7-LED Indicators	Green 570nm LED Indication - Discrete 2.2V (0805)	3	$0.180	$0.54	$0.095	$56.88	OSRAM Opto Semiconductors Inc.	LG R971-KN-1	Digi-Key	475-1410-1-ND	15	$2.70	15	5	10	D20, D21, D22
D-R	77	7-LED Indicators	Red 625nm LED Indication - Discrete 2.2V (0805)	1	$0.500	$0.50	$0.280	$56.06	Kingbright	APT2012SECK/J3-PRV	Digi-Key	754-1791-1-ND	5	$2.50	5	1	4	D24
D-Y	78	7-LED Indicators	Yellow 588nm LED Indication - Discrete 2.1V (0805)	1	$0.282	$0.28	$0.089	$17.82	Kingbright	APT2012YC	Digi-Key	754-1135-1-ND	10	$2.82	10	2	8	D23
J-6pos-FFC	79	7-LED Indicators	6 Position FFC, FPC Connector Contacts, Bottom 0.020" (0.50mm) Surface Mount, Right Angle	2	$4.335	$8.67	$3.613	$1,445.12	Molex, LLC	514410693	Digi-Key	WM6473CT-ND	10	$43.35	10	4	6	J1, J14
R-1K	80	7-LED Indicators	1k Ohm ±1% 0.1W, 1/10W Chip Resistor (0603), Automotive AEC-Q200, Thick Film	5	$0.035	$0.18	$0.006	$6.34	Vishay Dale	CRCW06031K00FKTA	Mouser	71-CRCW0603-1.0K	30	$1.05	30	8	22	R42, R43, R44, R45, R46
wire	81	7-LED Indicators	6 Position FFC Cable 0.020" (0.50mm) 2.000" (50.80mm)	1	$2.600	$2.60	$2.023	$404.62	Molex, LLC	152660053	Digi-Key	WM10510-ND	5	$13.00	5	0	5	n/a

sort ref	Item #	Section Grouping	Part Name/Description	Unit Quantity	Unit Cost	Total Cost	Unit Production Cost	Total Production Cost	Manufacturer	Manufacturer Part #	Supplier	Supplier Part #	Qty Ordered	Total Order Cost	Qty Received	Qty Used	Surplus Qty	Schematic Reference
Z	6	7-LED Indicators Section End				$12.77		$1,986.84						$60.22				
A		8-Inductive Charging - Transmitter																
C-0.068uF	82	8-Inductive Charging - Transmitter	0.068µF ±10% 50V Ceramic Capacitor X7R (0603)	1	$0.088	$0.09	$0.039	$7.82	Murata Electronics North America	GRM188R71H683KA93D	Digi-Key	490-3288-1-ND	2	$0.18	2	1	1	C37
C-0.15uF	83	8-Inductive Charging - Transmitter	0.15µF ±5% 50V Ceramic Capacitor X7R (1206)	2	$0.420	$0.84	$0.277	$110.68	KEMET	C1206C154J5RACTU	Digi-Key	399-9320-1-ND	4	$1.68	4	2	2	Cx1, Cx2
C-0.47uF	84	8-Inductive Charging - Transmitter	0.47µF ±10% 25V Ceramic Capacitor X7R (0603)	1	$0.132	$0.13	$0.067	$13.36	KEMET	C0603C474K3RAC7867	Digi-Key	399-11934-1-ND	2	$0.26	2	1	1	C36
C-10000pF	85	8-Inductive Charging - Transmitter	10000pF (0.01uF) ±10% 50V Ceramic Capacitor X7R (0603)	2	$0.022	$0.04	$0.010	$3.84	Murata Electronics North America	GRM188R71H103KA01D	Digi-Key	490-1512-1-ND	50	$1.10	50	2	48	C40, C41
C-22uF	86	8-Inductive Charging - Transmitter	22µF ±20% 6.3V Ceramic Capacitor X5R (0603)	1	$0.167	$0.17	$0.095	$18.92	Murata Electronics North America	GRM188R60J226MEA0D	Digi-Key	490-7611-1-ND	2	$0.33	2	1	1	C38
C-330pF	87	8-Inductive Charging - Transmitter	330pF ±5% 50V Ceramic Capacitor C0G, NP0 (0603)	1	$0.089	$0.09	$0.040	$7.94	Murata Electronics North America	GRM1885C1H331JA01D	Digi-Key	490-1439-1-ND	2	$0.18	2	1	1	C39
C-4.7uF-50V	88	8-Inductive Charging - Transmitter	4.7µF ±10% 50V Ceramic Capacitor X5R (0805)	1	$0.242	$0.24	$0.145	$29.00	Murata Electronics North America	GRM21BR61H475KE51L	Digi-Key	490-10751-1-ND	2	$0.48	2	1	1	C35
D-40V	89	8-Inductive Charging - Transmitter	Diode Schottky 40V 1A (DC) Surface Mount 2-DSN (1.4x0.6)	2	$0.381	$0.76	$0.260	$103.84	ON Semiconductor	NSR10F40NXT5G	Digi-Key	NSR10F40NXT5GOSCT-ND	4	$1.52	4	2	2	D16, D17
D-40V	90	8-Inductive Charging - Transmitter	Diode Schottky 40V 2A Surface Mount PowerDI™ 123	1	$0.470	$0.47	$0.183	$36.60	Diodes Incorporated	DFLS240L-7	Digi-Key	DFLS240LDICT-ND	5	$2.35	5	1	4	D14
D-G	91	8-Inductive Charging - Transmitter	Green 570nm LED Indication - Discrete 2.2V (0805)	1	$0.180	$0.18	$0.095	$18.96	OSRAM Opto Semiconductors Inc.	LG R971-KN-1	Digi-Key	475-1410-1-ND	5	$0.90	5	1	4	D15
D-Zen	92	8-Inductive Charging - Transmitter	Zener Diode 300mW ±6% Surface Mount SOT-23-3	2	$0.208	$0.42	$0.113	$45.36	Diodes Incorporated	BZX84C16-7-F	Digi-Key	BZX84C16-FDICT-ND	4	$0.83	4	2	2	D18, D19
I-4.7uH	93	8-Inductive Charging - Transmitter	Fixed Inductors LPS4018 Low Profile 4.7uH 1.8A 20% SMD, 4mmX4mm	1	$1.140	$1.14	$0.778	$155.60	Coilcraft	LPS4018-472MRB	Mouser	994-LPS4018-472MRB	5	$5.70	5	1	4	L3
I-68uH	94	8-Inductive Charging - Transmitter	68µH Shielded Wirewound Inductor 400mA 460 mOhm Max Nonstandard	2	$1.274	$2.55	$0.823	$329.28	TDK	VLCF5028T-680MR40-2	Digi-Key	445-6568-1-ND	4	$5.10	4	2	2	L4, L5
J-4Pos-Fem	95	8-Inductive Charging - Transmitter	4 Position Spring Compression Contact, Female Connector Through Hole	1	$1.680	$1.68	$1.303	$260.62	Bourns Inc.	70ADH-4-FL0	Digi-Key	70ADH-4-F-ND	10	$16.80	10	2	8	J8
J-Power	96	8-Inductive Charging - Transmitter	Power Barrel Connector Jack 2.00mm ID (0.079"), 5.50mm OD (0.217") Through Hole, Right Angle	1	$0.760	$0.76	$0.543	$108.56	CUI Inc.	CP-102AH	Digi-Key	CP-102AH-ND	5	$3.80	5	1	4	J13
Q-N-30V	97	8-Inductive Charging - Transmitter	N-Channel 30V 20A (Ta) 3.1W (Ta) Surface Mount 8-SOIC	2	$0.489	$0.98	$0.318	$127.26	Alpha & Omega	AO4576	Digi-Key	785-1465-1-ND	4	$1.96	4	2	2	Q5, Q6
Q-N-60V	98	8-Inductive Charging - Transmitter	N-Channel 60V 115mA (Tc) 225mW (Ta) Surface Mount SOT-23-3 (TO-236)	1	$0.148	$0.15	$0.081	$16.14	ON Semiconductor	2N7002LT1G	Digi-Key	2N7002LT1GOSCT-ND	2	$0.30	2	1	1	Q4
Q-P-12V	99	8-Inductive Charging - Transmitter	P-Channel 12V 4.1A (Ta) 750mW (Ta) Surface Mount SOT-23-3 (TO-236)	1	$0.580	$0.58	$0.444	$88.86	Vishay Siliconix	SI2333DS-T1-E3	Digi-Key	SI2333DS-T1-E3CT-ND	2	$1.16	2	1	1	Q3
R-100	100	8-Inductive Charging - Transmitter	100 Ohm ±5% 0.1W, 1/10W Chip Resistor (0603), Moisture Resistant Thick Film	2	$0.016	$0.03	$0.006	$2.56	Bourns Inc.	CR0603-JW-101ELF	Digi-Key	CR0603-JW-101ELFCT-ND	20	$0.32	20	2	18	R40, R41
R-100K	101	8-Inductive Charging - Transmitter	100k Ohm ±5% 0.1W, 1/10W Chip Resistor (0603), Automotive AEC-Q200, Thick Film	2	$0.026	$0.05	$0.010	$4.16	Vishay Dale	CRCW0603100KJNEA	Digi-Key	541-100KGCT-ND	50	$1.30	50	2	48	R37, R38
R-150K	102	8-Inductive Charging - Transmitter	150k Ohm ±1% 0.063W, 1/16W Chip Resistor (0603), Thin Film	2	$0.131	$0.26	$0.051	$20.56	TE Connectivity Passive Product	CPF0603F150KC1	Digi-Key	A102216CT-ND	4	$0.52	4	2	2	R32, R36
R-1K	103	8-Inductive Charging - Transmitter	1k Ohm ±1% 0.1W, 1/10W Chip Resistor (0603), Automotive AEC-Q200, Thick Film	1	$0.035	$0.04	$0.006	$1.27	Vishay Dale	CRCW06031K00FKTA	Mouser	71-CRCW0603-1.0K	7	$0.25	20	1	19	R39
R-20K	104	8-Inductive Charging - Transmitter	20k Ohm ±1% 0.063W, 1/16W Chip Resistor (0603) Thin Film	1	$0.162	$0.16	$0.063	$12.68	TE Connectivity Passive Product	CPF0603F20KC1	Digi-Key	A102237CT-ND	5	$0.81	5	1	4	R34
R-40.2K	105	8-Inductive Charging - Transmitter	40.2k Ohm ±1% 0.1W, 1/10W Chip Resistor (0603), Automotive AEC-Q200, Thick Film	1	$0.035	$0.04	$0.014	$2.84	Vishay Dale	CRCW060340K2FKEA	Digi-Key	541-40.2KHCT-ND	2	$0.07	2	1	1	R33
R-536K	106	8-Inductive Charging - Transmitter	536k Ohm ±1% 0.1W, 1/10W Chip Resistor (0603), Automotive AEC-Q200, Thick Film	1	$0.035	$0.04	$0.014	$2.84	Vishay Dale	CRCW0603536KFKEA	Digi-Key	541-536KHCT-ND	2	$0.07	2	1	1	R35
TX	107	8-Inductive Charging - Transmitter	Wireless Charging Coils Tx coil 4.95uH 0.03 ohms 50x3mm	1	$7.620	$7.62	$4.700	$940.00	TDK	WT-505060-8K2-LT	Digi-Key Mouser	445-172646-ND 810-WT-505060-8K2-LT	3	$22.86	3	0	3	ANT2
U	108	8-Inductive Charging - Transmitter	Buck Switching Regulator IC Positive Adjustable 0.79V 1 Output 2A 10-WFDFN Exposed Pad	1	$6.930	$6.93	$4.060	$812.00	Linear Technology	LT3480EDD#PBF	Digi-Key	LT3480EDD#PBF-ND	2	$13.86	2	1	1	U8
Z	27	8-Inductive Charging - Transmitter Section End				$26.43		$3,281.55						$84.69				
A		9-Inductive Charging-Receiver & Battery Charging																
BAT	109	9-Inductive Charging-Receiver & Battery Charging	Lithium-Ion Battery Rechargeable (Secondary) 3.7V, 500mAh, Coin, 35.0mm, Wire leads	1	$22.230	$22.23	$16.960	$3,392.00	Illinois Capacitor	RJD355SHPPV30M	Mouser Digi-Key (more $)	598-RJD355SHPPV30M 1572-1627-ND	2	$44.46	3	0	3	n/a

sort ref	Item #	Section Grouping	Part Name/Description	Unit Quantity	Unit Cost	Total Cost	Unit Production Cost	Total Production Cost	Manufacturer	Manufacturer Part #	Supplier	Supplier Part #	Qty Ordered	Total Order Cost	Qty Received	Qty Used	Surplus Qty	Schematic Reference
C-0.022uF	110	9-Inductive Charging-Receiver & Battery Charging	0.022µF ±5% 50V Ceramic Capacitor X7R (0603)	1	$0.071	$0.07	$0.032	$6.32	Murata Electronics North America	GRM188R71H223JA01D	Digi-Key	490-14377-1-ND	5	$0.36	5	2	3	C29
C-10000pF	111	9-Inductive Charging-Receiver & Battery Charging	10000pF (0.01uF) ±10% 50V Ceramic Capacitor X7R (0603)	1	$0.022	$0.02	$0.010	$1.92	Murata Electronics North America	GRM188R71H103KA01D	Digi-Key	490-1512-1-ND	50	$1.10	50	2	48	C33
C-10uF-16V	112	9-Inductive Charging-Receiver & Battery Charging	10µF ±10% 16V Ceramic Capacitor X6S (0805)	1	$0.131	$0.13	$0.066	$13.26	Murata Electronics North America	GRM21BC81C106KE15L	Digi-Key	490-10498-1-ND	5	$0.66	5	2	3	C28
C-10uF-50V	113	9-Inductive Charging-Receiver & Battery Charging	10µF ±10% 50V Ceramic Capacitor X7S (1210)	1	$0.851	$0.85	$0.609	$121.82	Murata Electronics North America	GRJ32EC71H106KE11L	Digi-Key	490-10956-1-ND	5	$4.26	5	2	3	C26
C-1800pF	114	9-Inductive Charging-Receiver & Battery Charging	1800pF ±5% 50V Ceramic Capacitor X7R (0603)	1	$0.247	$0.25	$0.148	$29.60	KEMET	C0603C182J5RACTU	Digi-Key	399-9024-1-ND	5	$1.24	5	2	3	C30
C-2.2uF	115	9-Inductive Charging-Receiver & Battery Charging	2.2µF ±10% 6.3V Ceramic Capacitor X5R (0603)	1	$0.103	$0.10	$0.048	$9.68	Murata Electronics North America	GRM188R60J225KE19D	Digi-Key	490-1552-1-ND	5	$0.52	5	2	3	C32
C-4700pF	116	9-Inductive Charging-Receiver & Battery Charging	4700pF ±5% 50V Ceramic Capacitor X7R (0603)	2	$0.042	$0.08	$0.019	$7.44	KEMET	C0603C472J5RACTU	Digi-Key	399-1088-1-ND	10	$0.42	10	4	6	C27, C31
C-47uF	117	9-Inductive Charging-Receiver & Battery Charging	47µF ±10% 16V Ceramic Capacitor X5R (1210)	1	$0.664	$0.66	$0.455	$91.08	Murata Electronics North America	GRM32ER61C476KE15K	Digi-Key	490-6538-1-ND	5	$3.32	5	2	3	C34
D-40V	118	9-Inductive Charging-Receiver & Battery Charging	Diode Schottky 40V 2A Surface Mount PowerDI™ 123	3	$0.404	$1.21	$0.183	$109.79	Diodes Incorporated	DFLS240L-7	Digi-Key	DFLS240LDICT-ND	15	$6.06	15	6	9	D10, D12, D13
D-Zen	119	9-Inductive Charging-Receiver & Battery Charging	Zener Diode 1W ±5% Surface Mount PowerDI™ 123	1	$0.426	$0.43	$0.290	$58.00	Diodes Incorporated	DFLZ39-7	Digi-Key	DFLZ39DICT-ND	5	$2.13	5	2	3	D11
I-15uH	120	9-Inductive Charging-Receiver & Battery Charging	Fixed Inductors LPS4018 Low Profile 15uH 1.12A 20% SMD	1	$1.000	$1.00	$0.778	$155.60	Coilcraft	LPS4018-153MRB	Mouser	994-LPS4018-153MRB	5	$5.00	6	2	4	L2
J-4Pos-Male	121	9-Inductive Charging-Receiver & Battery Charging	4 Position Spring Compression Contact, Male Connector Through Hole	1	$1.860	$1.86	$1.446	$289.18	Bourns Inc.	70ADH-4-ML0	Digi-Key	70ADH-4-M-ND	10	$18.60	10	2	8	J20
J-BAT	122	9-Inductive Charging-Receiver & Battery Charging	2 Positions Header Connector 0.049" (1.25mm) Through Hole Tin	1	$0.320	$0.32	$0.020	$4.02	Molex, LLC	530470210	Digi-Key	WM1731-ND	5	$1.60	5	2	3	J12
R-0	123	9-Inductive Charging-Receiver & Battery Charging	0.0 Ohm Jumper 0.1W, 1/10W Chip Resistor (0603), Automotive AEC-Q200, Thick Film	4	$0.022	$0.09	$0.007	$5.54	Vishay Dale	CRCW06030000ZSTA	Mouser	71-CRCW0603-0	50	$1.10	50	4	46	R23, R25, R28, R31
R-1.4M	124	9-Inductive Charging-Receiver & Battery Charging	1.4M Ohm ±1% 0.1W, 1/10W Chip Resistor (0603), Automotive AEC-Q200, Thick Film	1	$0.021	$0.02	$0.009	$1.72	Stackpole Electronics Inc.	RMCF0603FT1M40	Digi-Key	RMCF0603FT1M40CT-ND	10	$0.21	10	2	8	R24
R-100K	125	9-Inductive Charging-Receiver & Battery Charging	100k Ohm ±5% 0.1W, 1/10W Chip Resistor (0603), Automotive AEC-Q200, Thick Film	2	$0.026	$0.05	$0.010	$4.16	Vishay Dale	CRCW06031000KJNEA	Digi-Key	541-100KGCT-ND	50	$1.30	50	4	46	R22, R29
R-10K	126	9-Inductive Charging-Receiver & Battery Charging	10k Ohm ±1% 0.1W, 1/10W Chip Resistor (0603), Automotive AEC-Q200, Thick Film	1	$0.035	$0.04	$0.014	$2.84		CRCW060310K0FKTA	Mouser	71-CRCW0603-10K	100	$3.50	100	2	98	R27
R-3.01K	127	9-Inductive Charging-Receiver & Battery Charging	3.01k Ohm ±1% 0.1W, 1/10W Chip Resistor (0603), Moisture Resistant, Thick Film	1	$0.021	$0.02	$0.009	$1.72	Bourns Inc.	CR0603-FX-3011ELF	Digi-Key	CR0603-FX-3011ELFCT-ND	10	$0.21	10	2	8	R26
R-412K	128	9-Inductive Charging-Receiver & Battery Charging	412k Ohm ±1% 0.1W, 1/10W Chip Resistor (0603), Automotive AEC-Q200 Thick Film	1	$0.035	$0.04	$0.014	$2.84	Vishay Dale	CRCW0603412KFKEA	Digi-Key	541-412KHCT-ND	10	$0.35	10	2	8	R30
RT	129	9-Inductive Charging-Receiver & Battery Charging	NTC THERMISTOR 10K OHM 5% 0603	1	$0.894	$0.89	$0.605	$121.00	Vishay Dale	NTHS0603N02N1002JE	Digi-Key	541-1107-1-ND	5	$4.47	5	2	3	RT1
RX	130	9-Inductive Charging-Receiver & Battery Charging	1 Coil, 1 Layer 47µH Wireless Charging Coil Receiver 460 mOhm	1	$11.400	$11.40	$9.117	$1,823.40	Wurth Electronics Inc.	7.60308E+11	Digi-Key	732-6207-ND	2	$22.80	2	2	0	ANT1
SW-SPST	131	9-Inductive Charging-Receiver & Battery Charging	Slide Switch SPST Through Hole, Right Angle	1	$4.080	$4.08	$3.230	$646.00	NKK Switches	AS11CH	Digi-Key	360-2728-ND	4	$16.32	4	2	2	SW4
U	132	9-Inductive Charging-Receiver & Battery Charging	400mA Wireless Synchronous Buck Battery Charger, Lithium-Ion/Polymer, 3mmX3mmQFN16	1	$6.910	$6.91	$3.950	$790.00	Linear Technology	LTC4120EUD-4.2#PBF	Digi-Key	LTC4120EUD-4.2#PBF-ND	4	$27.64	4	3	1	U7
Z	24	**9-Inductive Charging-Receiver & Battery Charging Section End**		31		$52.76		$7,688.92						$167.61				
						$0.00		$0.00						$0.00			0	
	Total Number of Items			Total Quantity of Parts		Total Cost		Total Production Cost						Total Order Cost				

sort ref	Item #	Section Grouping	Part Name/Description	Unit Quantity	Unit Cost	Total Cost	Unit Production Cost	Total Production Cost	Manufacturer	Manufacturer Part #	Supplier	Supplier Part #	Qty Ordered	Total Order Cost	Qty Received	Qty Used	Surplus Qty	Schematic Reference
	131			265		$ 175.02		$22,267.22						$662.00				
							Projected Unit Production Cost (Inductive w/out Base)											
							$70.26											

APPENDIX E

CODE FOR THE WIRELESS STRAIN TRANSMITTER

Arduino code file name: “ARAMS_w_BT-Main.ino”

```
#include "HX711.h"
// HX711.DOUT  - pin #D3
// HX711.PD_SCK - pin #D2
HX711 scale;
int GainA=128; //gain value for Ch A/switch to Ch A (working only with 64 or 128)
int GainB=32; //ONLY gain value to access CH B
long int Load_A,Load_B;
float Calibration_A=21.05;
float Calibration_B=1.0;
float KnownWeightA=501; //grams
float KnownWeightB=501; //grams
float tempFactor, tempLoad;
float LowWeightA=100.0; //grams
float LowWeightB=35.0; //grams
float LowWeightASq, LowWeightBSq;
int CHA_On,CHB_On,FilterOn;
int Wait=1;
void setup() {
   Serial.begin(115200); // speed needed for the Bluetooth
   CHA_On=1;
   FilterOn=1;
   while (Wait==1){
    Serial.println("Waiting Bluetooth connection,");
    Serial.println("Send a 't' when connected");
    if(Serial.available()){
     char temp = Serial.read();
     if (temp=='t'){
       Wait=2;
     }
    }
    delay(1000);
   }
   scale.begin(3, 2); // parameter "gain" is omitted; the default value 128 is used by the
library
   Serial.println(" ");
   Serial.println("Code that is loaded is 'ARAMS_w_BT-Main v1.4'");
   Serial.println("CH A: On");
   Serial.println("Ch B: Off");
   Serial.println("Low weight reading Filter: On");
   LowWeightASq=LowWeightA*LowWeightA;
   LowWeightBSq=LowWeightB*LowWeightB;
   Instruction();
   Serial.println(" ");
```

```
  Serial.println("Each load calculation is the average of 20 readings.");
  Serial.println("There is a delay between displayed strain reading.");
  Serial.println("This is to make it easy to read results.");
  Serial.println(" ");
  Serial.println("Finalizing system initialization");
}

void loop() {
  if (Wait==2){ // to finalizing system initialization
    Wait=3;
    Calibration();}

  if (CHA_On==0 && CHB_On==0){
    Serial.println("Both HX711 channel are OFF");
    Serial.println("If need help with control commands, send 'q'");}
  if(CHA_On==1){
      scale.set_gain(GainA); // Set gain to read Channel A
      scale.set_scale(Calibration_A);
      Load_A=scale.get_units(20);
      if(FilterOn==1){
        tempLoad=Load_A*Load_A;
        if (tempLoad<=LowWeightASq){
          Load_A=0;}
        }
      Serial.print("Load Value of A (grams): ");
      Serial.println(Load_A);
      Serial.print("\t| Last raw ADC reading of A: ");
      Serial.println(scale.read());
    } // End of CHA

 if(CHB_On==1){
      scale.set_gain(GainB); // Set gain to read Channel A
      scale.set_scale(Calibration_B);
      Load_B=scale.get_units(20);
      if(FilterOn==1){
        tempLoad=Load_B^2;
        if (tempLoad<=LowWeightBSq){
          Load_B=0;
          }
        }
      Serial.print("Load Value of B (grams): ");
      Serial.println(Load_B);
      Serial.print("\t| Last raw ADC reading of B: ");
      Serial.println(scale.read());
    } // End of CHB
```

```
    if(Serial.available()){
      char temp = Serial.read();
      switch(temp){
        case 'A':
          CHA_On= 1;
          Serial.println("Channel A turned On.");
          break;
        case 'a':
          CHA_On= 0;
          Serial.println("Channel A turned Off.");
          break;
        case 'B':
          CHB_On=1;
          Serial.println("Channel B turned On.");
          break;
        case 'b':
          CHB_On=0;
          Serial.println("Channel B turned Off.");
          break;
        case 'C':
           Calibration();
           break;
        case'F':
           FilterOn=1;
           Serial.println("Filtering of low/miss calculated zero point turned On.");
           break;
        case 'f':
           FilterOn=0;
           Serial.println("Filtering of low/miss calculated zero point turned Off.");
           break;
        case 'q':
          Instruction();
          break;
        default:
          Serial.println("Error in command");
          Instruction();
          break;
      } //End of character Switch
    } //End of Serial Available
    delay(1000); // to slow the printing
  } // End of loop command

  void DotDown(){
    int w=1;
    while (w<=10){
```

```
    Serial.print(".");
    delay(1000);
    w++;}
}

void CountDown(){
  int w=1;
  int n=20;
  while (w<=20){
    Serial.print(n);
    Serial.print(", ");
    delay(1000);
    w++;
    n--;}
}

void Calibration() {
  Serial.println("Calibrating active HX channel(s).");
  if(CHA_On==0 && CHB_On==0){
    Serial.println("Need to turn on a HX channel to complete step.");}
  Serial.println("Remove all weights from scale.");
  if(CHA_On==1){
    scale.set_gain(GainA); // Set gain to read Channel A
    scale.get_units();
    int w=1;
    while (w<=15){
      Serial.print(".");
      delay(1000);
      w++;}
    Serial.println("Resetting");
    scale.set_scale();
    scale.tare();
    Serial.println("Calibrating Channel 'A'.");
    Serial.print("Place the channel 'A' weight of ");
    Serial.print(KnownWeightA);
    Serial.println(" grams on now.(got 20 sec)");
    CountDown();
    Serial.println(" ");
    Serial.println("Calculating");
    tempFactor=scale.get_units(50);
    Calibration_A=tempFactor/KnownWeightA;
    Serial.print("New calibration factor: ");
    Serial.println(Calibration_A);}
  if(CHA_On==1 && CHB_On==1){
    Serial.println("Remove all weights to calibrate Channel B.");}
```

```
  if(CHB_On==1){
    scale.set_gain(GainB); // Set gain to read Channel A
    DotDown();
    DotDown();
    Serial.println("Resetting");
    scale.set_scale();
    scale.tare();
    Serial.println("Calibrating Channel 'B'.");
    Serial.print("Place the channel 'B' weight of ");
    Serial.print(KnownWeightB);
    Serial.print(" grams on now.(got 20 sec)");
    CountDown();
    Serial.println(" ");
    Serial.println("Calculating");
    tempFactor=scale.get_units(50);
    Calibration_B=tempFactor/KnownWeightB;
    Serial.print("New calibration factor: ");
    Serial.println(Calibration_B);}
}

void Instruction() {
  Serial.println(" ");
  Serial.println("Here is the list of Serial control characters.");
  Serial.println("Channel A of the HX711");
  Serial.println("Turn on with: 'A'");
  Serial.println("Turn off with: 'a'");
  Serial.println("Channel B of the HX711");
  Serial.println("Turn on with: 'B'");
  Serial.println("Turn off with: 'b'");
  Serial.println("**** Other commands are:  *****");
  Serial.println("To calibrate of a load: 'C'");
  Serial.println("Turn on Low weight Filtering: 'F'");
  Serial.println("Turn off Low weight Filtering: 'f'");
  Serial.println("To recall character command list/help: 'q'");
  DotDown();
}
```

APPENDIX F

SCHEMATIC FOR THE FLEXIBLE SENSOR MODULES

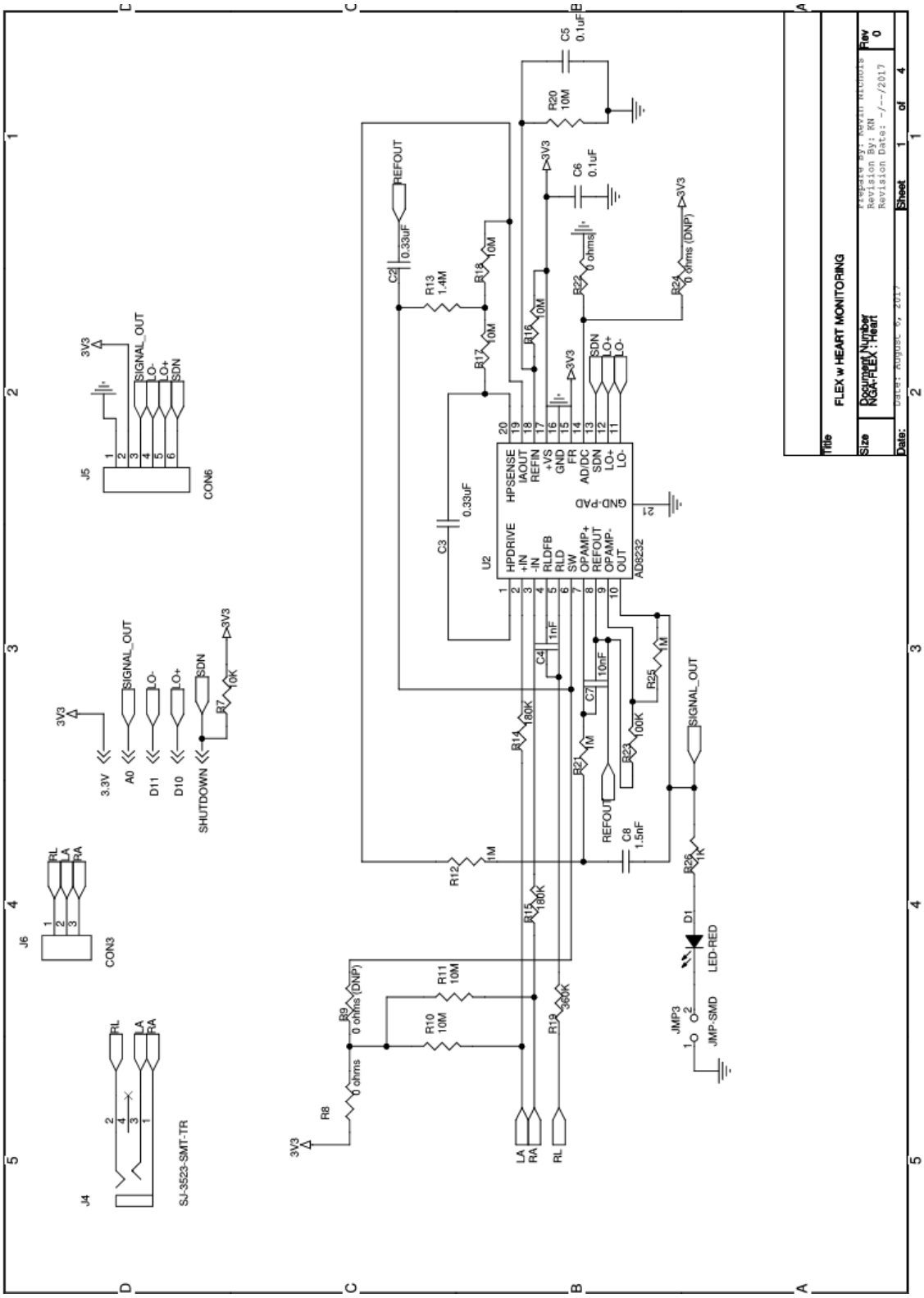
FLEX w HEART MONITORING
Document Number
NGA-FLEX : Heart
Rev
0
Sheet 1 of 4
Date:
Size
Title
J4
SJ-3523-SMT-TR
J6
CON3
J5
CON6
U2
AD8232
HPDRIVE
+IN
-IN
RLDFB
RLD
SW
OPAMP+
REFOUT
OPAMP-
OUT
HPSENSE
IAOUT
REFIN
+VS
GND
FR
AD/DC
SDN
LO+
LO-
GND-PAD
SIGNAL_OUT
3.3V
A0
D11
D10
SHUTDOWN
3V3
REFOUT
LA
RA
RL
D1
LED-RED
JMP3
JMP-SMD
R8
0 ohms
R9
0 ohms (DNP)
R10
10M
R11
10M
R12
1M
R13
1.4M
R14
180K
R15
180K
R16
360K
R17
10M
R18
10M
R19
10M
R20
10M
R21
1M
R22
0 ohms
R23
100K
R24
0 ohms (DNP)
R25
1M
R26
1K
R7
10K
C2
0.33uF
C3
0.33uF
C4
1nF
C5
0.1uF
C6
0.1uF
C7
10nF
C8
1.5nF

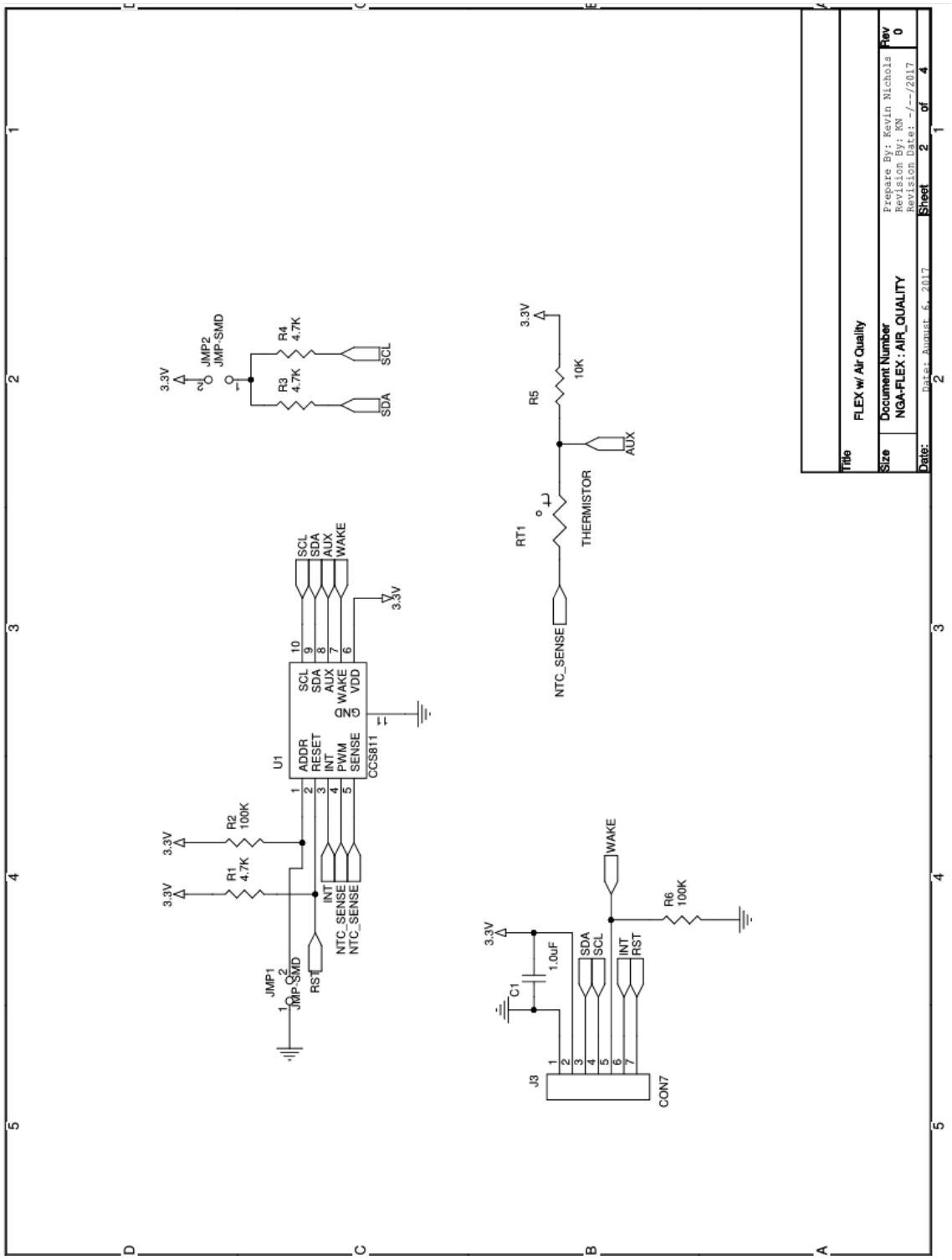
Title
FLEX w/ Air Quality
Size
Document Number
NGA-FLEX : AIR_QUALITY
Rev
0
Date: August 6, 2017
Sheet 2 of 4
Prepare By: Kevin Nicholas
Revision By: KN
Revision Date: -/--/2017
3.3V
JMP2
JMP-SMD
R4
4.7K
R3
4.7K
SCL
SDA
R5
10K
AUX
RT1
THERMISTOR
NTC_SENSE
U1
ADDR
RESET
INT
PWM
SENSE
GND
SCL
SDA
AUX
WAKE
VDD
CCS811
R2
100K
R1
4.7K
INT
NTC_SENSE
NTC_SENSE
RST
JMP1
JMP-SMD
WAKE
R6
100K
C1
1.0uF
SDA
SCL
INT
RST
J3
CON7

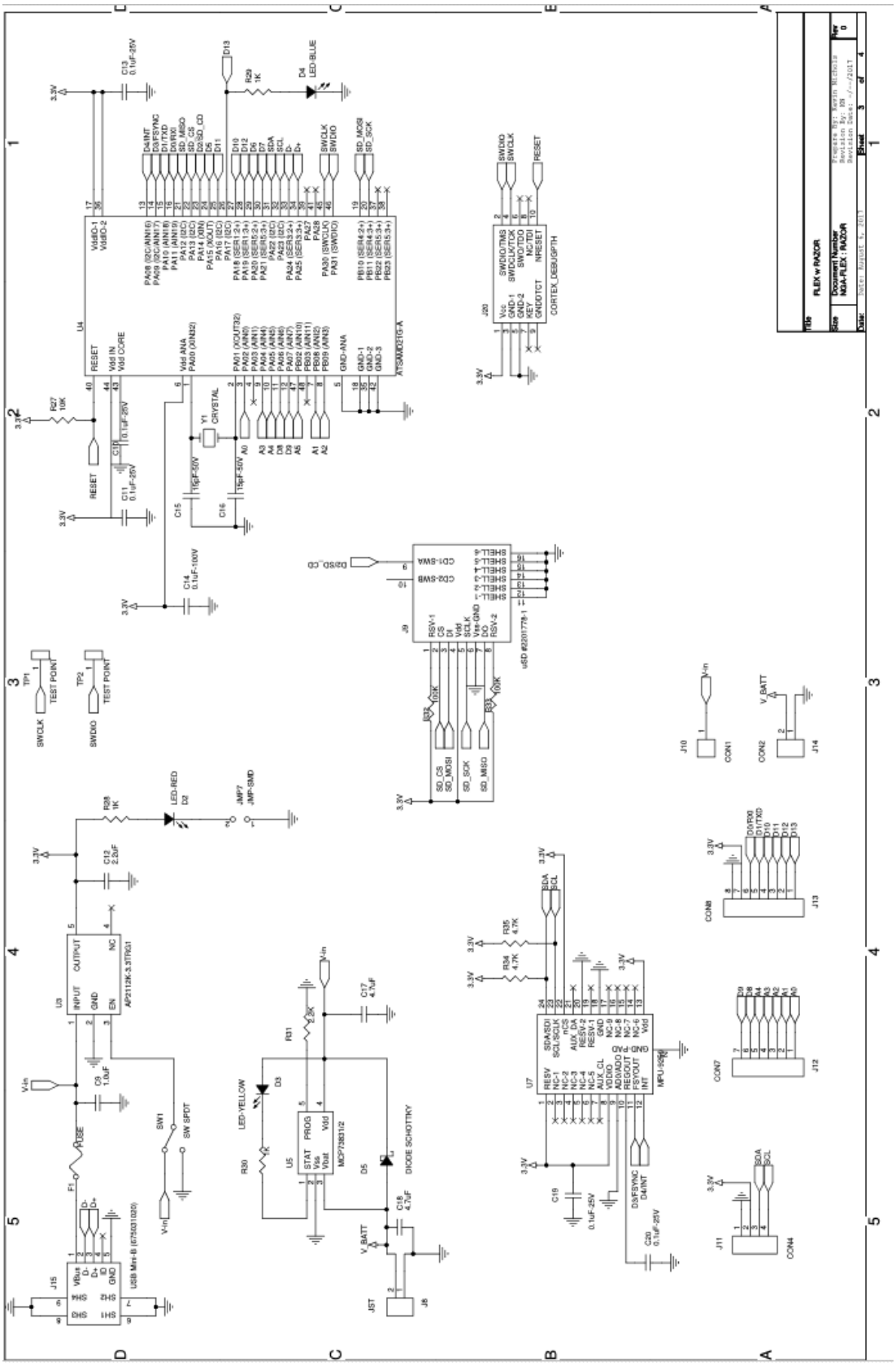
FLEX w RAZOR
NBA-FLEX-RAZOR
U4
XTSAM21G-A
U3
AP2112K-3.3TRG1
U5
MCP73831/2
U7
MPU-9250
J15
USB Mini-B (67503-0100)
J20
CORTEX_DEBUGPTH
J9
CD1-SWA
CD2-SWB
uSD #22011778-1
Y1
CRYSTAL
D4
LED-BLUE
D2
LED-RED
D3
LED-YELLOW
D5
DIODE SCHOTTKY
SW1
SW SPDT
TP1
TEST POINT
TP2
TEST POINT
J10
CON1
J14
CON2
J13
CON8
J12
CON7
J11
CON4
J8
J5T
V_BATT
SWCLK
SWDIO
RESET
SD_CS
SD_MOSI
SD_SCK
SD_MISO
SDA
SCL
D3/SD_CD
Vin
3.3V
Title
FLEX w RAZOR
Document Number
NBA-FLEX-RAZOR
Rev
0
Sheet 3 of 4

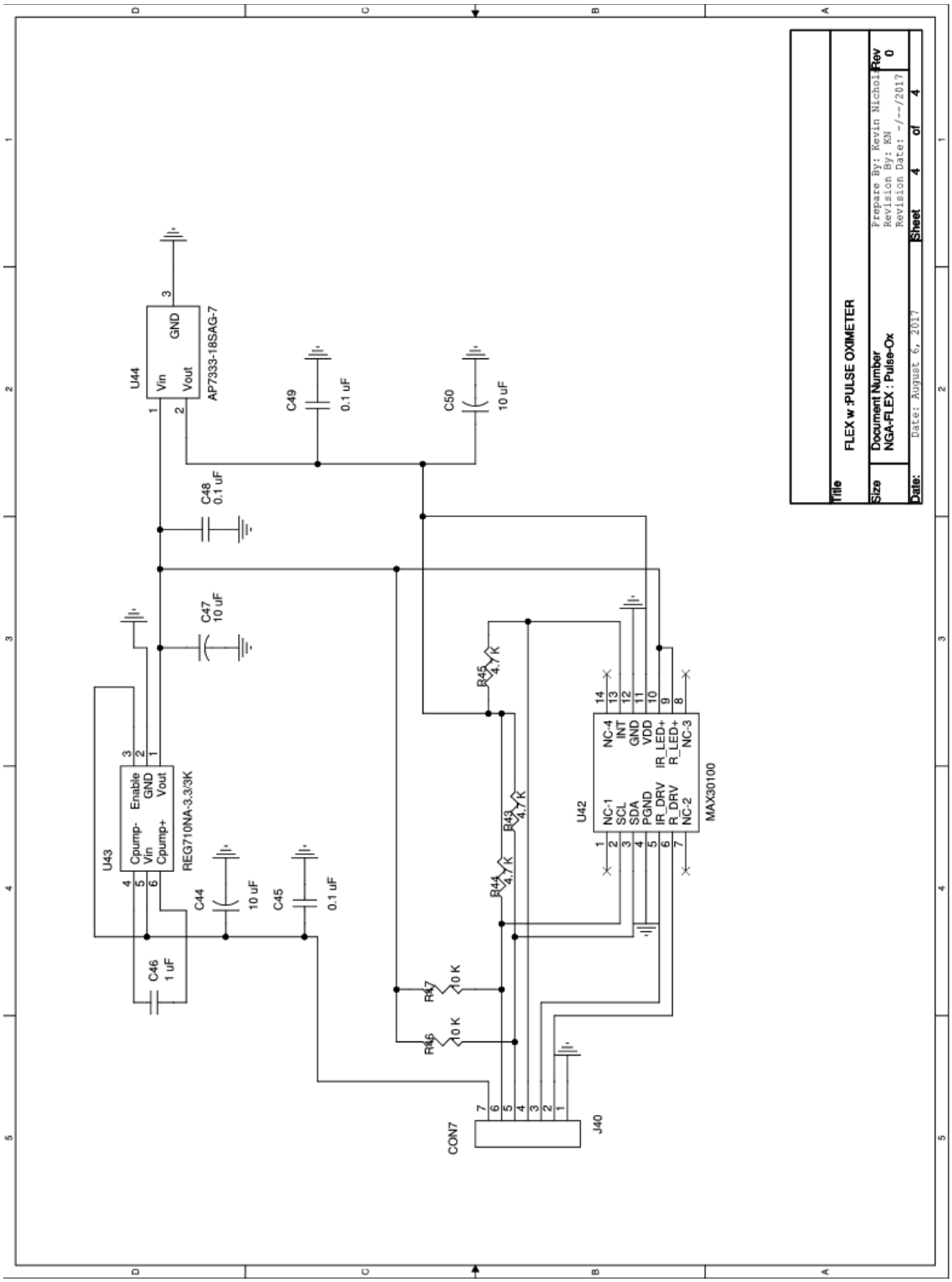
U44
Vin
Vout
GND
AP7333-18SAG-7
C49
0.1 uF
C50
10 uF
C48
0.1 uF
C47
10 uF
U43
Enable
GND
Vout
Cpump-
Vin
Cpump+
REG710NA-3.3/3K
C44
10 uF
C45
0.1 uF
C46
1 uF
R45
4.7 K
R43
4.7 K
R44
4.7 K
R47
10 K
R46
10 K
U42
NC-4
INT
GND
VDD
IR_LED+
R_LED+
NC-3
NC-1
SCL
SDA
PGND
IR_DRV
R_DRV
NC-2
MAX30100
CON7
J40
Title
FLEX w /PULSE OXIMETER
Size
Document Number
NGA-FLEX : Pulse-Ox
Rev
0
Date: August 6, 2017
Sheet 4 of 4
Prepare By: Kevin Nichol
Revision By: KN
Revision Date: -/--/2017

APPENDIX G

BILL OF MATERIAL FOR THE FLEXIBLE SENSOR MODULES

		Project Name:	FLEX Project													
		Prepared By:	Kevin Nichols													
		Version Number:	Alpha 1.3													
		Version Date:	11/28/2017													
			Bill of Material													
a-sort ref	**Item #**	**1-Section Grouping**	**Part Name/Description**	**Unit Qty**	**Unit Cost**	**Total Cost**	**Manufacturer**	**Manufacturer Part #**	**Supplier**	**Supplier Part #**	**Qty Ordered**	**Total Order Cost**	**Qty Received**	**Qty Used**	**Surplus Qty**	**Schematic Reference**
b		**9dof-Razor-IMU**														
C0.1uF-100	1	9dof-Razor-IMU	0.1µF ±10% 100V Ceramic Capacitor X7S 0603 (1608 Metric)	1	$0.133	$0.13	TDK Corporation	C1608X7S2A104K080AB	Digi-Key	445-5201-1-ND	10	$1.33	10	3	7	C14
C0.1uF-25	2	9dof-Razor-IMU	0.1µF ±20%, 25V, Ceramic Capacitor, X7R, 0603 (1608 Metric)	5	$0.047	$0.24	KEMET	C0603C104M3RACTU	Digi-Key	399-1283-1-ND	30	$1.41	30	15	15	C10, C11, C13, C19. C20
C15pF	3	9dof-Razor-IMU	15pF ±5% 50V Ceramic Capacitor C0G, NP0 0603 (1608 Metric)	2	$0.042	$0.08	KEMET	C0603C150J5GACTU	Digi-Key	399-1051-1-ND	20	$0.84	20	6	14	C15, C16
C1uF	4	9dof-Razor-IMU	1µF ±10% 16V Ceramic Capacitor X7R 0603 (1608 Metric)	1	$0.070	$0.07	KEMET	C0603C105K4RACTU	Digi-Key	399-7847-1-ND	10	$0.70	10	3	7	C9
C2.2uF	5	9dof-Razor-IMU	2.2µF ±10% 10V Ceramic Capacitor X7R 0603 (1608 Metric)	1	$0.171	$0.17	KEMET	C0603C225K8RACTU	Digi-Key	399-11681-1-ND	10	$1.71	10	3	7	C12
C4.7uF	6	9dof-Razor-IMU	4.7µF ±10% 16V Ceramic Capacitor X5R 0603 (1608 Metric)	2	$0.228	$0.46	TDK Corporation	C1608X5R1C475K080AC	Digi-Key	445-7478-1-ND	20	$4.56	20	6	14	C17, C18
D	7	9dof-Razor-IMU	Diode Schottky, 1A, 23V, Surface Mount SOD-323	1	$0.350	$0.35	STMicroelectronics	BAT20JFILM	Digi-Key	497-3381-1-ND	10	$3.50	10	3	7	D5
D-B	8	9dof-Razor-IMU	Blue 470nm LED Indication - Discrete 2.9V 0603 (1608 Metric)	1	$0.460	$0.46	Rohm Semiconductor	SMLE13BC8TT86	Digi-Key	846-1177-1-ND	5	$2.30	5	3	2	D4
D-R	9	9dof-Razor-IMU	Red 625nm LED Indication - Discrete 2.2V 0603 (1608 Metric)	1	$0.390	$0.39	Kingbright	APT1608SECK/J3-PRV	Digi-Key	754-1786-1-ND	5	$1.95	5	3	2	D2
D-Y	10	9dof-Razor-IMU	Yellow 590nm LED Indication - Discrete 2.2V 0603 (1608 Metric)	1	$0.340	$0.34	Rohm Semiconductor	SML-D12Y8WT86	Digi-Key	511-1582-1-ND	5	$1.70	5	3	2	D3
F	11	9dof-Razor-IMU	Polymeric PTC Resettable Fuse 6V Ih Surface Mount 1206 (3216 Metric), Concave, Long Side Terminals	1	$0.310	$0.31	Eaton	PTS12066V050	Digi-Key	283-3139-1-ND	5	$1.55	5	3	2	F1
J-JST	12	9dof-Razor-IMU	JST 2 pin Connector	1	$0.580	$0.58	JST Sales America Inc.	S2B-PH-SM4-TB(LF)(SN)	Digi-Key	455-1749-1-ND	5	$2.90	5	3	2	J8
J-SD	13	9dof-Razor-IMU	8 Position Card Connector microSD™ Surface Mount, Right Angle Gold-Palladium	1	$4.280	$4.28	TE Connectivity AMP Connectors	2201778-1	Digi-Key	A118117CT-ND	5	$21.40	5	3	2	J9
J-USB	14	9dof-Razor-IMU	USB - mini B USB 2.0 OTG Receptacle Connector 5 Position Surface Mount, Right Angle	1	$1.030	$1.03	Molex, LLC	675031020	Digi-Key	WM5461CT-ND	5	$5.15	5	3	2	J15
R100K	15	9dof-Razor-IMU	100K OHM Chip Resistor, ±1%, 1/10W, 0603 (1608 Metric), Moisture Resistant, Thick Film	2	$0.021	$0.04	Bourns Inc.	CR0603-FX-1003HLF	Digi-Key	CR0603-FX-1003HLFCT-ND	10	$0.21	10	6	4	R32, R33
R10K	16	9dof-Razor-IMU	10K OHM Chip Resistor, ±1%, 1/10W, 0603 (1608 Metric), Moisture Resistant, Thick Film	1	$0.056	$0.06	Bourns Inc.	CR0603-FX-1002GLF	Digi-Key	CR0603-FX-1002GLFCT-ND	25	$1.40	25	3	22	R27
R1K	17	9dof-Razor-IMU	1K OHM Chip Resistor, ±1%, 1/10W, 0603 (1608 Metric), Moisture Resistant, Thick Film	3	$0.021	$0.06	Bourns Inc.	CR0603-FX-1001ELF	Digi-Key	CR0603-FX-1001ELFCT-ND	75	$1.58	75	9	66	R28, R29, R30
R2.2K	18	9dof-Razor-IMU	2.2K OHM Chip Resistor, ±1%, 1/10W, 0603 (1608 Metric), Moisture Resistant, Thick Film	1	$0.056	$0.06	Bourns Inc.	CR0603-FX-2201ELF	Digi-Key	CR0603-FX-2201ELFCT-ND	10	$0.56	10	3	7	R31
R4.7K	19	9dof-Razor-IMU	4.7K OHM Chip Resistor, ±1%, 1/10W, 0603 (1608 Metric), Moisture Resistant, Thick Film	2	$0.009	$0.02	Bourns Inc.	CR0603-FX-4701ELF	Digi-Key	CR0603-FX-4701ELFCT-ND	30	$0.26	30	6	24	R34, R35
SW-SPDT	20	9dof-Razor-IMU	Slide Switch SPDT, 0.4VA, 28V, Surface Mount, Right Angle	1	$3.020	$3.02	NKK Switches	SS312SAH4	Digi-Key	360-3250-ND	5	$15.10	5	3	2	SW1
U	21	9dof-Razor-IMU	Accelerometer, Gyroscope, Magnetometer, 3 Axis Sensor I²C, SPI Output, 24QFN	1	$9.322	$9.32	TDK InvenSense	MPU-9250	Digi-Key	1428-1019-1-ND	5	$46.61	5	3	2	U7
U	22	9dof-Razor-IMU	ARM® Cortex®-M0+ SAM D21G Microcontroller IC 32-Bit 48MHz 256KB (256K x 8) FLASH 48-TQFP (7x7)	1	$3.220	$3.22	Microchip Technology	ATSAMD21G18A-AUT	Digi-Key	ATSAMD21G18A-AUTCT-ND	5	$16.10	5	3	2	U4
U	23	9dof-Razor-IMU	IC CONTROLLR LI-ION 4.2V (SOT23-5)	1	$0.580	$0.58	Microchip Technology	MCP73831T-2ACI/OT	Digi-Key	MCP73831T-2ACI/OTCT-ND	5	$2.90	5	3	2	U5
U-3V3	24	9dof-Razor-IMU	Linear Voltage Regulator IC Positive Fixed Output 3.3V 600mA SOT-23-5	1	$0.480	$0.48	Diodes Incorporated	AP2112K-3.3TRG1	Digi-Key	AP2112K-3.3TRG1DICT-ND	5	$2.40	5	3	2	U3
Y	25	9dof-Razor-IMU	32.768kHz ±20ppm Crystal 12.5pF 70 kOhm -40°C ~ 125°C AEC-Q200 Surface Mount 2-SMD, No Lead	1	$1.030	$1.03	NDK America, Inc.	NX3215SA-32.768K-STD-MUS-2	Digi-Key	644-1159-1-ND	5	$5.15	5	3	2	Y1
	26	9dof-Razor-IMU				$0.00						$0.00		0	0	

a-sort ref	Item #	1-Section Grouping	Part Name/Description	Unit Qty	Unit Cost	Total Cost	Manufacturer	Manufacturer Part #	Supplier	Supplier Part #	Qty Ordered	Total Order Cost	Qty Received	Qty Used	Surplus Qty	Schematic Reference
z	26	9dof-Razor-IMU Section End		35		$26.78						$143.26				
b		Air Quality														
C1uF	27	Air Quality	1µF ±10% 16V Ceramic Capacitor X7R 0603 (1608 Metric)	1	$0.070	$0.07	KEMET	C0603C105K4RACTU	Digi-Key	399-7847-1-ND	10	$0.70	10	3	7	C1
R100K	28	Air Quality	100K OHM Chip Resistor, ±1%, 1/10W, 0603 (1608 Metric), Moisture Resistant, Thick Film	2	$0.021	$0.04	Bourns Inc.	CR0603-FX-1003HLF	Digi-Key	CR0603-FX-1003HLFCT-ND	10	$0.21	10	6	4	R2, R6
R10K	29	Air Quality	10K OHM Chip Resistor, ±1%, 1/10W, 0603 (1608 Metric), Moisture Resistant, 10K ohms 0603 1/10W 1%	1	$0.056	$0.06	Bourns Inc.	CR0603-FX-1002GLF	Digi-Key	CR0603-FX-1002GLFCT-ND	25	$1.40	25	3	22	R5
R4.7K	30	Air Quality	4.7K OHM Chip Resistor, ±1%, 1/10W, 0603 (1608 Metric), Moisture Resistant, Thick Film	3	$0.009	$0.03	Bourns Inc.	CR0603-FX-4701ELF	Digi-Key	CR0603-FX-4701ELFCT-ND	35	$0.30	35	9	26	R1, R3, R4
RT1	31	Air Quality	NTC THERMISTOR 10K OHM 3% BEAD	1	$0.900	$0.90	Vishay BC Components	NTCLE100E3103HT1	Digi-Key	BC2395CT-ND	5	$4.50	5	1	4	RT1
U	32	Air Quality	Air Quality Sensor I²C	1	$12.424	$12.42	ams	CCS811	Digi-Key	CCS811CT-ND	5	$62.12	5	3	2	U1
z	6	Air Quality Section End		9		$13.52						$69.23				
b		Heart Monitor														
C0.1uF-16	33	Heart Monitor	0.1µF ±10% 16V Ceramic Capacitor X7R 0603 (1608 Metric)	2	$0.025	$0.05	KEMET	C0603C104K4RACTU	Digi-Key	399-1096-1-ND	15	$0.38	15	4	11	C5, C6
C0.33nF	34	Heart Monitor	0.33µF ±10% 10V Ceramic Capacitor X7R 0603 (1608 Metric)	2	$0.094	$0.19	KEMET	C0603C334K8RACTU	Digi-Key	399-4917-1-ND	20	$1.88	20	4	16	C2, C3
C1.5nF	35	Heart Monitor	1500pF ±10% 50V Ceramic Capacitor X7R 0603 (1608 Metric)	1	$0.040	$0.04	KEMET	C0603C152K5RACTU	Digi-Key	399-1084-1-ND	10	$0.40	10	2	8	C8
C10nF	36	Heart Monitor	10000pF ±10% 25V Ceramic Capacitor X7R 0603 (1608 Metric)	1	$0.029	$0.03	KEMET	C0603C103K3RACTU	Digi-Key	399-7840-1-ND	10	$0.29	10	2	8	C7
C1nF	37	Heart Monitor	1000pF ±10% 16V Ceramic Capacitor X7R 0603 (1608 Metric)	1	$0.028	$0.03	KEMET	C0603C102K4RACTU	Digi-Key	399-7835-1-ND	10	$0.28	10	2	8	C4
D-R	38	Heart Monitor	Red 625nm LED Indication - Discrete 2.2V 0603 (1608 Metric)	1	$0.390	$0.39	Kingbright	APT1608SECK/J3-PRV	Digi-Key	754-1786-1-ND	5	$1.95	5	2	3	D1
h	39	Heart Monitor	SENSOR CABLE - ELECTRODE PADS (3 connector)	1	$5.000	$5.00	SparkFun Electronics	CAB-12970	Digi-Key	CAB-12970-ND	3	$15.00	3	0	3	n/a
H	40	Heart Monitor	BIOMEDICAL SENSOR PAD (10 PACK)	1	$7.950	$7.95	SparkFun Electronics	SEN-12969	Digi-Key	SEN-12969-ND	2	$15.90	2	0	2	n/a
J	41	Heart Monitor	CONN JACK, 3.50mm (0.141", 1/8", Mini Plug) - Headphone Phone Jack Stereo Connector Solder, SMD, R/A	1	$1.020	$1.02	CUI Inc.	SJ-3523-SMT-TR	Digi-Key	CP-3523SJCT-ND	5	$5.10	5	1	4	J4
R0	42	Heart Monitor	0.0OHM Jumper-Chip Resistor, 1/10W, 0603 (1608 Metric), Moisture Resistant, Thick Film	2	$0.010	$0.02	Bourns Inc.	CR0603-J/-000ELF	Digi-Key	CR0603-J/-000ELFCT-ND	25	$0.26	25	4	21	R8, R22
R-DNP	43	Heart Monitor	DO NOT PLACE: 0.0 OHM Jumper-Chip Resistor	2		$0.00						$0.00				R9, R24
R1.4M	44	Heart Monitor	1.4M OHM Chip Resistor, ±1%, 1/10W, 0603 (1608 Metric), Automotive AEC-Q200, Thick Film	1	$0.021	$0.02	Stackpole Electronics Inc.	RMCF0603FT1M40	Digi-Key	RMCF0603FT1M40CT-ND	10	$0.21	10	2	8	R13
R100K	45	Heart Monitor	100K OHM Chip Resistor, ±1%, 1/10W, 0603 (1608 Metric), Moisture Resistant, Thick Film	1	$0.021	$0.02	Bourns Inc.	CR0603-FX-1003HLF	Digi-Key	CR0603-FX-1003HLFCT-ND	10	$0.21	10	2	8	R23
R10K	46	Heart Monitor	10K OHM Chip Resistor, ±1%, 1/10W, 0603 (1608 Metric), Moisture Resistant, Thick Film	1	$0.056	$0.06	Bourns Inc.	CR0603-FX-1002GLF	Digi-Key	CR0603-FX-1002GLFCT-ND	25	$1.40	25	2	23	R7
R10M	47	Heart Monitor	10M OHM Chip Resistor, ±1%, 1/10W, 0603 (1608 Metric), Automotive AEC-Q200, Thick Film	6	$0.035	$0.21	Vishay Dale	CRCW060310M0FKEA	Digi-Key	541-10.0MHCT-ND	40	$1.40	30	12	18	R10, R11, R16, R17, R18, R20
R180K	48	Heart Monitor	180K OHM Chip Resistor, ±1%, 1/10W, 0603 (1608 Metric), Moisture Resistant, Thick Film	2	$0.056	$0.11	Bourns Inc.	CR0603-FX-1803ELF	Digi-Key	CR0603-FX-1803ELFCT-ND	10	$0.56	10	4	6	R14, R15
R1K	49	Heart Monitor	1K OHM Chip Resistor, ±1%, 1/10W, 0603 (1608 Metric), Moisture Resistant, Thick Film	1	$0.021	$0.02	Bourns Inc.	CR0603-FX-1001ELF	Digi-Key	CR0603-FX-1001ELFCT-ND	25	$0.53	25	2	23	R26
R1M	50	Heart Monitor	1M OHM Chip Resistor, ±1%, 1/10W, 0603 (1608 Metric), Moisture Resistant, Thick Film	3	$0.006	$0.02	Bourns Inc.	CR0603-FX-1004ELF	Digi-Key	CR0603-FX-1004ELFCT-ND	20	$0.11	20	6	14	R12, R21, R25
R360K	51	Heart Monitor	360K OHM Chip Resistor, ±1%, 1/10W, 0603 (1608 Metric), Moisture Resistant, Thick Film	1	$0.015	$0.02	Yageo	RC0603FR-07360KL	Digi-Key	311-360KHRCT-ND	10	$0.15	10	2	8	R19
U	52	Heart Monitor	AD8232 IC, ECG Front End IC Heart Rate Monitoring, 20-LFCSP-WQ (4x4)	1	$3.960	$3.96	Analog Devices Inc.	AD8232ACPZ-WP	Digi-Key	AD8232ACPZ-WP-ND	5	$19.80	5	2	3	U2
z	20	Heart Monitor Section End		32		$19.15						$65.80				
b		Pulse-Oxygen														

a-sort ref	Item #	1-Section Grouping	Part Name/Description	Unit Qty	Unit Cost	Total Cost	Manufacturer	Manufacturer Part #	Supplier	Supplier Part #	Qty Ordered	Total Order Cost	Qty Received	Qty Used	Surplus Qty	Schematic Reference
c0.1uF-16	1	Pulse-Oxygen	0.1µF ±10% 16V Ceramic Capacitor X7R (0603)	3	$0.025	$0.08	KEMET	C0603C104K4RACTU	Digi-Key	399-1096-1-ND	25	$0.63	25	9	16	C45, C48, C49
C10uF	2	Pulse-Oxygen	10µF ±10% Molded Tantalum Capacitors 16V (1206)	3	$0.312	$0.94	KEMET	T491A106K016AT	Digi-Key	399-8269-1-ND	20	$6.24	20	9	11	C44, C47, C50
c1uF	3	Pulse-Oxygen	1µF ±10% 16V Ceramic Capacitor X7R 0603 (1608 Metric)	1	$0.070	$0.07	KEMET	C0603C105K4RACTU	Digi-Key	399-7847-1-ND	10	$0.70	10	3	7	C46
R10K	4	Pulse-Oxygen	~~10K OHM Chip Resistor, ±1%, 1/10W, 0603 (1608 Metric), Moisture Resistant, Thick Film~~	2	$0.056	$0.11	Bourns Inc.	CR0603-FX-1002GLF	Digi-Key	CR0603-FX-1002GLFCT-ND	25	$1.40	25	6	19	~~R46, R47~~
R4.7K	5	Pulse-Oxygen	4.7K OHM Chip Resistor, ±1%, 1/10W, 0603 (1608 Metric), Moisture Resistant, Thick Film	3	$0.009	$0.03	Bourns Inc.	CR0603-FX-4701ELF	Digi-Key	CR0603-FX-4701ELFCT-ND	35	$0.30	35	11	24	R43, R44, R45
U	6	Pulse-Oxygen	IC SENSOR OXIMETER/HEARTRATE	1	$7.030	$7.03	Maxim Integrated	MAX30100EFD+T	Digi-Key	MAX30100EFD+TCT-ND	5	$35.15	5	3	2	U42
U-1V8	7	Pulse-Oxygen	Linear Voltage Regulator IC Positive Fixed Output 1.8V 500mA TSOT-23-6	1	$0.430	$0.43	Diodes Incorporated	AP7333-18SAG-7	Digi-Key	AP7333-18SAG-7DICT-ND	5	$2.15	5	3	2	U44
U-3V3	6	Pulse-Oxygen	Charge Pump Switching Regulator IC Positive Fixed 3.3V 30mA SOT-23-6	1	$1.280	$1.28	Texas Instruments	REG710NA-3.3/3K	Digi-Key	296-39168-1-ND	5	$6.40	5	3	2	U43
z	8	**Pulse-Oxygen Section End**		15		$9.96						$52.97				
						$0.00						$0.00			0	
	Total Number of Items			Total Quantity of Parts		Total Cost						Total Order Cost				
	60			91		$69.40						$331.26				